Marine Geology 412 (2019) 139–172

Contents lists available at ScienceDirect

Marine Geology

journal homepage: www.elsevier.com/locate/margo

Invited review article

Geological evidence for past large earthquakes and tsunamis along the Hikurangi subduction margin, New Zealand

Kate Clark[a,*], Jamie Howarth[b], Nicola Litchfield[a], Ursula Cochran[a], Jocelyn Turnbull[a,c], Lisa Dowling[b], Andrew Howell[b], Kelvin Berryman[a], Franklin Wolfe[d]

[a] GNS Science, PO Box 30368, Lower Hutt, New Zealand
[b] School of Geography, Environment and Earth Sciences, Victoria University of Wellington, PO Box 600, Wellington, New Zealand
[c] CIRES, University of Colorado at Boulder, Boulder, CO, USA
[d] Department of Earth and Planetary Science, Harvard University, 20 Oxford Street, Cambridge, MA 02138, USA

ARTICLE INFO

Editor: Edward Anthony

Keywords:
Subduction margin
Paleoearthquake
Hikurangi
Marine terrace
Tsunami deposit
Coastal subsidence

ABSTRACT

The Hikurangi subduction margin, New Zealand, has not produced large subduction earthquakes within the short written historic period (~180 years) and the potential of the plate interface to host large (M > 7) to great (M > 8) earthquakes and tsunamis is poorly constrained. The geological record of past subduction earthquakes offers a method for assessing the location, frequency and approximate magnitude of subduction earthquakes to underpin seismic and tsunami hazard assessments. We review evidence of Holocene coseismic coastal deformation and tsunamis at 22 locations along the margin. A consistent approach to radiocarbon age modelling is used and earthquake and tsunami evidence is ranked using a systematic assessment of the quality of age control and the certainty that the event in question is an earthquake. To identify possible subduction earthquakes, we use temporal correlation of earthquakes, combined with the type of earthquake evidence, likely primary fault source and the earthquake certainty ranking. We identify 10 past possible subduction earthquakes over the past 7000 years along the Hikurangi margin. The last subduction earthquake occurred at 520–470 years BP in the southern Hikurangi margin and the strongest evidence for a full margin rupture is at 870–815 years BP. There are no apparent persistent rupture patches, suggesting segmentation of the margin is not strong. In the southern margin, the type of geological deformation preserved generally matches that expected due to rupture of the interseismically locked portion of the subduction interface but the southern termination of past subduction ruptures remains unresolved. The pattern of geological deformation on the central margin suggests that the region of the interface that currently hosts slow slip events also undergoes rupture in large earthquakes, demonstrating different modes of slip behaviour occur on the central Hikurangi margin. Evidence for subduction earthquakes on the northern margin has not been identified because deformation signals from upper plate faults dominate the geological record. Large uncertainties remain in regard to evidence of past subduction earthquakes on the Hikurangi margin, with the greatest challenges presented by temporal correlation of earthquake evidence when working within the uncertainties of radiocarbon ages, and the presence of upper plate faults capable of producing deformation and tsunamis similar to that expected for subduction earthquakes. However, areas of priority research such as improving the paleotsunami record and integration of submarine turbidite records should produce significant advances in the future.

1. Introduction

Subduction zones produce the largest earthquakes and tsunamis on earth and can have devastating impacts on societies both near and far from the earthquake source. Great (M_W > 8.0) subduction earthquakes have occurred in modern times and within the period of written histories on many subduction margins worldwide providing indisputable evidence of the seismic potential of the subduction zone (Cisternas et al., 2005; Garrett et al., 2016; Lay, 2015). Subduction zones that have not produced large earthquakes within the time of written historical records pose a problem in which the potential size and recurrence of subduction earthquakes is poorly constrained. Therefore, a lack of historic subduction earthquakes hampers the ability to forecast the likelihood and impacts of future earthquakes. This is the case for the

* Corresponding author.
E-mail address: K.Clark@gns.cri.nz (K. Clark).

https://doi.org/10.1016/j.margeo.2019.03.004
Received 23 October 2018; Received in revised form 12 March 2019; Accepted 13 March 2019
Available online 25 March 2019

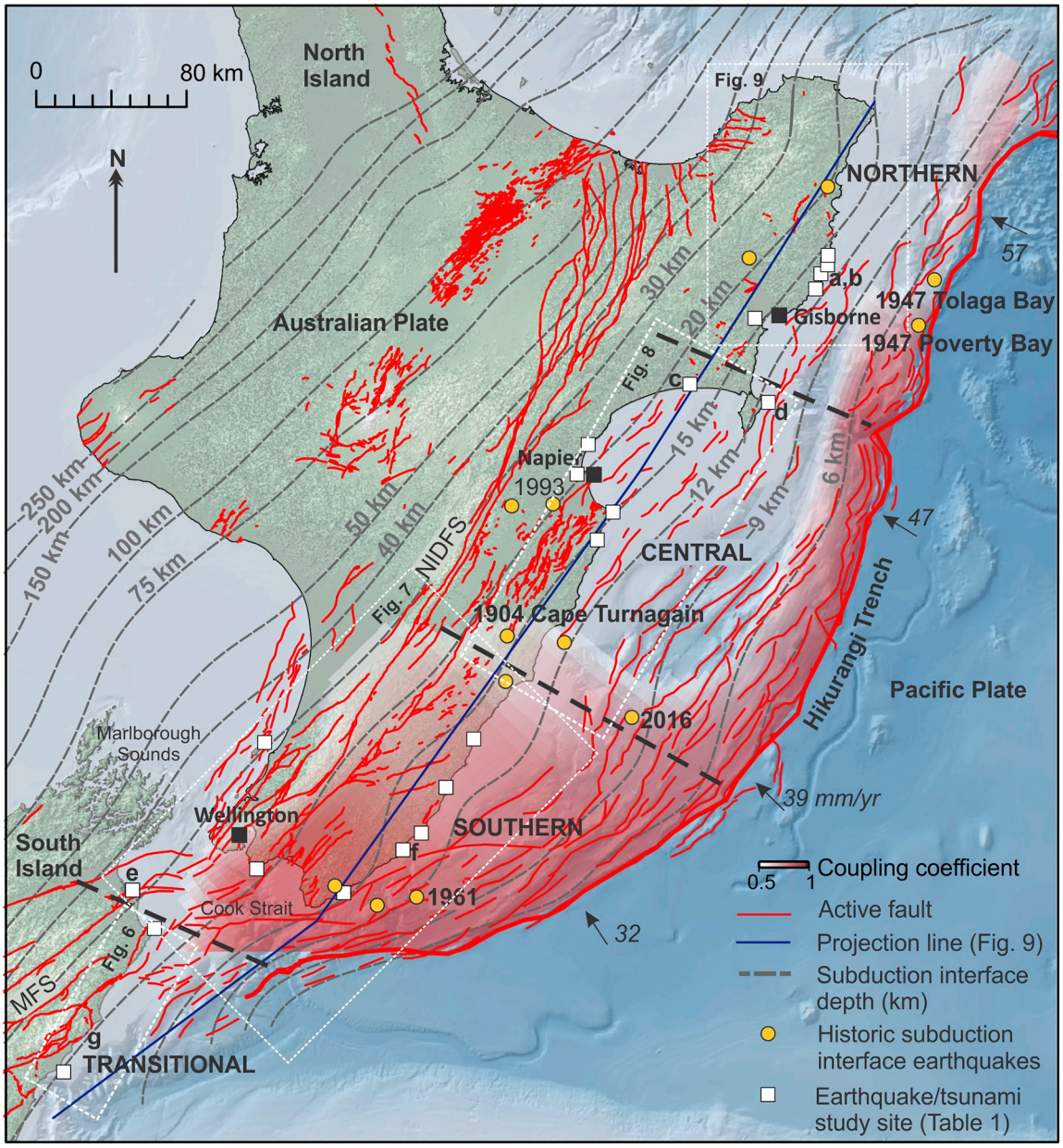

Fig. 1. Active tectonic map of the Hikurangi margin. Dashed black lines delineate the approximate boundaries between the regions discussed in the text and white squares show the study sites from which earthquake and paleotsunami ages have been obtained and compiled in Table 1 and Fig. 10. The projection line in dark blue shows the line to which all study sites were projected to calculate the distance along-margin of the horizontal axis in Fig. 10. Onshore active faults from the New Zealand Active Faults Database (Langridge et al., 2016) and offshore active faults from Barnes and Audru (1999), Barnes et al. (2002, 2010), Nodder et al. (2007), Mountjoy et al. (2009), Pondard and Barnes (2010), Mountjoy and Barnes (2011), Paquet et al. (2009). MFS: Marlborough Fault System, NIDFS: North Island Dextral Fault System. Subduction interface contours from Williams et al. (2013) and the subduction interface coupling coefficient is from Wallace et al. (2012b). Locations of historic interface seismicity (all < M_W 7.2) are from Wallace et al. (2014) and references therein, along with a 2016 earthquake from Wallace et al. (2017). Letters a–e show the locations of photos in Fig. 4A–G, and white dashed-line boxes show the areas covered in Figs. 7–10.

Hikurangi subduction margin, where the Pacific Plate subducts beneath the Australian Plate along the east coast of the North Island, New Zealand (Fig. 1).

New Zealand has a short written historic period of only ~180 years since European arrival and during that time the Hikurangi subduction margin has not produced any earthquakes of > M 7.2. Māori have inhabited New Zealand since ~700–800 years before present (BP) and although accounts of earthquakes and tsunamis occur within Maori oral histories (King et al., 2018), they are difficult to attribute to specific sources. Lacking historical examples, the seismic and tsunami potential of subduction zones can be characterised using geophysical techniques. For example, geodetic methods can monitor the accommodation of plate motion on the plate interface by detecting areas that are currently locked and accumulating stress versus areas that are unlocked or undergoing periodic slow slip (Wallace et al., 2009; Wallace et al., 2012b) and magnetotelluric methods can reveal electrically resistive patches on the interface that correspond with areas of increased coupling (Heise et al., 2017). However, geophysical methods provide a contemporary snapshot of plate interface stress and their utility as an indicator of long-term plate boundary behaviour is debatable (e.g. Witter et al., 2018). To understand longer-term earthquake behaviour at subduction zones, geological records are required.

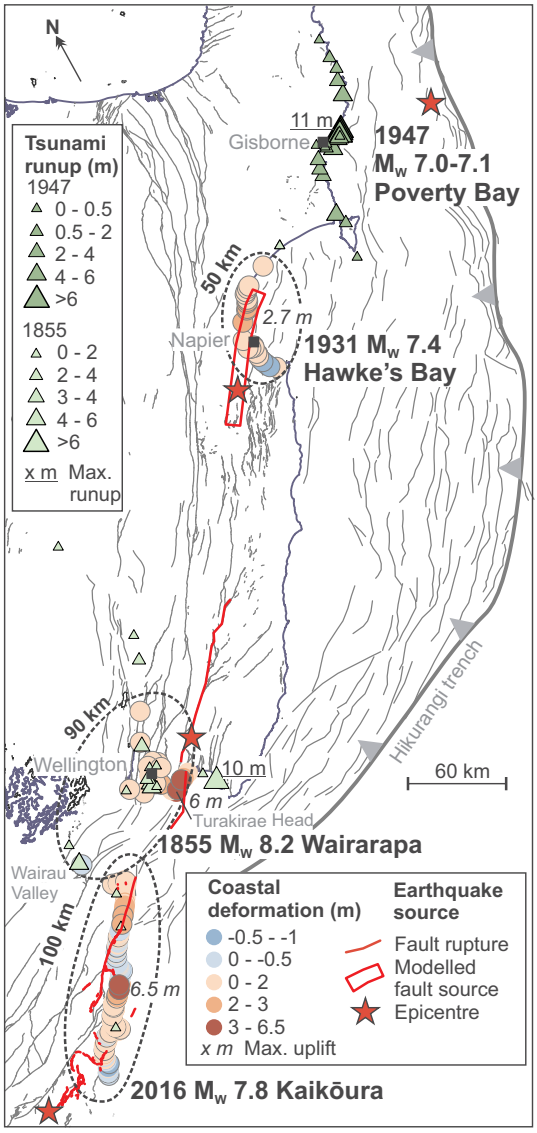

Fig. 2. Historic coseismic coastal deformation and significant local source tsunami runup on the Hikurangi margin. The dashed black ellipses show the extent of coastal deformation for each earthquake and the bold numbers note the margin-parallel extent of coastal deformation. The 1931 Hawke's Bay earthquake deformation data is from Hull (1990) and the fault source (a blind thrust fault, red rectangle) is from McGinty et al. (2001). The 1855 Wairarapa deformation and fault rupture data is from Grapes and Downes (1997) and Begg and McSaveney (2005). The Kaikōura earthquake deformation and fault rupture data is from Clark et al. (2017) and Litchfield et al. (2018a, b). Tsunami runup heights for the 1855 Wairarapa tsunami and 25 March 1947 Poverty Bay tsunami are compiled from the New Zealand Historic Tsunami Database (Downes et al., 2017) and are a mixture of maximum tsunami wave heights and runup elevations estimated from historic documents and instrumental recordings.

Geological records of past earthquakes and tsunamis at subduction zones provide powerful evidence of the magnitude and frequency of subduction earthquakes to underpin seismic and tsunami hazard assessments (González et al., 2009; Mueller et al., 2015; Priest et al., 2017; Sawai et al., 2012; Witter et al., 2013). However, identifying subduction earthquakes in the geological record of the Hikurangi margin is particularly challenging due to the number of upper plate faults (Clark et al., 2015). On margins with few active upper plate faults, the distinction between subduction and upper plate fault earthquakes is rarely considered. However, the Hikurangi margin is characterised by ubiquitous onshore and offshore upper plate faults and, although lacking a historic subduction earthquake occurrence, there is a rich record of large upper plate fault earthquakes such as the 1855 CE M_W 8.2 Wairarapa, 1931 M_W 7.4 Hawke's Bay and 2016 M_W 7.8 Kaikōura earthquakes (Fig. 2). These historical examples have demonstrated that at certain locations upper plate fault earthquakes can cause coastal deformation, ground shaking and tsunamis, similar to the effects expected at that site for a subduction earthquake (Hull, 1990; Grapes and Downes, 1997; Clark et al., 2017).

Studies of Holocene coastal deformation and paleotsunamis along the Hikurangi margin have been undertaken since the early 1980's (Berryman et al., 1992, Berryman, 1993a; Ota et al., 1988, 1989, 1990a, b, 1992, 1995) and since 2004 studies have been focused specifically toward trying to determine whether there is evidence for subduction earthquakes (e.g. Berryman et al., 2011; Cochran et al., 2006; Clark et al., 2010). Compilations and high-level summaries of evidence for past Hikurangi subduction earthquakes have appeared in several studies with successive publications iteratively improving the age control and/or number of sites examined (Hayward et al., 2016; Wallace et al., 2009, 2014). In this study we provide a critical review of the evidence for past subduction earthquakes and tsunamis on the Hikurangi margin. We aim to: 1) compile and evaluate the ages of past earthquakes and tsunamis along the Hikurangi margin using modern calibration curves, revised marine reservoir corrections and Bayesian statistical methods; 2) develop a chronology of past coastal deformation on the Hikurangi margin with an associated ranking of the certainty of evidence; 3) evaluate evidence for past subduction earthquakes; and 4) recommend how future research can improve our understanding of subduction earthquake and tsunami hazards along the Hikurangi margin.

2. Understanding past subduction earthquakes using the geological record

Multiple types of evidence yield information on the nature and timing of past subduction zone earthquakes and tsunamis. The most useful and reliable evidence for a particular subduction zone is a function of: (i) the location of the coastline relative to the subduction interface rupture patch; (ii) climate, glacio- and isostatic sea-level change; and (iii) coastal geomorphology. In general for a subduction earthquake, coseismic uplift occurs above the rupture patch while coseismic subsidence occurs inboard of the downdip end of the rupture patch, so the position of the coastline relative to a rupture patch can control whether coseismic uplift or subsidence occurs. It is possible that some locations (e.g., at the edges of rupture boundaries), may experience uplift in some earthquakes and subsidence in others if the slip distributions differ (e.g. Briggs et al., 2014; Ely et al., 2014). Tsunami deposits can be powerful evidence of past subduction earthquakes, particularly when they are preserved in the near-field region where coastal accommodation space is created by coseismic subsidence or where deep coastal lakes provide persistent accommodation space (e.g. Kempf et al., 2017). While most evidence of subduction earthquakes and tsunamis comes from the coastline, submarine and lacustrine turbidite records are increasingly being utilised as primary or complimentary records of subduction earthquakes (e.g. Goldfinger et al., 2012; Moernaut et al., 2014).

Evidence for coseismic subsidence is predominantly derived from peat-mud couplets preserved within tidal wetland sedimentary sequences and, to a lesser extent, from coastal geomorphology. Peat-mud couplets are the most widely-documented evidence of past subduction earthquakes: the underlying peat represents the pre-earthquake terrestrial or high-marsh surface and the overlying mud represents a post-earthquake marine environment. Several studies have defined criteria that a peat-mud couplet should satisfy in order to provide reliable evidence of a subduction earthquake (Nelson et al., 1996; Shennan

et al., 2016). Long subduction earthquake records have been compiled on the Cascadia subduction margin primarily from peat-mud couplets (e.g. Atwater, 1987; Witter et al., 2003) and peat-mud couplets have also been documented on the Alaska (Shennan and Hamilton, 2006; Shennan et al., 2016), Chile (Cisternas et al., 2005; Garrett et al., 2015), Japan (Fujiwara et al., 2016; Sato and Fujiwara, 2017) and Hikurangi margins (Clark et al., 2015; Hayward et al., 2016). Evidence of subduction earthquake coseismic subsidence has also been documented from the geomorphology of prograding beach ridge systems (Meyers et al., 1996; Kelsey et al., 2015b).

Coseismic uplift related to subduction earthquakes is recorded by coastal geomorphology, coral microatolls and mud-peat couplets within tidal wetland sequences (Briggs et al., 2014; Marshall and Anderson, 1995; Merritts, 1996; Ramírez-Herrera et al., 2011; Sieh et al., 2008; Shennan et al., 2014). Uplift is less commonly used as an indicator of subduction earthquakes primarily because the zone of uplift occurs closer to the trench than the zone of subsidence, and there are often fewer landmasses close to the trench.

Subduction earthquakes produce the largest tsunamis on earth and numerous studies have summarised the evidence bearing on paleotsunami deposits, including criteria that can aid in distinguishing between tsunami and storm surge sedimentary deposits (e.g. Dura et al., 2016b; Goff et al., 2012; Pilarczyk et al., 2014; Shanmugam, 2012). The concurrence of tsunami sediments and coastal deformation provides powerful evidence of past subduction earthquakes, but at some localities, tsunami sediments alone provide the record of past subduction earthquakes (e.g. Kelsey et al., 2005; Rubin et al., 2017). Submarine and lacustrine turbidites can record seismic shaking of a sufficient amplitude to trigger subaqueous slope instability and associated gravity flows. Some of the longest subduction earthquake records are from turbidites, and spatial correlation of turbidite deposits of similar age and lithostratigraphic signature means they have been used to understand earthquake behaviour and infer rupture segments (e.g. Goldfinger et al., 2012, 2013, 2017; Moernaut et al., 2018). The degree to which turbidite records are tied to subduction earthquakes varies because subaqueous sediment instability can also be triggered by upper plate fault earthquakes and non-seismic processes, but records are strengthened when turbidites are correlated to historic earthquakes or onshore evidence of subduction earthquakes.

All types of subduction earthquake evidence described above (barring coral microatolls) are found at various locations along the Hikurangi margin. An overarching challenge with the Hikurangi margin is to determine if the evidence of coastal deformation, tsunamis and turbidites relates to subduction earthquakes, or whether it may relate to upper plate faults instead.

3. Geological and geophysical characteristics of the Hikurangi subduction margin

The Hikurangi subduction margin marks the boundary between the Australian and Pacific plates at which the plates converge obliquely at rates ranging from 27 mm/yr in the south to 57 mm/yr in the north (Fig. 1). Along the North Island, plate motion is partitioned with the margin normal component occurring largely on the subduction thrust (Nicol and Beavan, 2003) and the margin parallel component accommodated by strike-slip faulting in the upper plate and clockwise rotation of the North Island fore arc (Cashman et al., 1992; Beanland and Haines, 1998; Wallace et al., 2004) At the southern end of the Hikurangi subduction margin, plate motion is transferred onto upper plate faults and there is a transition to oblique continental transpression through the Marlborough fault system. The northern end of the Hikurangi margin is marked by the northward transition from the high topography of the Raukumara Ranges into the deep (> 10 km sediment thickness, > 2 km water depth) Raukumara Basin (Bassett et al., 2010). Overthickened oceanic crust of the Hikurangi Plateau is being subducted at the margin (Davy and Wood, 1994) and the buoyancy of the Plateau is thought to drive the low rates of regional long-term uplift (~1 mm/yr) documented along the whole margin (Litchfield et al., 2007). Beneath much of the coastline of the Hikurangi margin, the plate interface lies at relatively shallow depths of 12–15 km (Fig. 1, Barker et al., 2009; Williams et al., 2013).

A number of geophysical and geological properties of the Hikurangi margin vary along-strike and these have been comprehensively described by Wallace et al. (2009). The southern Hikurangi margin is characterised by strong and deep interseismic coupling, it has a well-developed accretionary wedge and long-term tectonic contraction in the onshore forearc (Wallace et al., 2009). Between the southern and central margin is a pronounced shallowing of the contemporary interseismic coupling zone. The northern margin is characterised by shallow and weak interseismic coupling, frontal subduction erosion, numerous subducting seamounts, and a mildly extensional upper plate. A diverse array of slow slip event behaviour has been documented along the Hikurangi subduction interface (Wallace and Beavan, 2010; Wallace et al., 2012a, b; Bartlow et al., 2014). The southern part of the margin hosts deep, long duration and large slow slip events near the downdip limit of interseismic coupling (~40 km) while in the central and northern parts of the margin more frequent, short duration, small slow slip events occur at < 10–15 km depth at the downdip end of the shallow interseismic coupling zone (Wallace and Beavan, 2010).

The Hikurangi subduction margin has many active upper plate faults and their distribution, activity and style of faulting has impacts on understanding coastal deformation related to subduction earthquakes (Fig. 1). In the North Island, the North Island dextral fault system (NIDFS) is the largest fault system in the upper plate (Beanland, 1995; Beanland and Haines, 1998). Along the length of the Hikurangi margin contractional faults splay from the subduction interface and form a zone of offshore reverse faults within the accretionary wedge (Barnes et al., 2002, 2010; Pondard and Barnes, 2010; Mountjoy and Barnes, 2011). The southern end of the Hikurangi margin has the most pervasive and complex upper plate faulting. Faults of the NIDFS terminate within Cook Strait and there are complex submarine stepover zones onto the faults of the Marlborough fault system (MFS) (Pondard and Barnes, 2010; Wallace et al., 2012a, b). The faults of the MFS carry most (~80%) of the slip from the Hikurangi subduction margin into the zone of onshore oblique continental collision (Wallace et al., 2012a, b; Litchfield et al., 2014), although interpretations of the coseismic and postseismic deformation from the 2016 Kaikōura earthquake suggests that the Hikurangi subduction interface may be seismogenic in the northern South Island (Bai et al., 2017; Wallace et al., 2018; Wang et al., 2018).

4. The historical record of earthquakes and tsunamis on the Hikurangi subduction margin

Most historical earthquakes on the Hikurangi margin have been on upper plate faults but there is a sparse record of historical subduction interface seismicity (Fig. 1). The largest well-documented subduction interface earthquakes and tsunamis were the 25 March 1947 Poverty Bay (M_W 7.0–7.1) and 17 May 1947 Tolaga Bay (M_W 6.9–7.1) earthquakes in the northern Hikurangi margin (Fig. 1). These were both tsunami earthquakes (Kanamori, 1972) each with characteristic low shaking intensity relative to the moment magnitude and generation of larger than expected tsunamis relative to the earthquake magnitude (Doser and Webb, 2003). Both earthquake epicentres were shallow (< 10 km), and located near the trench on the subduction interface over subducting seamounts (Bell et al., 2014). The March 1947 earthquake generated a tsunami that affected ~120 km of coastline with maximum run up heights of up to 10–11 m above sea level recorded ~20 km northeast of Gisborne (Fig. 2). The May 1947 tsunami was slightly smaller with maximum run up height of ~6 m ~45 km northeast of Gisborne. After the 1947 earthquakes, the next largest earthquakes to have ruptured the subduction interface were the 1961 (M_W

6.4–6.5) earthquake, 40 km offshore of Cape Palliser on the southern Hikurangi margin and the 1993 M_W 5.6–6.0 Tikokino earthquake on the central part of the margin (Wallace et al., 2009). In addition there have been several M > 5 earthquakes near Gisborne, Cape Palliser, and in central Hawkes Bay that ruptured, or probably ruptured the subduction interface and Downes (2006) suggested that the 1904 M_W 7–7.2 Cape Turnagain earthquake was also on the subduction interface.

Significant upper plate fault earthquakes that have impacted the Hikurangi margin during the historic period are the 1855 M_W 8.2 Wairarapa, 1931 M_W 7.6 Hawke's Bay and 2016 M_W 7.8 Kaikōura earthquakes (Fig. 2). While each of these earthquakes had interesting characteristics in terms of what they revealed about upper plate fault behaviour and seismic hazard, here we focus on the extents of coastal deformation and tsunami generation that each earthquake produced, as these effects have implications for the interpreting the geological record of past subduction earthquakes.

The 1855 M_W 8.2 Wairarapa earthquake ruptured ~120 km of the dextral strike-slip Wairarapa fault onshore and most likely ruptured up to 40 km offshore into Cook Strait along the Wharekahau thrust and Nicholson Banks fault (Fig. 2, Grapes and Downes, 1997; Rodgers and Little, 2006; Little et al., 2009). A significant tsunami was generated with maximum observed runups of 10 m approximately 40 km east of Wellington and 4–5 m of run up around Wellington and on the northern Marlborough coast (Fig. 2, Grapes and Downes, 1997). The Wairarapa earthquake produced widespread coastal uplift across the southwestern North Island, with maximum uplift of 6 m near Turakirae Head recorded by an uplifted beach ridge and historic observations (Fig. 2). At least 40 km of the coastline parallel to the subduction margin was uplifted and the total margin-parallel extent of deformation is up to 90 km if subsidence in the lower Wairau Valley is assumed to be of tectonic origin. Subsidence of up to 1.5 m of the Wairau Valley, northeastern South Island, was recorded in historical documents, although whether this is tectonic subsidence or sediment compaction/liquefaction related remains unresolved (Grapes and Downes, 1997; Hayward et al., 2010b; Clark et al., 2015). Elastic dislocation models of the 1855 rupture that fit subsidence in the lower Wairau Valley require rupture of the deep subduction interface (~18–30 km depth) synchronous with the Wairarapa fault (Darby and Beanland, 1992; Beavan and Darby, 2005).

The 1931 M_W 7.4 (M_S 7.8) Hawke's Bay earthquake occurred on a predominantly blind reverse fault listric to the subduction interface (Hull, 1990; McGinty et al., 2001). Coastal deformation associated with the 1931 earthquake extended along a margin-parallel length of ~50 km (Fig. 2). The highest coastal uplift of 2.7 m occurred 28 km north of Napier at the Aropaoanui River mouth and moderate coastal subsidence of up to 0.7 m was recorded south of Napier. Ahuriri Lagoon was uplifted by 1–1.5 m changing the large intertidal embayment into a terrestrial surface (Hull, 1990). Despite the causative fault running offshore and certainly displacing seafloor, there was no significant tsunami generated by the 1931 earthquake. A notable aspect of the Napier earthquake is that the uplift of Ahuriri Lagoon contrasts with long-term subsidence of the site (Hull, 1986; Hayward et al., 2016).

The 2016 M_W 7.8 Kaikōura earthquake primarily occurred on a sequence of onshore and offshore upper plate faults that span the transition zone from the Hikurangi subduction margin to the continental transpressional plate boundary of the northern South Island (Fig. 2, Hamling et al., 2017; Litchfield et al., 2018a). Multiple fault ruptures crossed the coastline and the pattern of coastal deformation, spanning 100 km, was highly variable and ranged from −2.5 m to 6.5 m (Figs. 2, 3h; Clark et al., 2017). The Kaikōura earthquake generated a tsunami of significant wave amplitudes (4 m peak-to-trough at the Kaikōura tide gauge, and maximum runup of 7 m, Power et al., 2017). A much-discussed aspect of the Kaikōura earthquake is the extent to which the underlying subduction interface ruptured (summarised by Litchfield et al., 2018a). Afterslip of up to 0.5 m occurred on the subduction interface in the months following the Kaikōura earthquake, suggesting the subduction interface does accommodate plate motion (Wallace et al., 2018). Of relevance to the interpretation of marine terraces elsewhere along the Hikurangi margin, the Kaikōura earthquake showed that multiple upper plate faults can rupture synchronously and in unexpected combinations, producing variable coastal deformation along > 100 km lengths of coastline.

5. Holocene relative sea-level change in New Zealand

Relative sea level (RSL) change influences the capacity of coastal environments to preserve sedimentary and geomorphic records of past earthquakes (Nelson et al., 2009; Dura et al., 2015, 2016a; Kelsey et al., 2015a). Stratigraphic records of coseismic subsidence and tsunamis will be preferentially preserved on coastlines undergoing moderate RSL rise due to eustatic and glacio- and hydro-isostatic factors. Geomorphic evidence of coseismic uplift will be less well preserved on coastlines undergoing RSL rise as rising sea level can erode evidence of uplift (e.g. Berryman et al., 2018), but coastal wetland stratigraphic records of uplift may be well preserved under conditions of RSL rise. Understanding non-tectonic RSL change through time is essential for evaluating the completeness of the coastal deformation record along tectonically active coasts as well as for constraining the amount of coastal deformation that occurred in past earthquakes.

Holocene RSL change in New Zealand can broadly be characterised as rising in the early Holocene and reaching present mean SL by about 8000–7000 years BP (Fig. 4). This peak was followed by a mid-Holocene highstand of 1.2–3 m above present mean SL, which persisted until about 3000–2500 years BP, followed by a gradual fall in SL to the present mean SL (Fig. 4, Clement et al., 2016; Hayward et al., 2016). In detail, the amount and timing of the peak and mid-Holocene highstand are not well constrained. Hayward et al. (2016) used a compilation of sea level index points from tectonically stable parts of New Zealand to constrain the end of the mid-Holocene highstand to 2500 years BP. Clement et al. (2016) suggest that RSL likely varies around New Zealand and so argue against the amalgamation of sea level index points to form a single New Zealand-wide RSL curve. Instead, they favour a regional approach to sea level reconstructions and their northern North Island RSL compilation suggests sea level was up to 3 m higher than present, with the highstand persisting until at least c. 3000 years BP. Glacial isostatic adjustment models for northern North Island (Fig. 4), suggest a gradual fall in RSL from 3000 years BP to present, but fossil sea level indicators (molluscs) suggest RSL in northern New Zealand was at or below present between 2300 and 300 years BP (Clement et al., 2016). Hayward et al. (2016) record a late Holocene sea level fall to a lowstand of −0.6 m at c. 600 years BP and the rise to present mean SL occurred mostly with an accelerated burst of sea level rise in the 20th Century (Gehrels et al., 2008; Hayward et al., 2012a).

Non-tectonic Holocene RSL change has several implications for the completeness and accuracy of the coseismic coastal deformation record along the Hikurangi margin (Fig. 4). From c. 3000 to just prior to 600 years BP, RSL was generally falling. Therefore accommodation space in coastal environments was decreasing and there is a higher possibility during this period that evidence of coseismic subsidence may not have been preserved. This is thought to be the case at Ahuriri Lagoon, where between 2700 and 1700 years BP, unconformities within saltmarsh and estuarine sediment cores mean evidence of coseismic subsidence becomes sparser compared to the more continuous sediment records before and after the period of falling RSL (Hayward et al., 2015a). During the past 600 years, when sea level was rising, coseismic subsidence may be preferentially preserved while coseismic uplift may be eroded (Fig. 4). This appears to be the case along the Wairarapa coastline and north of Gisborne where rapid coastal erosion means only fragmentary evidence of the lowest marine terraces remain. The varying sea level trends need to be considered as the geological record of subduction earthquakes is interpreted, particularly when there appear to be large temporal gaps in the earthquake record and when amounts of coseismic vertical change are calculated.

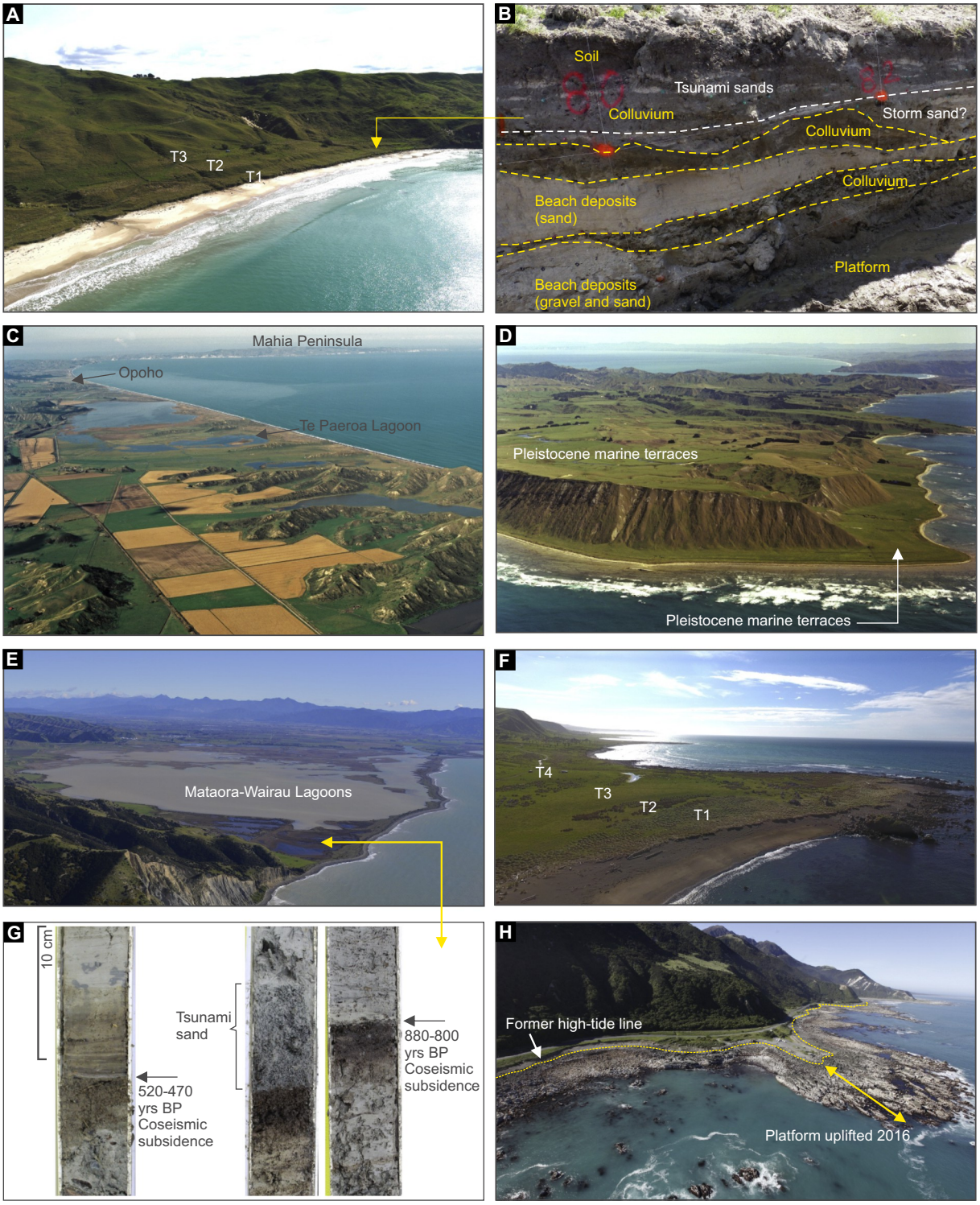

Fig. 3. Coastal tectonic geomorphology and stratigraphy of the Hikurangi margin, broadly from north to south (see Figs. 5–8 for locations). (A) Three Holocene marine terraces at Puatai Beach, northern Hikurangi margin. (B) Trench excavation across the lowest terrace (T1) at Puatai Beach, dated at 455–260 years BP (Litchfield et al., submitted). Image shows beach deposits sitting directly on a bedrock platform. Overlying the beach deposits are colluvial units and sand layers that could be storm or tsunami deposits. (C) Coastal lagoons of Te Paeroa and Opoho, central Hikurangi margin. These lagoons record Holocene coseismic subsidence and tsunamis (Cochran et al., 2006, photo by Lloyd Homer, GNS Science). (D) Pleistocene and Holocene marine terraces of Mahia Peninsula, central Hikurangi margin (photo by Lloyd Homer, GNS Science). (E) Mataora/Wairau Lagoon, transitional region. Saltmarsh sediments fringing the lagoon record coseismic subsidence in the last two earthquakes on the southern Hikurangi margin (Clark et al., 2015, photo by Graham Hancox, GNS Science). (F) Holocene marine terraces (T1-T4) at Honeycomb Rock-Glenburn area, southern Hikurangi margin. The youngest terrace here is dated at 560–410 years BP (Litchfield et al., 2013). (G) Examples of sediment cores stratigraphy from Mataora/Wairau Lagoon (E) showing the peat-mud couplets that record two past subduction earthquakes. (H) Historical coseismic coastal uplift at Paparoa Point north of Kaikōura Peninsula. This section of coastline was uplifted 3.5–5.5 m in the 2016 Kaikōura earthquake (Clark et al., 2017), the white and dark brown areas on the coastal platform is the former subtidal algae zone.

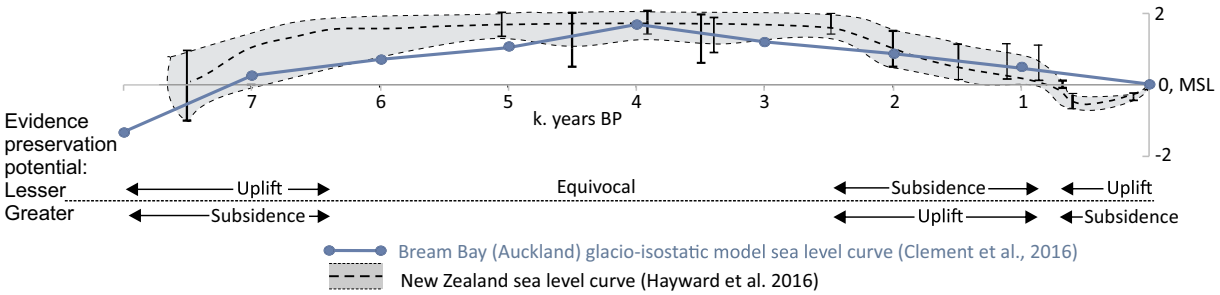

Fig. 4. Holocene sea level curves for New Zealand. The Hayward et al. (2016) curve is a compilation of Holocene sea level markers from around New Zealand. The sea level curve of Clement et al. (2016) is a glacial isostatic adjustment model prediction for northern North Island. The trend of sea level rise or fall can influence the preservation potential of coseismic coastal deformation evidence. MSL: mean sea level.

6. Marine reservoir correction for the Hikurangi subduction margin

The dominant form of age control for dating past coastal deformation on the Hikurangi margin is radiocarbon dating of marine shells. Calibrated radiocarbon ages derived from marine shells have a ~400 year reservoir correction applied to account for the offset between ^{14}C in the atmosphere and in the ocean. The 400 yr correction is a global average but there are regional and local deviations, quantified by ΔR. The regional marine reservoir correction (ΔR) for the Hikurangi margin is poorly constrained and this impacts the calibration of marine shell radiocarbon ages that are used to date past earthquakes and tsunamis. New Zealand has relatively few locally derived ΔR values and notably no values from the Hikurangi margin, except at Turakirae Head in Cook Strait (http://calib.org/marine/; Reimer and Reimer, 2001; Fig. 5a). Past studies of paleoearthquakes along the Hikurangi margin have typically used ΔR values of: 1) −30 ± 13 years (a widely accepted New Zealand average based on 11 shells growing from 1923 to 1957 CE, McFadgen and Manning, 1990); 2) 3 ± 14 years (based on 10 dates from shells that died in the 1855 CE Wairarapa earthquake, McSaveney et al., 2006); or 3) 0 years (chosen in the absence of a robust local value, Berryman et al., 2018). Individual published ΔR values around the mainland of New Zealand vary from −107 ± 61 year to 77 ± 57 years (Fig. 5a; Higham and Hogg, 1995; Hinojosa et al., 2015; McSaveney et al., 2006; Sikes et al., 2000). The variation in these values demonstrates that ΔR around the New Zealand coast is not uniform, therefore the application of the New Zealand-wide averages are inappropriate (Fig. 5a).

Efforts have been made recently to better constrain ΔR for the Hikurangi margin. Although there are still too few measurements to support either a robust ΔR value or an understanding of factors controlling variation, the new values provide a significant advance on using a New Zealand-wide average. The strategy has been to date shells from museum collections that have a known date of live collection prior to 1950 CE, avoiding post-1950s samples where interpretation of ΔR is complicated by the large temporal 14C variability induced by bomb 14C. Litchfield et al. (submitted) obtained four measurements of pre-1950s shells from Gisborne and Ruatoria (northern Hikurangi margin) and for the purposes of this review we obtained new ΔR measurements on 5 shells from Flat Point (southern Hikurangi margin) and 5 shells from Port Ahuriri (central Hikurangi margin) (Fig. 5a) [Supplementary Data 1]. The shell species selected for ΔR measurements were from tidal inlet or rocky open coast nearshore environments similar to the paleoenvironments from which shells are typically obtained for dating past earthquakes and tsunamis. This allows for equivalence between the modern specimens for which we obtain ΔR and those that we calibrate from the geological record. To calculate the average ΔR for a region from a given set of historical shell dates we use the weighted mean of the ΔR values and the uncertainty range is the 1-σ standard deviation on the ΔR values. Although a standard error yields a narrower

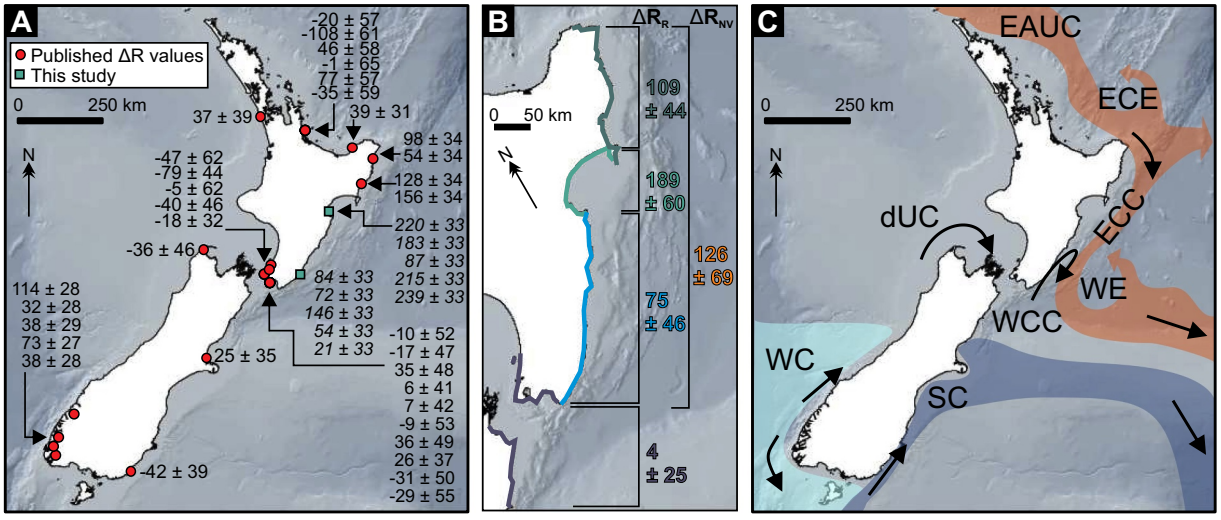

Fig. 5. (A) Marine reservoir correction values (ΔR) around the New Zealand mainland. Data sourced from the 14CHRONO Marine Reservoir Database (http://calib.org/marine/) and Higham and Hogg (1995), Hinojosa et al. (2015), McSaveney et al. (2006) and Sikes et al. (2000). (B) Locally-derived ΔR values for the Hikurangi margin used in this study. ΔR_R = regional marine reservoir correction, ΔR_{NV} = an average marine reservoir correction for the Hikurangi margin based on an assumption of non-spatially-variable ΔR. (C) Surface circulation around New Zealand from Chiswell et al. (2015). East Auckland Current (EAUC), East Cape Current (ECC), d'Urville Current (dUC), Wairarapa Coastal Current (WCC), Westland Current (WC), Southland Current (SC), East Cape Eddy (ECE), Wairarapa Eddy (WE).

uncertainty range, we do not use this as there may be variation in ΔR between the species and using the 1-σ standard deviation produces a wider spread to account for this (Coulthard et al., 2010; Hinojosa et al., 2015).

Our approach for ΔR values of the Hikurangi margin is to use locally-derived ΔR values (ΔR_R) within the region from which they were collected, but we also consider the scenario of a non-spatially-varying ΔR and provide a margin-wide average (ΔR_{NV}). Fig. 5a shows the locations from which the new ΔR values were obtained, and Fig. 5b shows the ΔR_R values that we use over four sections of the Hikurangi margin coastline. The extent of coastline over which we apply each ΔR_R is based on proximity to measurement site and on the circulation of ocean surface waters shown in Fig. 5c. Variation in ΔR along the Hikurangi margin is not unexpected given the oceanographic setting, with surface currents from the south (the Wairarapa Coastal Current, WCC) and the north (the East Cape Current) flowing along the east coast of the North Island and mixing marine water bodies with different aged carbon in a non-uniform manner (Fig. 5c, Chiswell et al., 2015). An alternative approach to using a variable ΔR_R along the margin is to contend that ΔR may be the same along the margin and therefore use a mean value of all ΔR values (ΔR_{NV}). To account for a non-varying ΔR we combine all ΔR values from Flat Point, Port Ahuriri, Gisborne and Ruatoria to yield $\Delta R_{NV} = 126 \pm 69$ years. When using ΔR_{NV} within OxCal for event age modelling we apply a uniform probability distribution to give equal weight to any ΔR values within the range. When using ΔR_R within OxCal we use the default normal distribution. Along with spatial variation, there could be temporal variation in ΔR as past climate variability and oceanic circulation changes can drive variability in ΔR at centennial to millennial timescales. Recent work in the southwest Pacific indicates that during the Holocene open ocean ΔR values have been similar to the modern day (Sikes and Guilderson, 2016), so for this study we assume modern ΔR is a reasonable representation of Holocene ΔR. However, we acknowledge that temporal variations in ΔR could have occurred and this introduces an uncertainty that we cannot quantify at this stage.

7. A review of geological evidence of past subduction earthquakes and tsunamis along the Hikurangi subduction margin

We subdivide the Hikurangi subduction margin into four regions along-strike: the transitional, southern, central and northern regions (Fig. 1, Table 1). The subdivisions align with previous divisions of the margin, based on overall characteristics of the subduction margin, historical seismicity, and distribution of interseismic coupling (Wallace et al., 2009; Stirling et al., 2012). For each region we review the geological evidence relating to past earthquakes and tsunamis, present age constraints and, where appropriate, provide revised age models. We also summarise previous interpretations on the faults that drive the coastal deformation or tsunami generation. Often there are multiple ways to interpret the cause of past coastal deformation. Fig. 6 is a conceptual illustration of various rupture scenarios for a hypothetical location along the Hikurangi margin where the subduction interface and reverse faults in the upper plate are both possible earthquake sources. The information and data compiled in this review are derived primarily from published papers and we also draw on theses, reports and peer-reviewed extended conference abstracts. At Pakuratahi Valley, Hawke Bay, we present unpublished data bearing on the age of earthquakes and tsunamis, and further information on this site is presented in Supplementary Data 2.

Radiocarbon ages are presented at the 2σ (95%) age range in calibrated years before present (years BP). For terrestrial samples, we calibrate the conventional radiocarbon age using the SHCal13 curve (Hogg et al., 2013). For marine samples, we use the Marine13 curve (Reimer et al., 2013) with the ΔR_R value as described in Section 6 and in Fig. 3B. Over 700 radiocarbon ages have been obtained from coastal sediments of the Hikurangi margin and to facilitate re-calibration and interpretation of the ages, a GIS database of all coastal radiocarbon dates (provided in Supplementary Data 3) was compiled by Dowling et al. (2018). Where appropriate we have undertaken Bayesian age modelling to constrain the ages of earthquake and tsunamis using OxCal (v4.3, Bronk Ramsey, 2009). In some cases pertaining to more recent publications our OxCal models do not differ from that in the publication (e.g. Clark et al., 2015), but in others our revision of data and use of a different ΔR value produces a different age model to that previously published (e.g. Hayward et al., 2016 and Berryman et al., 2018). The majority of OxCal models use a sequence model with phases (Bronk Ramsey, 2009). The sequence model makes no assumptions of deposition rates based on sample location and radiocarbon ages are placed in stratigraphic order, or grouped in phases when stratigraphic order is unknown. Exceptions to the sequence model are (i) lake cores, where a P-sequence model is used (deposition rate between radiocarbon ages is assumed to be random, Bronk Ramsey, 2008) and (ii) some marine terrace radiocarbon age datasets where a combine function is used to combine several similar probability distributions into a single probability distribution. All age models are presented in Supplementary Data 4. We use a generic earthquake or tsunami naming and numbering convention, with marine terraces named T1 (youngest) up to T6 (oldest), and earthquakes or tsunamis labelled Eq1/Tsu1 (youngest) up to Eq9 (Table 1).

In compiling earthquake ages from paleoseismic data there are a number of uncertainties to take into account; these can generally be separated into epistemic and aleatoric uncertainties. The aleatoric uncertainty is the statistical uncertainty associated with the calculation of the earthquake ages and is derived from uncertainties introduced by the radiocarbon measurements, calibrations, and marine reservoir corrections. The aleatoric uncertainty is quantified by the 95% highest probability density function range of the earthquake ages. Epistemic uncertainty relates to the overall interpretation of the earthquake evidence and the stratigraphic relationship between radiocarbon ages and earthquake horizons. The different influences of epistemic and aleatoric uncertainty can be demonstrated by the example of a small but sudden sea-level change recorded in a salt marsh sequence. The timing of the sea-level change could be precisely dated by radiocarbon ages that bound the change horizon (=low aleatoric uncertainty). However, there may be other reasons than an earthquake for the sudden sea-level change. Further, the radiocarbon material above the change horizon may not be in-situ and therefore provides erroneous constraint on the timing of the event (=high epistemic uncertainty). To account for the epistemic uncertainty in earthquake ages we assign each earthquake age a certainty ranking of 1 (low) to 3 (high). Our ranking combines qualitative assessments of the likelihood that the age data represents the earthquake age, and the certainty that the event in question is an earthquake (Table 2). For example, a marine terrace with a well-defined platform surface and riser is strong evidence of an earthquake, so would have an earthquake evidence ranking of 3. If the timing of uplift can be constrained by multiple radiocarbon ages from the beach sediments prior to the earthquake and tephra deposited immediately after uplift, then the quality of age control is also “high” (3), and so it would have an overall earthquake certainty ranking of 3 (high). Alternatively if the terrace age was constrained by only three ages on shells that pre-date uplift, we would assign an “average” (2) quality of age control, yielding an overall ranking of 2 (average). If the terrace age was only controlled by one shell age (age quality 1) it would have an overall ranking of 1.

7.1. Transitional region

The southern extent of the Hikurangi subduction zone is not a sharply defined boundary as there is a gradual transfer of plate motion from the subduction interface onto the transpressional crustal faults of the Marlborough Fault System (Fig. 1; Wallace et al., 2012a, b). Following the findings of Wallace et al. (2018) that afterslip following the 2016 Kaikōura earthquake occurred on the subduction interface as far

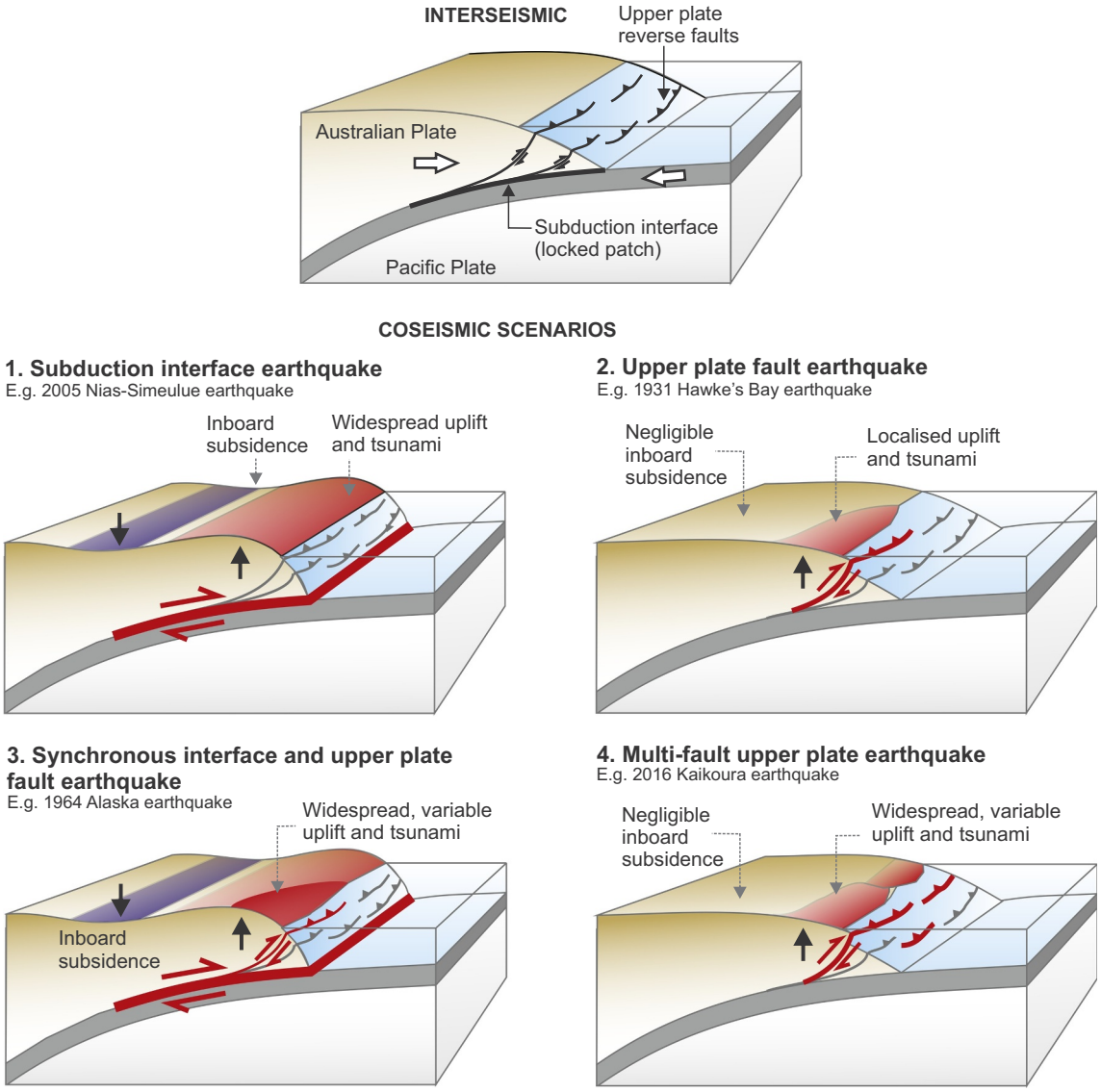

Fig. 6. Illustration of onshore vertical deformation patterns from various rupture scenarios at a hypothetical location along a subduction margin, where the subduction interface and upper plate reverse faults are both possible earthquake sources. Scenario (1): rupture of the subduction interface causes widespread upper plate deformation. Heterogenous slip on the interface can produce variability in the deformation pattern but in general the changes in deformation signal and amount occur over a long wavelength. An example is the 2005 M_W 8.7 Nias-Simeulue earthquake (Briggs et al., 2006). Scenario (2): rupture of an upper plate fault, producing localised upper plate deformation, for example, the 1931 M_W 7.6 Hawke's Bay earthquake (Hull, 1990). Scenario (3): synchronous interface and upper plate fault rupture, producing a widespread but variable deformation pattern, for example, the 1964 M_W 9.2 Alaska earthquake when the Patton Bay fault ruptured with the subduction interface (Plafker, 1967). Scenario (4): rupture of multiple upper plate faults, producing widespread and variable deformation, an example is the 2016 M_W 7.8 Kaikōura earthquake (Clark et al., 2017). The deformation produced by scenarios 3 and 4 may be particularly difficult to differentiate in the geological record.

south as beneath the Kaikōura Peninsula, we place the southern limit of our review at Kaikōura Peninsula.

At Kaikōura Peninsula a sequence of three to four Holocene marine terraces have been mapped and dated by Duckmanton (1974), McFadgen (1987), Ota et al. (1995, 1996), and Litchfield et al. (2017). Fifteen radiocarbon dates have been obtained from the cover sediments of the terraces, however they were collected from 7 different locations and terrace correlations between sites are not clear. On the basis of their stratigraphic context and reliability of location information, we selected 5 ages to place constraints on the timing of terrace uplift and we assume all shells pre-date the uplift of the terrace on which they sit (see table in page 2–3 of Supplementary Data 4). The terrace ages are (T3) 3165–1240, (T2) 1005–480 and (T1) 400–105 years BP (Table 1). These earthquakes all have a low certainty due to the poor age control. Our revision disagrees with McFadgen (1987) who suggested two earthquakes post-500 years BP, but we concur with the interpretation of Barrell (2015) that the geomorphology suggests only one terrace younger than 500 years BP. The Kaikōura Peninsula uplifted 0.8–1 m in the 2016 Kaikōura earthquake, uplift is thought to have been controlled by rupture of the offshore Kaikōura Peninsula fault, a NE-striking reverse fault (Figs. 2, 7; Clark et al., 2017). The geometry of uplift in 2016 appears to generally replicate the pattern of paleo-uplift recorded by Holocene and Pleistocene marine terraces of the Kaikōura Peninsula. We suggest the Kaikōura Peninsula fault has been the primary driver of Kaikōura Peninsula uplift in the late Holocene (Fig. 7).

Holocene marine terraces have been mapped and dated intermittently between Half Moon Bay and Cape Campbell but the radiocarbon ages are sparse and no reliable age constraints can be placed on any single paleoearthquake (Fig. 7; Litchfield et al., 2017). The radiocarbon ages were measured in the 1980's and are problematic because

Table 1
Summary of earthquake evidence along the Hikurangi margin with type of evidence, earthquake certainty ranking (see Table 2) and age.

Region	Locality	Distance along margin (km)[a]	Earthquake	Evidence	Quality of age control	Certainty of earthquake evidence	Earthquake certainty rank	Earthquake age (years BP, ΔR_R)	Earthquake age (years BP, ΔR_NV)	Most likely fault source	Other plausible fault sources[b]
Transitional	Kaikoura Peninsula	19	Eq1 (T1)	Holocene marine terrace	1	3	1	400–150	No change	Kaikoura Peninsula fault	+ subduction interface
	Kaikoura Peninsula	19	Eq1 (T2)	Holocene marine terrace	1	3	1	1005–480	No change	""	""
	Kaikoura Peninsula	19	Eq3 (T3)	Holocene marine terrace	1	3	1	3165–1240	No change	""	""
	Cape Campbell	103	Eq1 (T1)	Holocene marine terrace	1	3	1	280–140	No change	Needles fault	+ subduction interface
Southern	Mataora-Wairau Lagoon	106	Eq1	Subsidence	3	3	3	520–470	No change	Subduction interface	
	Mataora-Wairau Lagoon	106	Eq2	Subsidence and tsunami	3	3	3	880–800	No change	Suduction interface	Wairarapa fault
	Mataora-Wairau Lagoon	106	Tsu1	Tsunami	1	1	1	2010–990	No change	Unknown - numerous possible sources	
	Okupe Lagoon, Kapiti Island	234	Eq1	Subsidence and tsunami	3	3	3	620–564	No change	Rangatira fault	
	Turakirae Head	166	Eq3	Holocene beach ridge	1	3	1	2400–2090	No change	Wairarapa fault	+ subduction interface
	Turakirae Head	166	Eq5	Holocene beach ridge	1	3	1	6845–6400	No change	""	""
	Palliser, Wairarapa coast	195	Eq1 (T1)	Holocene marine terrace	1	3	1	1260–955	No change	Palliser-Kaiwhata fault	Subduction interface OR + subduction interface
	Palliser, Wairarapa coast	195	Eq2 (T2)	Holocene marine terrace	2	3	2	2115–1755	2105–1655	""	""
	Palliser, Wairarapa coast	195	Eq3 (T3)	Holocene marine terrace	1	3	1	3970–3510	No change	""	""
	Honeycomb, Wairarapa coast	230	Eq1 (T1)	Holocene marine terrace	3	3	3	560–410	560–395	Most likely fault source is uncertain - could be Palliser-Kaiwhata fault, subduction interface or an unmapped nearshore reverse fault.	
	Honeycomb, Wairarapa coast	230	Eq2 (T2)	Holocene marine terrace	2	3	2	1050–805	995–750	""	""
	Flat Point, Wairarapa coast	243	Eq2 (T2)	Holocene marine terrace	2	3	2	1590–1350	1600–1280	""	""
	Whareama, River, Wairarapa coast	270	Eq1 (T1)	Holocene marine terrace	1	3	1	2295–1775	2280–1685	""	""
	Whareama, River, Wairarapa coast	270	Eq2 (T2)	Holocene marine terrace	1	3	1	3940–3615	3920–3505	""	""
	Mataikona, Wairarapa coast	299	Eq1 (T1)	Holocene marine terrace	1	3	1	1560–1295	1555–1240	""	""

(*continued on next page*)

Table 1 (*continued*)

Region	Locality	Distance along margin (km)[a]	Earthquake	Evidence	Quality of age control	Certainty of earthquake evidence	Earthquake certainty rank	Earthquake age (years BP, ΔR_R)	Earthquake age (years BP, ΔR_NV)	Most likely fault source	Other plausible fault sources[b]
Central	Waimarama	422	Eq2 (T2)	Holocene marine terrace	1	3	1	5030–4490	4970–4400	Kidnappers/Kairakau fault	Subduction interface OR + subduction interface
	Waimarama-Cape Kidnappers	439	Eq1 (T1)	Holocene marine terrace	3	3	3	2310–2065	2305–1955	""	""
	Ahuriri Lagoon	444	Eq1	Subsidence	2	3	2	460–185	505–215	Subduction interface	Unmapped offshore reverse fault
	Ahuriri Lagoon	444	Eq2	Subsidence	3	3	3	1015–815	1020–820	""	""
	Ahuriri Lagoon	444	Eq3	Subsidence	3	1	1	1460–1140	1480–1170	""	""
	Ahuriri Lagoon	444	Eq4	Subsidence	3	3	3	1725–1545	1730–1570	""	""
	Ahuriri Lagoon	444	Eq5	Subsidence	3	3	3	2815–2405	2815–2405	""	""
	Ahuriri Lagoon	444	Eq6	Subsidence	2	1	1	4140–3475	4235–3525	""	""
	Ahuriri Lagoon	444	Eq7	Subsidence	3	2	2	5205–4625	5225–4685	""	""
	Ahuriri Lagoon	444	Eq8	Uplift within sedimentary sequence	2	1	1	5595–5015	5595–5030	Napier fault	
	Ahuriri Lagoon	444	Eq9	Subsidence	2	2	2	7260–6755	7265–6800	Subduction interface	Unmapped offshore reverse fault
	Pakuratahi Valley	460	Eq1	Subsidence and tsunami	3	2	2	910–690	983–690	Subduction interface	Unmapped offshore reverse fault
	Pakuratahi Valley	460	Eq2	Subsidence	3	3	3	1820–1620	No change	""	""
	Pakuratahi Valley	460	Eq3	Subsidence	2	3	2	3320–3105	No change	""	""
	Pakuratahi Valley	460	Eq4	Subsidence	3	2	2	4860–4455	4970–4520	""	""
	Pakuratahi Valley	460	Eq5	Subsidence	3	2	2	5855–4830	5940–4900	""	""
	Pakuratahi Valley	460	Eq6	Subsidence and tsunami	2	3	2	7010–6355	7110–6430	""	""
	Te Paeroa/Opoho	517	Eq1	Subsidence and tsunami	3	3	3	5600–5105	No change	Subduction interface	Lachlan fault
	Te Paeroa/Opoho	517	Eq2	Subsidence and tsunami	3	3	3	7250–7020	No change	""	""
	Auroa Point, Mahia Peninsula	531	T5 (Eq5)	Holocene marine terrace	1	3	1	5025–3570	5034–3621	Lachlan fault	Subduction interface OR + subduction interface
	Table Cape, Mahia Peninsula	531	T4 (Eq4)	Holocene marine terrace	3	3	3	3490–3280	3630–3330	""	""
	Table Cape, Mahia Peninsula	531	T3 (Eq3)	Holocene marine terrace	3	3	3	1795–1710	1840–1710	""	""
	Table Cape, Mahia Peninsula	531	T2 (Eq2)	Holocene marine terrace	3	3	3	1360–1120	1337–1047	""	""

(*continued on next page*)

Table 1 (*continued*)

Region	Locality	Distance along margin (km)[a]	Earthquake	Evidence	Quality of age control	Certainty of earthquake evidence	Earthquake certainty rank	Earthquake age (years BP, ΔR_R)	Earthquake age (years BP, ΔR_NV)	Most likely fault source	Other plausible fault sources[b]
Northern	Poverty Bay	565	Eq1	Uplift within sedimentary sequence	1	2	1	4710–4195	4715–4190	""	""
	Poverty Bay	565	Eq2	Subsidence	1	2	1	6115–5125	6120–5085	Unknown - nearby upper plate fault or subduction interface	
	Pakarae River	595	T2 (Eq2)	Holocene marine terrace	3	3	3	700–530	720–500	Upper plate fault (Gable End or other)	+ subduction interface
	Pakarae River	595	T3 (Eq3)	Holocene marine terrace	3	3	3	1530–1300	1560–1265	""	""
	Pakarae River	595	T4 (Eq4)	Holocene marine terrace	1	3	1	2080–1500	2090–1485	""	""
	Pakarae River	595	T5 (Eq5)	Holocene marine terrace	1	3	1	3360–2240	3448–2210	""	""
	Pakarae River	595	T6 (Eq6)	Holocene marine terrace	1	3	1	4150–3510	4160–3490	""	""
	Puatai Beach	603	T1 (Eq1)	Holocene marine terrace	3	3	3	455–260	475–145	Upper plate fault (Gable End or other)	+ subduction interface
	Puatai Beach	603	T2 (Eq2)	Holocene marine terrace	3	3	3	1160–920	1200–855	""	""
	Puatai Beach	603	T3 (Eq3)	Holocene marine terrace	3	3	3	1785–1710	1790–1710	""	""
	Puatai Beach	603	Tsu1	Tsunami	1	1	1	260–0	245–0	Unknown - nearby upper plate fault or subduction interface	
	Puatai Beach	603	Tsu2	Tsunami	1	1	1	1065–805	1100–750	""	""
	Waihau Bay	609	T2 (Eq2)	Holocene marine terrace	1	3	1	1870–1460	1870–1395	Upper plate fault (Gable End or other)	+ subduction interface
	Tolaga Bay	614	T2 (Eq2)	Holocene marine terrace	1	3	1	4595–3780	4585–3775	Unknown - nearby upper plate fault or subduction interface	

[a] Distance measured along the projection line shown in Fig. 1.
[b] "+" means additional fault source along with the fault listed in column to the left.

Table 2
Matrix table showing the relationship between the ranking of the quality of earthquake or tsunami age control and the quality of earthquake evidence, and how this results in the earthquake certainty ranking.

Earthquake certainty ranking 3 = high, 2 = moderate, 1 = low		Quality of age control		
		Good	Average	Poor
Quality of earthquake evidence	Strong	3	2	1
	Moderate	2	2	1
	Weak	1	1	1

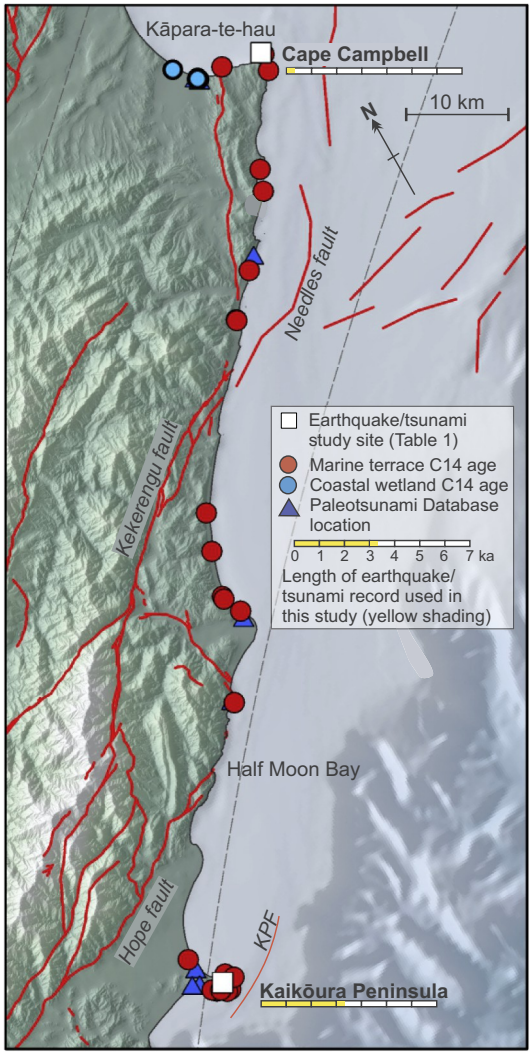

Fig. 7. Topography, active fault (red lines) and coastal deformation data locations along the transitional region of the southern Hikurangi margin. KPF: Kaikōura Peninsula fault. The white boxes show locations at which we have determined a past earthquake or tsunami age. The red and blue dots show locations at which radiocarbon dates have been obtained by past studies, and all ages are entered in a GIS database (Dowling et al., 2018 and Supplementary Data 3). The blue triangles are location entries from the New Zealand Paleotsunami Database (NZPD, 2018, accessed August 2018).

they have very large uncertainties (> ± 160 years), multiple shells were dated, and the depositional environments are unclear. Only shell ages obtained in 2017 from the lowest terrace at Cape Campbell have 2σ uncertainty ranges of < 200 years. If we assume the shell mortality was caused by earthquake uplift, then the combined age of two shells from the lowest terrace at Cape Campbell date the earthquake at 280–140 years BP (Table 1). This earthquake has a low certainty due to the sparse radiocarbon age control. Uplift of Cape Campbell in the 2016 earthquake was driven by rupture of the submarine Needles fault and it is likely that past uplift of the Cape Campbell region was also driven by Needles fault rupture (Fig. 7). Evidence to support this includes the temporal correlation between the last earthquake on the Kekerengu fault (the onshore continuation of the Needles fault, Fig. 7) dated at 249–108 years BP (Little et al., 2018) and the two radiocarbon ages from the lowest terrace at Cape Campbell (280–140 years BP).

At the Kāpara-te-hau (Lake Grassmere embayment), just 8 km northwest of Cape Campbell (Fig. 7), the Holocene record of vertical tectonics is unclear. Sediments underlying the margins of the lake have yielded several intertidal estuarine shells dating from the mid to late Holocene (Ota et al., 1995). Ota et al. inferred 1 m of uplift since 2300 (uncalibrated) years BP, and a period of non-deposition or erosion between 5200 and 2400 (uncalibrated) years BP. Once the radiocarbon ages are re-calibrated and compared to more recent sea level curves (Fig. 4) then the elevation of the estuarine shells falls within the uncertainty envelope of past sea level, suggesting no significant vertical deformation of Kāpara-te-hau over the mid to late Holocene. With existing data, the radiocarbon dating, and stratigraphic/geomorphic control at Kāpara-te-hau does not have the resolution to decipher the vertical tectonics and no coseismic events have been clearly identified.

7.1.1. Paleotsunami of the transitional region

There are very few paleotsunami records from the transitional region coastline but this is likely to reflect an absence of targeted paleotsunami studies and few sites with good preservation potential, rather than a true lack of occurrence. The coastline has been impacted by at least four historical tsunamis (post ~1840 CE) and there are pūrākau (traditional Māori narrative) of events possibly related to extreme waves (NZPD, 2018, Fig. 7). At several locations, including Kaikōura Peninsula and near Kāpara-te-hau there are indications of anomalous sand or gravel deposits overlying archaeological occupation horizons but detailed studies of the origins of the anomalous deposits have not been undertaken. It was noted by Power et al. (2017) that evidence of the 2016 Kaikōura tsunami, consisting of gravel clasts on gravel beaches and biological material that rapidly decays, had low long-term preservation potential despite runup reaching up to 7 m above tide level at the time of the tsunami. This implies the steep, rocky coastline that dominates the transitional region is generally not ideal for paleotsunami studies although the historic and archaeological records suggest the coast is prone to tsunami.

7.2. Southern region

In the southern region of the Hikurangi margin, there is clear evidence for two past subduction earthquakes and a wealth of evidence of late Holocene coastal deformation that has been attributed to upper plate fault paleoseismicity (Fig. 8). The ubiquity of upper plate faults makes this region the most complicated for disentangling past subduction earthquakes from the geological record, yet we are also fortunate that the onshore and submarine faults have been mapped in detail and there are paleoseismic records spanning the last ~1200 years on most of the major upper plate faults.

The most compelling evidence for southern Hikurangi margin subduction earthquakes comes from two peat-mud couplets at Mataora-Wairau Lagoon (called Big Lagoon by Clark et al., 2015) in the northern South Island (Fig. 8). In the southeastern corner of the lagoon, Clark et al. (2015) documented two subsided saltmarsh paleosols overlain by marine mud (Fig. 3E, G). These were interpreted as evidence of subduction earthquakes causing 0.25 ± 0.1 m and 0.45 ± 0.1 m of coseismic subsidence at 520–470 years BP (EQ1) and 880–800 years BP (EQ2), respectively (Table 1). The older saltmarsh soil was overlain by sand interpreted to have been deposited by a tsunami. EQ2 overlaps in

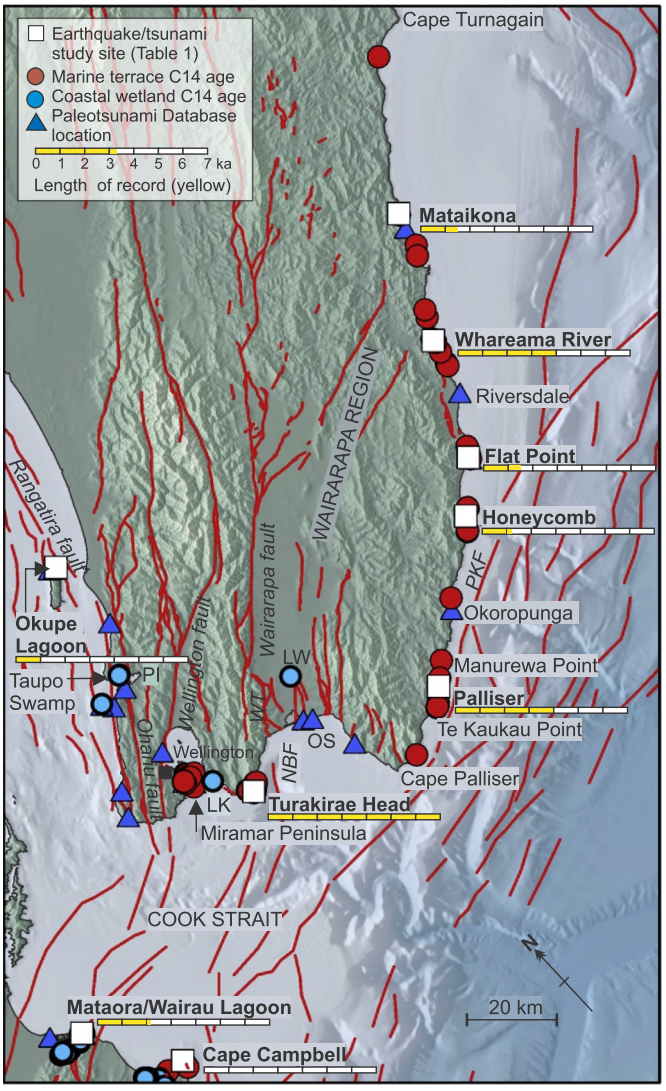

Fig. 8. Topography, active fault and coastal deformation data locations along the southern region of the Hikurangi margin. PI: Pauatahanui Inlet, LK: Lake Kohangapiripiri, WT: Wharekauhau thrust, LW: Lake Wairarapa, NBF: Nicholson Bank fault, OS: Okourewa Stream, PKF: Palliser-Kaiwhata fault.

time with the penultimate rupture of the Wairarapa fault at 920–800 years BP (Little et al., 2009). Clark et al. (2015) suggested EQ2 represented either (i) a subduction earthquake that occurred close in time, but in a separate event, from the penultimate Wairarapa fault earthquake, or (ii) a synchronous rupture of the subduction interface and Wairarapa fault. Fourteen radiocarbon ages from terrestrial organic fragments were used in a Bayesian age model to constrain the ages of EQ1 and EQ2 by Clark et al. (2015). Because a marine reservoir correction was not required in their age model and the calibration curve has not changed, we adopt the earthquake ages of Clark et al. (2015) in this review without modification.

Later work by King et al. (2017) at Mataora-Wairau Lagoon focussed on tsunami evidence and they found geochemical and diatom evidence to further support the interpretation of a tsunami associated with EQ2 and evidence of an older tsunami on which they place a maximum age of 2095 years BP. The maximum age constraint is based on two radiocarbon dates on wood from within the interpreted tsunami unit. Using minimum age constraints from Clark et al. (2015) and maximum age constraints from King et al. (2017) we can only constrain the older tsunami age to 2010–990 years BP, but the tsunami age is most likely closer to the older end of this age at c. 2000 years BP. The older tsunami has a low certainty ranking due to poor age control and uncertainty the tsunami was generated by a local fault source (Table 1).

There are no other sites in the northern South Island that duplicate the subduction earthquake evidence found at Mataora-Wairau Lagoon. Northwards from Mataora-Wairau Lagoon the coastal geomorphology changes to steep and rocky shorelines of the Marlborough Sounds and there are few sites amenable for high-resolution RSL studies. Hayward et al. (2010a) studied intertidal sediment cores from the inner Marlborough Sounds and found evidence of Holocene subsidence at rates of 0.2–2.4 mm/yr but there was no foraminiferal or sedimentary evidence for sudden, coseismic subsidence found in any cores. They concluded that Holocene subsidence of the Marlborough Sounds is most likely gradual, but acknowledged that coseismic displacements of < 0.5 m may have been below the detection thresholds of the paleoenvironments they encountered in the cores.

Okupe Lagoon, located on Kapiti Island off the west coast of the lower North Island, was recently the subject of a study aimed at constraining possible vertical deformation associated with the Hikurangi subduction margin (Fig. 8, Cochran et al., 2015). Early work at Okupe Lagoon identified marine inundation and lagoon water depth change at 716–306 years BP (based on one radiocarbon date) (Goff et al., 2000; Cochran et al., 2007). Cochran et al. (2015) replicated the tsunami and earthquake evidence and refined the earthquake age to 620–564 years BP using twelve radiocarbon ages (Table 1). They demonstrated no temporal overlap with the EQ1 identified at Mataora-Wairau Lagoon at 520–470 years, although did note evidence of weak catchment disturbance at 540–494 years BP which could have resulted from strong ground shaking. Utilising lidar topographic data, Cochran et al. (2015) identified two traces of the Rangatira fault running across Okupe Lagoon and they suggest that rupture of the Rangatira fault is the most likely explanation for the lagoon water depth change and tsunami at 620–564 years BP (Fig. 8). The age model developed by Cochran et al. (2015) for the earthquake and tsunami at Okupe Lagoon is adopted here without modification and the earthquake has a high certainty.

Around the Wellington and western Palliser Bay coastlines Holocene and Pleistocene marine terraces and coastal waterbodies record uplift that is primarily driven by reverse-dextral upper plate faults (Ninis, 2018; Cochran et al., 2007; Pillans and Huber, 1995; McSaveney et al., 2006). Although Holocene marine terraces have patchy preservation, extensive Pleistocene marine terraces show steps across the major upper plate faults: the Ohariu, Wellington and Wairarapa faults (Fig. 8, Ota et al., 1981; Ninis, 2018). Studies of two coastal waterbodies, Taupo Swamp and Lake Kohangapiripiri, show sudden changes in wetland paleoecology that are correlated to rupture of nearby upper plate faults, the Ohariu and Wairarapa faults respectively (Cochran et al., 2007). Two other coastal waterbodies, Pauatahanui Inlet and Lake Wairarapa were investigated for a record of land elevation change related to subduction earthquakes but no evidence of coseismic displacements was found (Fig. 8, Clark et al., 2011).

Uplifted Holocene shorelines around the Miramar Peninsula (Fig. 8) show evidence of eight coseismic uplift events in the past 6500 years (including the historically documented uplift of 1.35–1.5 m in the 1855 CE Wairarapa earthquake). Using shells from boreholes, Pillans and Huber (1995) estimated the penultimate uplift of the Miramar Peninsula was at 940–260 years BP. Re-calibration of shell ages they infer as “close to uplift of PS2” give an age range of 1170–470 years BP and the minimum age constraint is 485–155 years BP. The age range of this uplift event and its geomorphic evidence is too uncertain for inclusion in our earthquake compilation for the southern region. Pillans and Huber (1995) assumed SL had been stable over the 6500 years, yet we now know that relative SL has fallen since ~3000 years BP (Section 5) so it is also worth considering that evidence for a tectonic uplift of Miramar Peninsula (where it is not accompanied by strong stratigraphic or geomorphic evidence of sudden change) could be misinterpreted due to non-tectonic SL fall. Given the Miramar Peninsula uplifted in the Wairarapa earthquake, previous coseismic uplift is likely to have been

driven by the same upper plate fault.

Maximum coastal uplift of 6 m in the 1855 CE Wairarapa earthquake was recorded at Turakirae Head, southeast of Wellington (Fig. 2), and at this location three older beach ridges record prior coseismic uplift of similar or larger amounts (McSaveney et al., 2006). Radiocarbon ages on shell, peat, and wood, and ^{10}Be surface exposure dating were used to estimate the timing of the past beach ridge (BR) uplift at 2380–2060 (BR3), 5420–4110 (BR4), 6610–6920 (BR5) years BP. We consider the ages of McSaveney et al. (2006) for BR3 and BR5 are the best available to constrain the abandonment of the Turakirae Head beach ridges, and therefore focus recalibration efforts on these ages. Combining the two shell ages on the assumption they had the same time of death results in a minor change to the age of BR3 to 2400–2090 years BP. Recalibrating the terrestrial ages that constrain the age of BR5 and using the youngest of the three wood ages (rather than a weighted mean of the three) yields an age for BR5 of 6845–6400 years BP. These are maximum ages for both beach ridges as it assumes the shells and wood were living or deposited immediately prior to beach ridge uplift - the wood in particular would have an inherited age as it was not in growth position. We assign a low earthquake certainty to both earthquakes. McSaveney et al. (2006) did not directly date BR4 but instead used a slip-predictable relationship between beach ridge uplift and age, a method that we do not consider sufficiently reliable for inclusion in our earthquake age compilation because there is no independent evidence to suggest the Wairarapa fault and its offshore extensions conform to a slip-predictable earthquake behaviour model. The Turakirae Head beach ridges are all assumed to relate to rupture of the Wairarapa fault and its offshore extensions: the Wharekahau Thrust and Nicholson Bank fault, as occurred in the 1855 Wairarapa earthquake (Figs. 2, 7).

The southeastern Wairarapa coast (from Cape Palliser to Cape Turnagain) has a rich geomorphology of Holocene marine terraces (Wellman, 1971a, b; Singh, 1971; Ota et al., 1990a, b, Berryman et al., 2011, Litchfield and Clark, 2015; Litchfield et al., 2013; Fig. 3F). The most recent compilation of southeast Wairarapa Holocene terrace mapping and dating is by Berryman et al. (2011), and a short section of coastline from Honeycomb Rock to Riversdale has been the subject of a more detailed study by Litchfield et al. (2013). This review of the Holocene marine terrace chronology along the southeast Wairarapa coast makes minor changes to the terraces ages compared with Berryman et al. (2011) and Litchfield et al. (2013). The age changes are mainly due to the use of $\Delta R_R = 75 \pm 46$ years for this region, compared with previous calibrations that used $\Delta R = -30 \pm 13$. Detailed notes on the revised earthquake ages are in Supplementary Data 4; here we briefly describe the terrace chronology from southwest to northeast along the coast.

The youngest terrace (T1) in the Cape Palliser to Manurewa Point area (called Palliser, Table 1, Fig. 8) has an age of 1260–955 years BP; this age is derived from the peat sitting directly on top of the marine platform. This earthquake is assigned a low certainty due to the unknown lag time between uplift and peat formation. T2 in the Palliser area is dated at 2115–1755 years BP, the age is derived from the combined age of two shells in growth position within beach gravels on the platform. We assume the shell death was caused by coseismic uplift and this earthquake has a moderate certainty. T3 has an age of 3970–3510, based on one wood sample resting on the terrace platform; this earthquake has a low certainty due to the poor age control.

Fifteen radiocarbon ages from the youngest terrace on the Honeycomb Rock to Riversdale coastline (Honeycomb, Table 1; Figs. 3F, 7) mean this terrace has a well constrained uplift age of 560–410 years BP. The high concentration of ages on this terrace is because Litchfield et al. (2013) tested whether the terrace uplift age was similar to EQ1 at Mataora-Wairau Lagoon. When using the combined ages of 8 shell radiocarbon dates from the terrace platform and a $\Delta R = -30 \pm 13$, Litchfield et al. (2013) estimated T1 uplift occurred at 655–618 years BP. Our revised ΔR_R value and terrace age model, in which uplift immediately post-dates the platform shell ages, results in a younger terrace uplift age of 560–410 years BP which entirely overlaps with the 2σ age range for EQ1 at Mataora-Wairau Lagoon (Table 1). T2 along the Honeycomb Rock coastline has a revised age of 1051–806 years BP; this age was obtained from the combined age of two shells on the terrace platform and the earthquake has moderate certainty (Table 1). Berryman et al. (2011) correlated the T1 from the Cape Palliser-Manurewa Point area with T2 at Honeycomb Rock. Our calibration of the Honeycomb T2 shell ages places them younger than the Palliser T1 age and we no longer consider that the two terraces represent the same earthquake (although there is a small amount of overlap at the 2-σ age range). T2 terrace at Flat Point is slightly older than T2 at Honeycomb Rock and has a revised age of 1590–1350 years BP, based on the combined age of two shells in growth position on the terrace platform; this earthquake has a moderate certainty.

The revised terrace ages for the Whareama River (T1 and T2), Mataikona River (T1), and Cape Turnagain (T1) areas are ~100 years younger than the terrace ages presented by Berryman et al. (2011), with the age difference only due to the revised ΔR_R. Each terrace has a low earthquake age certainty because we select only one shell from near or resting directly on the terrace platform to constrain the time of uplift (Table 1). We assume the shell death was caused by coseismic uplift, an assumption better justified when there is an assemblage of similarly aged shells which in these cases we do not have. The recalibrated age for the shell at Cape Turnagain is mostly within the historic period, and there is no historical evidence for uplift there, so we consider this age to be unreliable.

In summary, nine past earthquakes that caused coseismic uplift of the southeast Wairarapa coast have been dated using radiocarbon ages from Holocene marine terraces (Table 1). There are many more terraces that have not been dated. Berryman et al. (2011) provide reconnaissance-level terrace mapping and dating which provides a valuable framework but Litchfield et al. (2013) demonstrate the increased certainty that can be placed on earthquake ages when targeted studies are undertaken. The recent acquisition of LiDAR from along the Wairarapa coast offers opportunity to improve the terrace mapping and better understand the faults driving uplift.

Marine terrace uplift along the southeast Wairarapa coast is usually attributed to offshore upper plate reverse faults (i.e. scenario 2 in Fig. 6; Berryman et al., 2011, Litchfield et al., 2013, Litchfield and Clark, 2015). Currently much of the reasoning for upper plate fault causation is the limited margin-parallel extent of the terraces. The maximum along-margin extent of a single terrace is ≤50 km (according to correlations by Berryman et al., 2011) and subduction earthquakes are speculated to cause greater extents of upper plate deformation (i.e. scenario 1, Fig. 6). Berryman et al. (2011) also reason that subduction earthquake deformation should be elastic and recovered during the interseismic period, while the permanent deformation recorded by the terraces is consistent with an upper plate mechanism.

Reasons to consider the southeast Wairarapa marine terraces could have been uplifted by subduction earthquakes include the absence of mapped nearshore faults along part of the coast (Fig. 8), the possibility of heterogeneous interface rupture producing small patches of high uplift, and the likelihood of synchronous upper plate-interface rupture (scenario 3, Fig. 6). From Cape Palliser up to Honeycomb Rock, the Palliser-Kaiwhata fault is located relatively close (3–6 km) to the coastline (Fig. 8, Barnes and Mercier de Lepinay, 1997; Barnes et al., 1998) and is a plausible causative fault for marine terrace uplift. However, north of Honeycomb Rocks nearshore upper plate faults have not been mapped (the faults mapped by Berryman et al. (2011) are inferences based on marine terrace data). There is no significant decrease in terrace occurrence or elevation north of Honeycomb Rocks suggesting either undocumented upper plate faults do exist or an alternative fault source, such as the subduction interface, drives uplift. The reasoning that a subduction earthquake would uplift greater extents of the coast than an upper plate fault could be reconsidered: heterogenous interface slip could produce localised coastal uplift and

patches of uplift separated by regions of negligible coastal change (e.g. Jara-Muñoz et al., 2015). Furthermore, the likelihood that upper plate reverse faults rupture synchronously with the subduction interface should be considered. The relatively shallow depth of the interface (< 15 km) beneath the offshore reverse faults of the Wairarapa coast could imply strong connectivity between the crustal faults and the interface, so synchronous (or closely spaced in time) rupture is a very plausible scenario. Untangling a subduction earthquake signal from the SE Wairarapa marine terraces may be complicated, but we contend that the terraces cannot be uniquely assigned to an upper plate fault signal and future studies should give greater consideration of subduction interface involvement in terrace uplift.

7.2.1. Paleotsunami of the southern region

The southern region of the Hikurangi margin has a rich paleotsunami record compared to other parts of the margin, with two tsunamis associated with coseismic coastal subsidence and several sites with only paleotsunami evidence (Fig. 8). Paleotsunamis associated with coastal deformation have been found at Mataora-Wairau Lagoon (Clark et al., 2015; King et al., 2017) and at Okupe Lagoon (Cochran et al., 2015). The NZPD lists 49 sites on the western side of Cook Strait and most of these are related by Goff and Chagué-Goff (2015) to a regionally significant paleotsunami in the 15th century. On the eastern side of Cook Strait, around the Wellington and Wairarapa coasts, there are surprisingly few paleotsunami records given the number of offshore faults and tectonic activity evident from the coastal deformation.

Paleotsunami studies on the western side of Cook Strait hint at a regional paleotsunami at ~1470–1510 CE (Goff and Chagué-Goff, 2015) although the tsunami source is unknown and we suggest there is low confidence the data relates to one event given the poorly-dated evidence. This region overlies the deep part of the Hikurangi subduction interface (> 30 km deep) and a large subduction earthquake could generate a tsunami either by vertical displacement of the seafloor west of Cook Strait or through propagation of a large tsunami from east to west through Cook Strait. Submarine upper plate faults are present on the western side of Cook Strait but they have relatively low rates of activity and relatively modest estimated maximum magnitudes of M_W 5.7–7.5 (Fig. 1, Nodder et al., 2007). Goff and Chagué-Goff (2015) point to eight key sites for evidence of the 1470–1510 CE paleotsunami. Of these eight sites, four sites have radiocarbon age data and the remaining four are dated by correlation to other sites or constrained as post-Maori occupation by archaeological horizons. One of the key sites is Okupe Lagoon, which we have discussed above. The refined earthquake and tsunami age for Okupe Lagoon at 620–564 years BP (1330–1386 CE) predates the 1470–1510 CE regional paleotsunami by c. 100 years. We acknowledge a wealth of evidence suggests a widespread coastal disturbance event post-Maori occupation on the western side of Cook Strait but chronological control to substantiate the correlation of region-wide tsunami evidence is lacking. The recent recognition of an active fault running through Okupe Lagoon (Cochran et al., 2015) demonstrates that local earthquake sources can cause local-scale disturbances which could be mis-correlated to regional signals when the age constraints are poor.

Along the Wellington and Wairarapa coasts there are 16 sites in the NZPD, but three relate to historical tsunamis and, of the remaining 13 sites, only two sites have a high validity status (according to the evidence ranking system employed by the NZPD) along with accompanying radiocarbon age data for chronological control. At Okourewa Stream, on the south Wairarapa coast (Fig. 8), a gravel layer that reaches 1.4 km inland with shell and marine microfauna, is interpreted as a tsunami deposit. The age constraints on this unit place it between ~1400 years BP and 1890 CE, so it may relate to the 1855 CE tsunami or an earlier event (Goff et al., 1998). At Okoropunga on the southeastern Wairarapa coast, an extensive sand layer overlying Māori horticultural features is attributed to tsunami deposition (Fig. 8, Goff et al., 2004). The only age constraints are two charcoal ages from the archaeological layers below the sand (McFadgen, 1980), and recalibration of these ages places the tsunami at < 500–280 years BP. Due to the large age uncertainties, neither of these paleotsunamis are added to our event age compilation for the southern region. There are many other paleotsunami records on the Wellington and Wairarapa coasts but they lack age control (for example, 11 sites in the NZPD without site-specific age control), and additionally Berryman et al. (2011) noted that shells of anomalously young ages for their elevation were found at Honeycomb Rock, Flat Point, Te Kaukau Point and Whareama River (Fig. 8). The anomalously young shells were signalled as potentially tsunami deposits, particularly because their ages coincided with terrace uplift ages from nearby locations, but studies of the depositional units around the shells were not undertaken. We don't include these shells in the event age compilation because there is not sufficient evidence they are, in fact, tsunami deposits. The lack of paleotsunami deposits along the Wellington and Wairarapa coast is likely a function of a lack of targeted studies and few ideal depositional environments (most of the coast is steep and rocky), rather than a lack of tsunami occurrence.

7.3. Central region

The central region of the Hikurangi margin encompasses a margin-parallel coastline with intermittent preservation of marine terraces (south of Cape Kidnappers and at Mahia Peninsula; Fig. 3D) and the large margin indentation of Hawke Bay where coastal lagoons (Fig. 3C) record the longest records of subduction earthquakes preserved along the Hikurangi margin. The transition zone from strong to weak interseismic coupling on the subduction interface occurs at the boundary between the southern and central regions, near Cape Turnagain (Fig. 1, Wallace et al., 2012a, b). Consequently, changes in the characteristics of subduction zone paleoseismology north and south of the locking transition is of particular relevance for understanding how past large earthquake rupture patches relate to the contemporary deformation of the plate interface.

The embayment of Porongahau, 20 km north of Cape Turnagain (Fig. 9), has a mixed history of Holocene vertical deformation with uplift in the west and subsidence in the east, but no identified coseismic displacements. Hayward et al. (2012b) collected 5 sediment cores across the Porongahau coastal plain and obtained four radiocarbon ages from the Holocene marine sediments underlying the plain. There may be potential to improve the Holocene vertical history of Porongahau as the existing cores are sparse for the extent of the coastal plain.

From Blackhead to Cape Kidnappers, a distance of 66 km, there is very patchy preservation of 1–3 Holocene marine terraces that most likely relate to uplift on the Kidnappers or Kairakau reverse faults located 4–12 km offshore (Fig. 9, Ota et al., 1990a, b; Miyauchi et al., 1989; Paquet et al., 2009; Mountjoy and Barnes, 2011). At Blackhead, Aramoana, and Pourere up to three marine terraces are preserved but only four radiocarbon ages have been obtained, and there are too few dates to derive robust earthquake ages from this site (Ota et al., 1990b). At Waimarama, ten radiocarbon ages have been obtained from across two terraces (Miyauchi et al., 1989; Hull, 1987). Ages from the older terrace, T2, have a spread of > 1500 years but if we assume the youngest age approximates terrace uplift then the earthquake occurred at 5030–4490 years BP; this earthquake has a low certainty due to the poor age control (Table 1). From the 11 ages on T1 between Waimarama and Cape Kidnappers, five ages cluster at the younger end of the age distribution and we suggest this cluster records the timing of uplift. A combined age for these five shell radiocarbon ages is 2310–2065 years BP; we assign a moderate certainty to this earthquake (Table 1).

One of the longest, and likely most complete, records of coseismic subsidence along the Hikurangi margin has been obtained from Ahuriri Lagoon, near Napier (Fig. 9), where 8 subsidence events and two uplift events are recorded within the ~7000 year history of lagoon infilling (Hull, 1986; Hayward et al., 2006, 2016). In 1931 Ahuriri Lagoon was

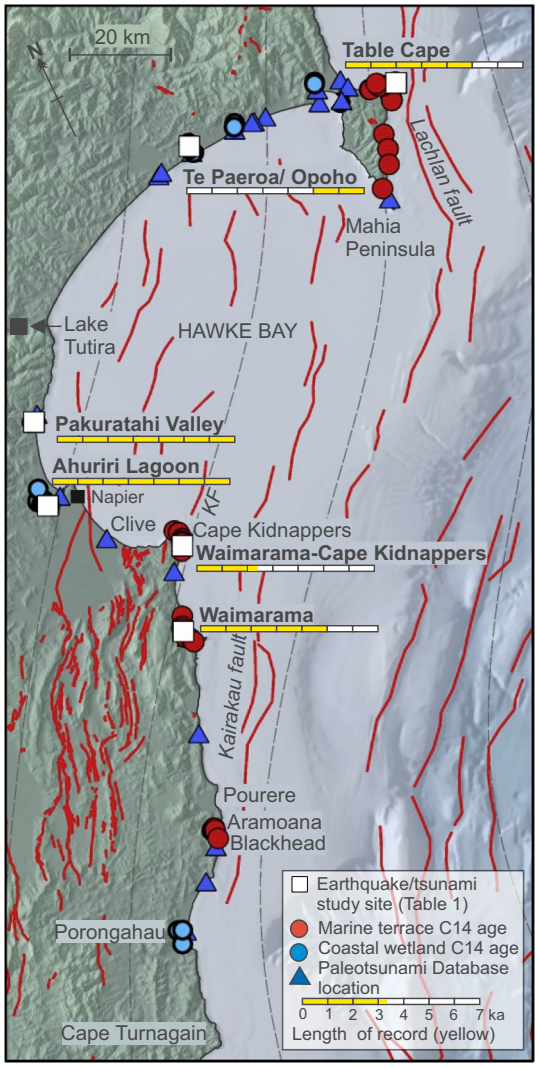

Fig. 9. Topography, active fault and coastal deformation data locations along the central region of the Hikurangi margin. KF: Kidnappers fault.

uplifted 1–1.5 m by rupture on a blind thrust fault (Fig. 2, Hull, 1990), but prior to this the lagoon had a vertical history dominated by co-seismic subsidence. The most recent study of Ahuriri Lagoon coseismic subsidence is by Hayward et al. (2016) who documented 10 past earthquakes using the foraminifera records of relative sea-level change across 45 sediment cores. The record is complex with the margins of the lagoon changing rapidly in time and space so that unconformities are common and any single core rarely contains evidence for more than four earthquakes. Hayward et al. (2016) provides a ranking of the strength of evidence for each past earthquake, ranging from weak to strong evidence and 33 radiocarbon ages and 3 tephras constrain the Bayesian age model of earthquake ages. We adopt the Hayward et al. (2016) age model with minor modification (we identified two outliers, see age model in Supplementary Data 4) in this review but use the $\Delta R_R = 189 \pm 60$ years obtained from shells collected prior to 1931 in Port Ahuriri (as Ahuriri lagoon was called prior to uplift). This shifts the earthquake ages slightly younger and broadens the age range due to the increased uncertainty margin on the ΔR value compared to the value of -30 ± 13 used by Hayward et al. (2016). The revised earthquake ages, and our assessments of the earthquake certainty are in Table 1.

Coseismic subsidence at Ahuriri Lagoon is inferred by Hayward et al. (2016) to be driven by subduction earthquakes, based largely upon temporal correlation to coastal deformation at widely-spaced sites along the Hikurangi margin. The inboard position of Ahuriri Lagoon (~150 km margin-normal distance from the trench and 20 km above the plate interface, Fig. 1) mean it is feasible it would subside in large subduction earthquakes, and forward elastic dislocation models support this (Fraser et al., 2013). Furthermore, an upper plate fault in a location capable of causing subsidence at Ahuriri Lagoon and with a slip rate sufficiently high to generate large earthquakes at recurrence intervals of ~1000 years, has not yet been identified despite reasonably dense seismic surveys within Hawke Bay (Paquet et al., 2009).

Coseismic subsidence is also recorded within sediment cores from Pakuratahi Valley, 15 km north of Ahuriri Lagoon, and at this location two of the six recorded earthquakes are accompanied by evidence of tsunami inundation (Fig. 9, Supplementary Data 2). The sediment and microfossil record found within three cores and a riverbank outcrop, shows reversals in paleoenvironment in a sequence that otherwise transitions from marginal marine to freshwater as the valley filled in over the past 7000 years. Six paleoearthquakes are identified and characterised by a sudden rise in relative sea level and/or increase in salinity (Supplementary Data 2). Bayesian age modelling incorporating 17 radiocarbon dates from shell and terrestrial organic fractions, and two tephras constrains the six earthquakes ages (Table 1). Like Ahuriri Lagoon, the most likely cause of subsidence at Pakuratahi Valley is a subduction earthquake.

In northern Hawke Bay, the coastal lagoons of Te Paeroa and Opoho hold records of coseismic subsidence and tsunamis (Figs. 3c, 8, Chagué-Goff et al., 2002; Cochran et al., 2006). In a detailed paleoecological study, Cochran et al. (2006) describe the sedimentary signatures of the events as "sudden interruptions of coarse-grained, marine-derived units associated with thick packages of chaotically mixed, reworked sediment from various sources across the coastal plain and little change in elevation from pre- to post-event paleoenvironments". Of note is the rapid infilling of accommodation space after the earthquake because post-event sediment reworking impacts the ability to constrain the earthquake ages. The Cochran et al. (2006) study has a wealth of radiocarbon age data but was undertaken prior to routine use of Bayesian age modelling. We construct age models for each Te Paeroa and Opoho core individually, enabling a more robust identification of radiocarbon dates from reworked material because the stratigraphic position is known (as opposed to constructing a composite chronological model by merging cores when the stratigraphic relationships are not known). The most reliable constraint on the oldest earthquake (Te Paeroa/Opoho Eq1) is obtained from Te Paeroa Core 1 and from Opoho cores 1 and 2. We combine the earthquake ages from each of these cores to obtain an age of 7250–7020 years BP for Eq1 (Table 1, see details in Supplementary Data 4). The age for Te Paeroa/Opoho Eq2 is most reliably obtained from Te Paeroa core 3 and is dated at 5600–5105 years BP (Table 1). The high-resolution paleoenvironmental data and age control mean both Eq1 and Eq2 have a high certainty.

Lagoon infilling and increasing isolation from the sea mean that after ~5000 years BP, Te Paeroa and Opoho have paleoenvironments dominated by freshwater and alluvial/dune systems which are not as sensitive for recording vertical coastal deformation. Chagué-Goff et al. (2002) noted evidence of a possible saltwater influx to Te Paeroa Lagoon just after deposition of the Waimihia tephra (3401 ± 108 years BP; Lowe et al., 2013) but the nature of the event was not explored in detail. The cause of coseismic subsidence and tsunami at Te Paeroa and Opoho could be rupture of the Lachlan fault (a listric reverse fault offshore of Mahia Peninsula, Fig. 9, Barnes et al., 2002) and/or a subduction earthquake (Cochran et al., 2006). Dislocation models by Fraser et al. (2013) show negligible subsidence at Te Paeroa and Opoho due to Lachlan fault rupture and significantly more subsidence due to a subduction interface rupture, suggesting the subduction interface is a more likely driver of subsidence at Te Paeroa and Opoho than the Lachlan fault.

Directly east of Te Paeroa and Opoho is Mahia Peninsula, where well-preserved sequences of Pleistocene and Holocene marine terraces (Fig. 3D) record coseismic uplift (Berryman, 1993a, b; Berryman et al.,

2018). The most recent compilation of marine terrace ages is in Berryman et al. (2018), who describe and date samples from trenches exposing the coverbeds of four terraces at Table Cape. Fifty one radiocarbon ages and two airfall tephras provide age control on terrace uplift. We adopt the Bayesian age model provided by Berryman et al. (2018) but use $\Delta R_R = 109 \pm 44$ years. Compared with Berryman et al. (2018) the ages of the third and fourth terraces remain essentially the same because they are bounded by tephra ages (Table 1). The second terrace age (Eq2) is refined to 1360–1120 years BP and the lowest terrace (Eq1) has an age of < 102 years BP. The modelled age of the lowest terrace places the terrace uplift within the historic period and yet there is no written record of an earthquake at Mahia Peninsula. To explain this very young terrace age either many shells on the lowest terrace post-date terrace uplift or the ΔR_R value is too high. We assign a high certainty to the earthquakes that uplifted terraces T2, T3 and T4 but do not use the age of T1 as it is unreliable. There is a 5th Holocene terrace on Mahia Peninsula but the age is only constrained by two radiocarbon dates at Auroa Point (Berryman, 1993b). Assuming the two dates are a maximum age for the terrace and a minimum age is provided by radiocarbon dates on the fourth terraces at Table Cape yields a broad terrace uplift age of 5025–3570 years BP. Due to the poor age control on T5, we assign this a low earthquake certainty. Uplift of the Mahia Peninsula Holocene terraces is assumed to be driven by earthquakes on the Lachlan fault (Fig. 9, Barnes et al., 2002, e.g. scenario 1 in Fig. 6). However, forward elastic dislocation models by Cochran et al. (2006) and Fraser et al. (2013) show that subduction earthquakes could also produce uplift at Mahia Peninsula (e.g. scenario 2 in Fig. 6).

Situated 85 km west of Mahia Peninsula and 30 km above the subduction interface is Lake Tutira (Fig. 9). A 37 m-long lake sediment core archives a continuous record of mass-transport deposits, tephra and autochthonous muds that spans the last ~7000 years (Orpin et al., 2010). 119 'homogenites' composed of fining upwards, largely autochthonous, silty clays are inferred to be formed by earthquake triggered subaqueous mass-wasting (Orpin et al., 2010; Gomez et al., 2015). Triggering earthquakes are inferred to generate shaking of Modified Mercalli Intensity (MMI) VII or greater at the lake site. Hence, Lake Tutira provides an integrated record of seismicity for the wider Hawkes Bay region with onshore and offshore upper plate faults, along with the subduction interface capable of generating a signal in the lake.

Chronology for the earthquake triggered homogenites in Lake Tutira is derived from linear interpolation between 17 Holocene tephra deposits identified in the sedimentary sequence. The age model provides very precise earthquake ages with 2σ uncertainties ranging from ± 2 to ± 210 years. Event based correlations between a subset of homogenite ages and the records of coseismic coastal subsidence and marine terrace uplift from Hawke Bay have been used to tentatively argue that Lake Tutira archives subduction interface and Lachlan fault earthquakes (Gomez et al., 2015). However, these event correlations are problematic because more than one homogenite in Lake Tutira correlates with the paleoearthquake age distributions. The problematic nature of these correlations are compounded by the Tutira age model itself. The use of strictly linear interpolation between tephra ages based on the assumption of constant autogenic sediment accumulation between events produces overly prescribed earthquake age uncertainties. Remodelling of the Tutira age model using a Bayesian approach that allows for variation in autogenic sediment accumulation (Bronk Ramsey and Lee, 2013) provides more realistic 2σ uncertainties that range from ± 3 to ± 412 years, which are twice that of the age model derived by linear interpretation (Fig. S4e). We acknowledge that the Tutira record probably records shaking from large subduction interface earthquakes in addition to a wide range of other fault sources. Given the non-unique correlations between earthquakes triggered homogenties in the lake records and other paleoseismic data we do not consider it further in the current review because it currently lacks the chronological precision required to inform the timing of subduction earthquake. Despite the low precision chronology, the Tutira paleoseismic record demonstrates time-independent (poissonian) recurrence large earthquake on the fault network in the Hawke's Bay region.

7.3.1. Paleotsunami of the central region

The central region of the Hikurangi margin has a relatively sparse record of paleotsunamis with most detailed studies coming from lagoons around Hawke Bay where paleotsunamis occur in association with lagoon subsidence (Fig. 9, Chagué-Goff et al., 2002; Cochran et al., 2006). Many sites in the NZPD relating to the central region coastline have preliminary and poorly dated evidence of paleotsunami, for example, pebbles in sand dunes or gravel layers separating Māori occupation horizons (NZPD, 2018; Goff, 2008). Such information is indicative of coastal disturbance but requires further study to confirm a tsunami origin and improved chronological control. Studies of paleotsunami were undertaken by Goff (2008) at Clive and Porongahau in an effort to improve the paleotsunami record of the Hawke Bay region. Sediment cores revealed anomalous sand layers with four possible tsunami deposits identified at Clive and three at Porongahau over the past ~5000 years but no events are sufficiently well dated to include in the tsunami age compilation. The sparse record of paleotsunamis in the central region is most likely a reflection of few detailed studies with appropriate age control. Of particular note is the lack of evidence to date of paleotsunami within Ahuriri Lagoon, despite its long record of coseismic subsidence. Studies at Ahuriri Lagoon have targeted the inland margins of the inlet for land level change studies (Hayward et al., 2016), but such sites are not optimal for paleotsunami study. Further seaward and/or deeper parts of the former lagoon may hold better potential for preserving paleotsunami deposits than the landward margins.

7.4. Northern region

The Raukumara Peninsula displays diversity in style and rates of coastal deformation: the highest uplift rates along the margin are at Puatai Beach; subsidence is recorded at Poverty Bay; and long stretches of the northern coast hold no records of Holocene coseismic deformation (Fig. 10, Ota et al., 1992; Clark et al., 2010). Contemporary earthquake behaviour on the northern margin is also quite diverse: slow slip events with equivalent moment releases of Mw 6.3–6.8 occur every ~2 years offshore of Gisborne (Wallace and Beavan, 2010), yet in 1947 the two largest earthquakes on the subduction interface occurred near the trench generating tsunamis with runup up to 11 m.

The Poverty Bay Flats near Gisborne are tilted, with Holocene uplift in the east and subsidence in the southwest (Brown, 1995; Berryman et al., 2000; Hayward et al., 2015b), but the tectonic structure driving this tilting is not well understood. In the region of subsidence, Hayward et al. (2015b) obtained 23 sediment cores extending to 5.5 m depth and back to 6000 years BP. The sediment cores showed evidence of two coseismic vertical movements - one uplift and one subsidence. The age constraints on each coseismic event are relatively sparse but we concur with the age model presented by Hayward et al. (2015b), only modifying the marine reservoir correction to $\Delta R_R = 109 \pm 44$ years. The earthquake causing coseismic subsidence occurred at 6115–5125 years BP and the coseismic uplift occurred at 4710–4195 years BP. We consider both of these earthquakes to have low certainty due to the relatively weak paleoenvironmental evidence for the coseismic displacements, and the sparse age control. The fault driving the uplift and subsidence at western Poverty Bay is unknown; no active faults have been identified proximal to Poverty Bay onshore or offshore (Fig. 10). Hayward et al. (2015b) speculate a subduction earthquake could have caused the subsidence, while an upper plate fault or a subduction interface rupture could have caused uplift.

At Pakarae River mouth and Puatai Beach, sites separated by ~9 km, high uplift rates (> 3 mm/ yr) are manifest by a well-defined Holocene marine terraces (Fig. 3A) that have been extensively studied

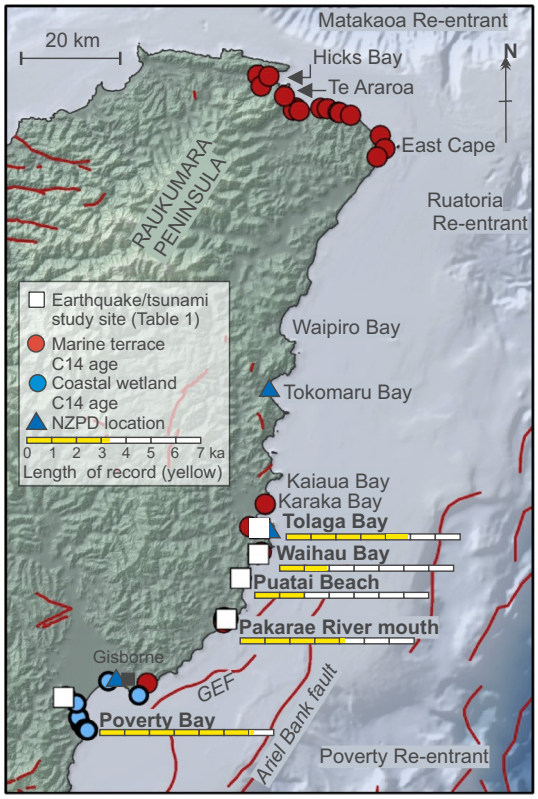

Fig. 10. Topography, active fault and coastal deformation data locations along the northern region of the Hikurangi margin. GEF: Gable End fault (existing mapping of Mountjoy and Barnes (2011), see Litchfield et al. (submitted) for revised offshore fault mapping).

(Fig. 10, Ota et al., 1991; Berryman et al., 1992; Wilson et al., 2006; Litchfield et al., 2010, 2016, submitted). The most recent and highest-resolution study of the Pakarae and Puatai terraces comes from Litchfield et al. (2016, submitted) who excavated trenches across the lowest three terraces at each location (e.g., Fig. 3B). Multiple shell radiocarbon ages from beach sediments on each terrace, coupled with tephra within the non-marine cover sediments and complete exposure of the stepped terrace strath resulted in well-constrained earthquake ages at each site. Litchfield et al. (submitted) used the same $\Delta R_R = 109 \pm 44$ years that we use in this study so we have not modified their earthquake age model. The earthquake ages at Puatai Beach are: T3: 1785–1710 years BP; T2: 1160–920 years BP; T1: 455–260 years BP (Table 1). The earthquake ages obtained from terrace trenches at Pakarae are: T3: 1530–1300 years BP; T2: 700–530 years BP and T1 could not be dated with any confidence (Litchfield et al., submitted). The older terraces at Pakarae have previously been dated by Ota et al. (1981) and Wilson et al. (2006). Using a Bayesian model that assumes uplift occurred after deposition of the dated shells on each terrace, and before deposition of shells on the next lowest terrace, we obtain broad terrace age ranges of: T4: 2080–1500 years BP; T5: 3360–2240 years BP; T6: 4150–3510 years BP. A further 4 km north of Puatai Beach, is Waihau Bay where three or four marine terraces were recorded by Ota et al. (1981). Two identical shell radiocarbon ages of 1870–1460 years BP were obtained from the second lowest terrace and we adopt this as the T2 earthquake age but assign a low certainty.

Uplift of the Pakarae-Puatai area is thought to be driven by near-shore upper plate faults, such as the Gable End fault (GEF on Fig. 10, Litchfield et al., 2010, submitted; Mountjoy and Barnes, 2011). Rupture of the subduction interface could produce uplift at Puatai and Pakarae, but the patch of interface rupture would need to be relatively large to produce the 2–3 m of uplift recorded at Pakarae and Puatai, and therefore would cause uplift at both sites synchronously (for example, see dislocation models in Litchfield et al., 2010). The temporal offset in earthquake ages between Puatai and Pakarae is more consistent with the heterogenous uplift pattern expected from a segmented, nearshore upper plate faults.

At multiple locations between Tolaga Bay and Hicks Bay (90 km apart) Holocene marine terraces are present and attest to tectonic uplift, although the driver of uplift, and whether it is driven by earthquakes or aseismic, gradual processes is currently unresolved (Wilson et al., 2007a; Ota et al., 1992). Ota et al. (1992) describe 2–3 Holocene marine terraces at Tolaga Bay, Kaiaua Bay, Karaka Bay, Tokomaru Bay and Waipiro Bay (Fig. 10). The ages are sparse however, so, with the exception of Tolaga Bay, we consider the ages of coseismic uplift events cannot be determined with any useful degree of certainty. At Tolaga Bay, three terraces have been identified. The middle terrace, T2, has three shell radiocarbon ages that pre-date uplift and a post-uplift wood age and Waimihia tephra. These age constraints yield an earthquake age of 4595–3780 years BP; we assign a low certainty to this earthquake age to reflect the sparse radiocarbon ages (Table 1). Terraces T1 and T3 at Tolaga Bay do not have sufficient age control to obtain an earthquake age.

The coastline between East Cape and Hicks Bay has multiple marine terraces, uplifted beach ridge sequences and uplifted early Holocene transgressive estuarine sequences (Fig. 10). These coastal geomorphic features all attest to high late Quaternary uplift rates (up to 3 mm/ yr), however it is not certain that large earthquakes drive the coastal uplift (Wilson et al., 2007a, b; Clark et al., 2010). Several shell radiocarbon ages have been collected from the marine terraces between Te Araroa and East Cape but no sites have sufficient dates to constrain the timing of coseismic uplift. Five shells collected from four sites on the lowest marine terrace have ages ranging from 1140 to 760 years BP to < 240 years BP, and from the second terrace only one age of 955–655 years BP. Clark et al. (2010) suggest uplift of the East Cape to Hicks Bay coastline is due to gradual and aseismic process driven by sediment underplating. The suggestion of gradual uplift largely rests upon the absence of evidence for large coseismic events, for example, no large steps in the beach ridge sequence at Te Araroa, no sudden paleoenvironmental changes in the estuarine sequence at Hicks Bay, and poorly defined marine terrace geomorphology (Wilson et al., 2007a). However, it is possible that small but frequent coseismic uplift could drive uplift of the East Cape region, with uplift amounts below the threshold detectable (i.e. < 0.85 m vertical movement) with the paleoenvironmental methods used by Wilson et al. (2007a). For the purposes of this review, the inability to derive a reliable terrace uplift age coupled with uncertainty about the tectonic mechanisms driving uplift mean we have not defined any earthquake ages for the East Cape to Hicks Bay section of coastline.

7.4.1. *Turbidite records of the northern Hikurangi margin*

The northern Hikurangi margin is currently the only region for which turbidite paleoseismology has been used to reconstruct the frequency and magnitude of prehistoric earthquakes (Pouderoux et al., 2012a, b, 2014). The turbidite paleoseismology studies have been isolated to three morphological re-entrants scars into the continental slope that form independent late Quaternary sedimentary systems (Poverty, Ruatoria and Matakaoa re-entrants, Fig. 10). The sediment sequences from these re-entrants are recorded in cores that span the last ~16,500 years and reveal interbedded hemipelagites and silty turbidites with isolated hyperpycnites and monomagmatic turbidites (Pouderoux et al., 2012b).

Paleoseismic interpretations of turbidite sequences from the Poverty, Ruatoria and Matakahoa re-entrants are based on correlation of turbidites between the distributary systems and the argument that large earthquakes are the primary mechanism triggering synchronous slope failures on the upper slope over length scales of hundreds of kilometers (cf. Goldfinger et al., 2012; Gràcia et al., 2010; Patton et al.,

2015). Correlations are based on four criteria: 1) primary air fall tephra that provide isolated but absolute time planes through the sequences (Lowe et al., 2008); 2) turbidite ages generated using Bayesian age/depth modelling of tephrochronology, pelagic foraminifera radiocarbon dates and accumulated hemipelagite thickness; 3) correlation of turbidite physical properties (density, magnetic susceptibility and p-wave velocity signatures (cf. Goldfinger et al., 2012; Patton et al., 2015); and 4) relative depth of hemipelagite between turbidites. Pouderoux et al. (2014) argue for 41 synchronous turbidite deposition events recorded in two or more re-entrants between 390 ± 170 and 16,450 ± 310 years BP. These 'margin wide' events imply synchronous triggering along ~170–200 km of the margin. An earthquake trigger was inferred for the 17 'margin wide events' that occurred during the Holocene sea level high stand, when seismic shaking is the only process likely to trigger synchronous upper slope mass-wasting in more than one re-entrant (Pouderoux et al., 2014). A minimum magnitude for these earthquakes of $M_w > 7.3$ was inferred through modelling that used ground motion prediction equations (Cousins et al., 1999) and an assumed triggering threshold of 0.08–0.1 g peak ground acceleration for mass-wasting. Using fault sources in the New Zealand Seismic Hazard model (Stirling et al., 2012), only three fault sources were calculated to be capable of generating the turbidite records: Raukumara subduction interface segment, the Ruatoria South 1 fault and the Ariel Bank fault (Pouderoux et al., 2014). The analysis by Pouderoux et al. (2014) also suggests that rupture of the Raukumara subduction interface segment is the only source capable of generating the 10 synchronous turbidite events in all three re-entrants that have occurred in the last ~7500 years and these are dated in Pouderoux et al. (2014).

We consider it robust that seismic shaking triggered the majority of turbidites recorded in the sediment cores studied by Pouderoux et al. (2014), however we consider some of the assumptions made in turbidite correlation and fault source attribution are not sufficiently robust, therefore we do not include the turbidite-derived earthquake ages in our earthquake compilation. Defining specific fault sources from the turbidite paleoseismic record on the Northern Hikurangi margin requires three major inferences to be made, these are: 1) spatial patterns of synchronous turbidite deposition are well supported by turbidite correlations between discrete sedimentary systems; 2) the triggering threshold for upper slope mass-wasting is known; and 3) the distribution of potential fault sources is well constrained (Pouderoux et al., 2014).

Absolute temporal correlations of turbidites between the Poverty, Ruatoria and Matakaoa re-entrants are limited by age model precision (Pouderoux et al., 2012b, 2014). For most cores very little time, if any, lies outside of the 2σ uncertainty of the age probability distributions for sequential turbidites, meaning that temporal turbidite correlations between re-entrants are non-unique (Pouderoux et al., 2012b, 2014). Hence, the primary basis for relating turbidites between distributary systems is the correlation of turbidite 'fingerprints' in core physical properties (density, magnetic susceptibility and P-wave velocity) data (Pouderoux et al., 2014). The approach of 'fingerprinting' turbidites based on peaks in physical properties data that provide a reliable proxy for grainsize was pioneered in Cascadia (Goldfinger et al., 2012). There the number and distribution of coarse grained pulses at the base of turbidites correlate between discrete sediment distributary systems along ~1000 km of that margin (Gutiérrez-Pastor et al., 2013). By comparison, correlations of turbidite 'fingerprints' based on physical properties data between re-entrants on the Northern Hikurangi margin are less compelling in that neither the number nor distribution of peaks in physical properties data from turbidite bases appear routinely consistent between correlated turbidites (see Figure SM2.03 of Pouderoux et al., 2014). Therefore, correlations based on this approach are less robust. Arguments for synchronous triggering are further compounded by the presence of stacked turbidites that record deposition from multiple turbidity currents closely spaced in time. These are considered as single depositional events for the purposes of correlation by Pouderoux et al. (2014), which ultimately precludes unequivocal spatial correlations for many events. Improved turbidite correlations will require more precise chronologies but the current record with non-unique correlations weakens the evidence for margin-wide earthquake triggering.

The inference of $M_w > 7.2$ earthquakes on the subduction interface also relies on an inferred threshold for upper slope mass wasting and accurate fault source knowledge. The ground motion threshold for triggering upper slope mass-wasting of peak ground acceleration (PGA) > 0.08–0.1 was derived from global data that range from 0.08 to 0.6 (Pouderoux et al., 2014). Slope failure is likely to be governed by local conditions mediated by sediment supply and earthquake rate, therefore a more robust analysis of earthquake source will require a locally derived triggering threshold. The spatial distribution of earthquake sources in the New Zealand National Seismic Hazard model is simplified, and recent data suggests it may be incomplete given the increased density of faults identified through new mapping based on high resolution seismic and multibeam bathymetry data (e.g. Böttner et al., 2018; Litchfield et al., submitted). The seismic hazard model also rarely takes into account the possibility of multi-fault rupture whereby several upper plate faults could rupture synchronously to produce more widespread ground shaking than otherwise expected for a single fault rupture (e.g. the 2016 Kaikōura earthquake, Hamling et al., 2017). The potential for a higher density of upper plate faults offshore of the northern Hikurangi margin and the recognition of multi-fault rupture potential complicates the interpretation that upper plate fault sources are unable to trigger slope failure in all three re-entrants.

The offshore sediment cores of the northern Hikurangi margin contain a rich record of seismically-triggered turbidites but our revision of the assumptions involved in deriving a subduction earthquake record suggests the earthquake ages and sources are relatively poorly constrained at present. With greater certainty in the core chronologies to bolster the turbidite correlations and increased knowledge of triggering thresholds and offshore fault distributions, the turbidite record does hold potential for understanding subduction earthquake characteristics of the northern margin.

7.4.2. Paleotsunami of the northern region

The northern region has a very sparse record of paleotsunami with only three sites recorded in the NZPD, and several possible deposits noted incidentally from marine terrace studies (Fig. 10). Given the northern region is the location of two of New Zealand's largest local source tsunamis (1947 Poverty Bay and Tolaga Bay earthquakes, Fig. 2), the contrasting sparseness of paleotsunamis is particularly notable. There have been few targeted studies of paleotsunamis on the northern Hikurangi margin, and additionally poor preservation of paleotsunamis may be due to the high coastal uplift rates that result in few optimum back-barrier/coastal plain depositional environments and, in some areas, rapid Holocene coastal progradation due to high fluvial sedimentation rates (e.g. Wolinsky et al., 2010). Sites in the NZPD include a pūrākau, a thick (possibly up to 15 m) deposit near Gisborne that may be fluvial-related, and a shelly sand layer near Tolaga Bay deposited post-Māori settlement; no records have good age control (NZPD, 2018).

During excavations across the marine terrace sequence at Puatai Beach, Litchfield et al. (2016) described 6 sand units within the colluvial silt coverbed sequences of the terraces. Of these 6 units, they identified two units with characteristics of a marine source and distribution most consistent with tsunami deposition (Fig. 3B). The older sand unit (S0) reached 9.3 ± 0.5 m elevation (elevation adjusted for post-depositional uplift of the site) and a shell within the sand was dated at 1065–805 years BP. The younger sand unit (S1) reached up to 9.0 ± 0.5 m elevation and assuming it correlates with the S3 sand on the lowest terrace, the combined age of two shells within the sand is < 260 years BP. Both the Puatai Beach paleotsunami deposits have a low certainty due to the lack of detailed exploration of the depositional

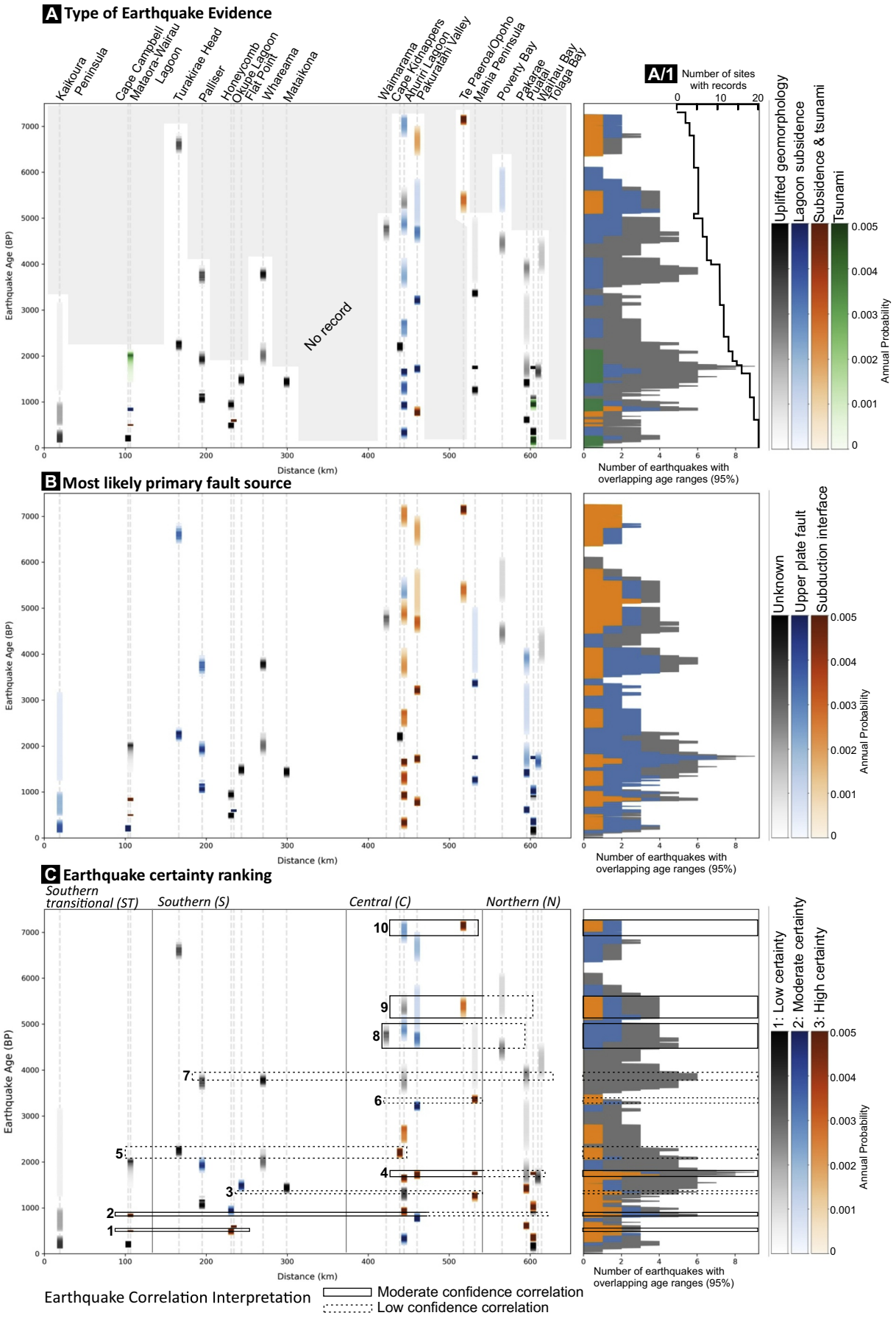

(caption on next page)

Fig. 11. Earthquake age correlation along the Hikurangi margin. The plots on the left show the earthquake ages plotted by distance along the margin (see projection line in Fig. 1) and earthquake ages are shaded by probability density in 5 year bins. The histograms show, for each 5 year bin through time, the number of earthquakes with 95% age ranges that overlap with that bin. On the right are shown the legends for each plot. (A) Earthquake ages are shaded by the type of evidence, the light grey shaded zone shows where no geological record exists. Plot A/1 shows the number of sites that record earthquake or tsunami evidence through time. (B) Earthquake ages are shaded by their most likely primary fault source. (C) Earthquake ages are shaded by their certainty (see text in Section 7 and Table 2), and subduction earthquake correlations are marked by the solid and dashed rectangles. Numbers 1–10 represent earthquakes Corr_Eq1-Eq10.

mechanism and poor age control.

8. Paleoearthquake correlations along the Hikurangi subduction margin

The primary basis for identifying a past subduction earthquake is the synchronous occurrence of coseismic coastal deformation and tsunamis at multiple sites (e.g. Garrett et al., 2016; Shennan et al., 2016; Witter et al., 2012; Philibosian et al., 2017). When using paleoearthquake and paleotsunami ages derived primarily from radiocarbon dates, the establishment of synchroneity across non-contiguous sites is impossible as there are always uncertainty ranges on radiocarbon dates. With this caveat in mind, to identify possible subduction earthquakes we use the number of earthquakes that occur through time, combined with the type of earthquake evidence, likely primary fault source and the earthquake certainty ranking (Fig. 11, Table 3). For each temporal cluster of earthquakes we consider possible fault sources aside from the subduction interface that could explain the pattern of coastal deformation and tsunami recorded (Fig. 6) and we also discuss how uncertainty in the marine reservoir correction for the Hikurangi margin affects paleoearthquake correlations.

We identify 10 past possible subduction earthquakes, named Corr_Eq10 (oldest) to Corr_Eq1 (youngest, Fig. 11C). In general the older earthquakes have broader age ranges and more limited spatial extent of evidence. Across the margin, earthquake age ranges narrow and the spatial coverage increases toward the present day; this is simply due to preservation potential rather than actual variation in earthquake rate through time (plot A/1, Fig. 11).

Corr_Eq10 and Corr_Eq9 are very similar in both having the bulk of evidence located within Hawke Bay; the subsided lagoons of this region provide the best preservation of older stratigraphy compared to other sites along the margin. Corr_Eq10 is represented by subsidence at Ahuriri, Pakuratahi and Te Paeroa/Opoho, with both Pakuratahi and Te Paeroa/Opoho recording tsunamis in association with the subsidence. Earthquake evidence at each of these three sites is consistent with subduction earthquake deformation: sudden subsidence recorded in multiple cores, tsunami inundation and no known upper plate faults that could cause the same deformation signature. Rupture of the Lachlan fault, outboard of Mahia Peninsula, could cause a small amount of subsidence at Te Paeroa and Opoho (Cochran et al., 2006) but the Lachlan fault is too far outboard and does not extend far enough southwest to cause subsidence at Pakuratahi and Ahuriri (Fraser et al., 2013). For Corr_Eq10, the 2σ age range of subsidence at Te Paeroa/Opoho overlaps entirely with the age range of subsidence at Ahuriri, but it does not overlap at all with the 2σ age range of subsidence at Pakuratahi Valley (Fig. 11). The mismatch of the age of Pakuratahi subsidence compared to Te Paeroa/Opoho is minor (they overlap at the 100% uncertainty range, but Fig. 11 and Table 2 show the 95% uncertainty ranges) and is likely due to poor age control at one of the sites, probably Pakuratahi Valley. We cannot rule out a scenario in which subsidence at Pakuratahi Valley occurred decades to centuries after subsidence at Te Paeroa/Opoho and Ahuriri, but synchronous subsidence of all three sites is a more credible scenario.

Corr_Eq9 is represented by uplift at Ahuriri lagoon, subsidence at Pakuratahi and Te Paeroa/Opoho and a tentative correlation with subsidence at Poverty Bay (Fig. 11). The contrast of uplift at Ahuriri compared to subsidence at Pakuratahi and Te Paeroa/Opoho is a puzzling aspect of this correlated earthquake; it suggests rupture of a local upper plate fault (perhaps the same one which ruptured in the 1931 Hawke's Bay earthquake) close in time or synchronous with subduction interface rupture.

Five sites from Hawke Bay to Poverty Bay record evidence for Corr_Eq8, although most of the sites have moderate to low earthquake certainty rankings and broad age ranges (Fig. 11). We are moderately confident with the correlation between uplift at Waimarama and subsidence at Ahuriri and Pakuratahi. These sites are all within a margin-parallel distance of 40 km and margin-normal distance of 30 km. Subduction interface rupture, perhaps with synchronous rupture of the Kidnappers/Kairakau fault could cause the observed uplift-subsidence deformation pattern. The correlation to uplift at Mahia Peninsula and Poverty Bay is less confident because of the broad age uncertainties.

Corr_Eq7 is the least robust earthquake correlation with low certainty evidence of coastal deformation at 5 sites spread from the southern region to the northern region and broad age ranges for earthquakes at each site. While subsidence of Ahuriri Lagoon and uplift of Whareama River is likely to be evidence of a subduction earthquake, uplift at Palliser, Pakarae and Tolaga Bay may have been driven by offshore, reverse upper plate faults. Nevertheless, the temporal overlap of deformation at these five sites means that a large subduction earthquake causing deformation at all sites is a possibility, albeit slim in this case.

Only two sites in the central region record evidence of Corr_Eq6: Pakuratahi Valley and Mahia Peninsula, but this is included as a potential subduction earthquake because both sites have narrow age ranges and moderate to high earthquake certainty rankings (Fig. 11). A subduction interface rupture is the most likely scenario for causing synchronous deformation at both sites. Dislocation modelling suggests the Lachlan fault, offshore of Mahia Peninsula, could not cause subsidence at Pakuratahi but the subduction interface could (Fraser et al., 2013).

Evidence for Corr_Eq5 occurs at 5 sites, with uplift of marine terraces from Palliser to Cape Kidnappers and a tsunami at Mataora-Wairau lagoon (Table 3). The tsunami has a very broad age range so this is a highly tentative correlation. No sites related to Corr_Eq5 show subsidence signatures classically associated with subduction earthquakes, and it is equivocal whether Corr_Eq5 is a series of closely-spaced-in-time upper plate fault earthquakes or a subduction earthquake.

There is a strong likelihood Corr_Eq4 represents a subduction earthquake on the central region of the Hikurangi margin, with less confident correlation to uplift of marine terraces of the northern region. Good agreement between the timing of subsidence at Ahuriri and Pakuratahi Valley is compatible with a subduction earthquake. Uplift of Mahia Peninsula within the same time period may indicate a subduction rupture caused deformation in northern Hawke Bay but unfortunately by this time the paleoenvironments at Te Paeroa/Opoho were not suitable for recording coastal deformation (Fig. 11). Marine terrace uplift at Puatai and Waihau Bay could have occurred in the same earthquake or the uplift may be related to upper plate fault rupture in the same time period.

Corr_Eq3 is represented by uplift of marine terraces at two locations on the Wairarapa coast and at Mahia Peninsula, along with subsidence at Ahuriri Lagoon. We have low confidence in the correlation of an earthquake between all of these sites because all of the marine terrace sites could be uplifted by upper plate faults, and the subsidence at Ahuriri lagoon has a weak certainty of earthquake evidence. The peat-

Table 3
Summary of earthquake evidence for each possible past subduction earthquake on the Hikurangi margin (Corr_Eq1–10), along with correlated earthquake age and minimum rupture length.

Earthquake name and age			Locality and geological evidence correlated to each subduction earthquake					
Past subduction earthquake	Age (years BP)	Minimum rupture length (km)	Locality[a]	Distance along margin (km)	Earthquake	Evidence	Earthquake age (years BP, ΔR_R)	Earthquake age (years BP, ΔR_NV)
Corr_Eq1	520–470	124	**Mataora-Wairau Lagoon**	**106**	**Eq1**	**Subsidence**	**520–470**	No change
			Honeycomb, Wairarapa coast	**230**	**Eq1 (T1)**	**Holocene marine terrace**	**560–410**	560–395
			Ahuriri Lagoon	*444*	*Eq1*	*Subsidence*	*460–185*	*505–215*
Corr_Eq2	870–815	354	**Mataora-Wairau Lagoon**	**106**	**Eq2**	**Subsidence and tsunami**	**880–800**	No change
			Honeycomb, Wairarapa coast	**230**	**Eq2 (T2)**	**Holocene marine terrace**	**1050–805**	995–750
			Ahuriri Lagoon	**444**	**Eq2**	**Subsidence**	**1015–815**	1020–820
			Pakuratahi Valley	**460**	**Eq1**	**Subsidence and tsunami**	**910–690**	983–690
			Puatai Beach	*603*	*Tsu2*	*Tsunami*	*1065–805*	1100–750
Corr_Eq3	1355–1300	288	*Flat Point, Wairarapa coast*	*243*	*Eq2 (T2)*	*Holocene marine terrace*	*1590–1350*	1600–1280
			Mataikona, Wairarapa coast	*299*	*Eq1 (T1)*	*Holocene marine terrace*	*1560–1295*	1555–1240
			Ahuriri Lagoon	*444*	*Eq3*	*Subsidence*	*1460–1140*	1480–1170
			Table Cape, Mahia Peninsula	*531*	*T2 (Eq2)*	*Holocene marine terrace*	*1360–1120*	1337–1047
Corr_Eq4	1815–1710	87	**Ahuriri Lagoon**	**444**	**Eq4**	**Subsidence**	**1725–1545**	1730–1570
			Pakuratahi Valley	**460**	**Eq2**	**Subsidence**	**1820–1620**	No change
			Table Cape, Mahia Peninsula	**531**	**T3 (Eq3)**	**Holocene marine terraces**	**1795–1710**	1840–1710
			Pakarae River	*595*	*T4 (Eq4)*	*Holocene marine terrace*	*2080–1500*	2090–1485
			Puatai Beach	*603*	*T3 (Eq3)*	*Holocene marine terrace*	*1785–1710*	1790–1710
			Waihau Bay	*609*	*T2 (Eq2)*	*Holocene marine terrace*	*1870–1460*	1870–1395
Corr_Eq5	2300–2070	333	*Mataora-Wairau Lagoon*	*106*	*Tsu1*	*Tsunami*	*2010–990*	No change
			Turakirae Head	*166*	*Eq3*	*Holocene beach ridge*	*2400–2090*	No change
			Palliser, Wairarapa coast	*195*	*Eq2 (T2)*	*Holocene marine terrace*	*2115–1755*	2105–1755
			Whareama, River, Wairarapa coast	*270*	*Eq1 (T1)*	*Holocene marine terrace*	*2295–1775*	2280–1685
			Waimarama-Cape Kidnappers	*439*	*Eq1 (T1)*	*Holocene marine terrace*	*2310–2065*	2305–1955
Corr_Eq6	3360–3265	71	*Pakuratahi Valley*	*460*	*Eq3*	*Subsidence*	*3320–3105*	No change
			Table Cape, Mahia Peninsula	*531*	*T4 (Eq4)*	*Holocene marine terrace*	*3490–3280*	3630–3330
Corr_Eq7	3930–3780	419	*Palliser, Wairarapa coast*	*195*	*Eq3 (T3)*	*Holocene marine terrace*	*3970–3510*	No change
			Whareama, River, Wairarapa coast	*270*	*Eq2 (T2)*	*Holocene marine terrace*	*3940–3615*	3920–3505
			Ahuriri Lagoon	*444*	*Eq6*	*Subsidence*	*4140–3475*	4235–3525
			Pakarae River	*595*	*T6 (Eq6)*	*Holocene marine terrace*	*4150–3510*	4160–3490
			Tolaga Bay	*614*	*T2 (Eq2)*	*Holocene marine terrace*	*4595–3780*	4585–3775
Corr_Eq8	5020–4450	38	**Waimarama**	**422**	**Eq2 (T2)**	**Holocene marine terrace**	**5030–4490**	4970–4400
			Ahuriri Lagoon	**444**	**Eq7**	**Subsidence**	**5205–4625**	5225–4685
			Pakuratahi Valley	**460**	**Eq4**	**Subsidence**	**4860–4455**	4970–4520
			Auroa Point, Mahia Peninsula	*531*	*T5 (Eq5)*	*Holocene marine terrace*	*5025–3570*	5034–3621
			Poverty Bay	*565*	*Eq1*	*Uplift within sedimentary sequence*	*4710–4195*	4715–4190
Corr_Eq9	5600–5100	73	**Ahuriri Lagoon**	**444**	**Eq8**	**Uplift within sedimentary sequence**	**5595–5015**	5595–5030
			Pakuratahi Valley	**460**	**Eq5**	**Subsidence**	**5855–4830**	5940–4900
			Te Paeroa/Opoho	**517**	**Eq1**	**Subsidence and tsunami**	**5600–5105**	No change
			Poverty Bay	*565*	*Eq2*	*Subsidence*	*6115–5125*	6120–5085
Corr_Eq10	7250–6900	73	**Ahuriri Lagoon**	**444**	**Eq9**	**Subsidence**	**7260–6755**	7265–6800
			Pakuratahi Valley	**460**	**Eq6**	**Subsidence and tsunami**	**7010–6355**	7110–6430
			Te Paeroa/Opoho	**517**	**Eq2**	**Subsidence and tsunami**	**7250–7020**	**7250–7020**

[a] Entries in bold indicate sites correlated with moderate confidence. Entries in italic indicate sites correlated with low confidence.

silt contact representing subsidence of Eq3 at Ahuriri is present in only three cores at 2 out of the 4 sites studied (Hayward et al., 2016), so while subsidence of Ahuriri lagoon is most likely caused by subduction interface ruptures, the evidence for Eq3 is weak. Uplift at Pakarae River mouth fits within the time range of Corr_Eq3 but it was probably driven by upper plate fault earthquake.

The strongest evidence for a past subduction earthquake on the Hikurangi margin is the evidence for Corr_Eq2 in which subsidence occurs at Mataora-Wairau Lagoon, Ahuriri Lagoon and Pakuratahi Valley, and uplift occurs at Honeycomb Rock on the Wairarapa coast (Fig. 11). Paleotsunami deposits are found in association with the subsidence evidence at Mataora-Wairau Lagoon and Pakuratahi Valley, and we also include a less confident correlation to a paleotsunami deposit at Puatai Beach (a less confident correlation because it is dated by only one shell with an age range of 260 years). Subsidence at Mataora-Wairau Lagoon, Ahuriri Lagoon and Pakuratahi Valley is most simply explained by subduction interface rupture. Uplift of the Honeycomb Rock area on the Wairarapa fault could be caused by a subduction earthquake or by the Palliser-Kaiwhata fault. The temporal correlation with subsidence at sites north and south of Honeycomb Rock is quite convincing evidence that the Honeycomb Rock area uplift, in this case, was caused by a subduction earthquake.

Corr_Eq1 is represented by subsidence at Mataora-Wairau Lagoon and uplift of the Honeycomb Rock area on the Wairarapa coast. Both earthquakes have a high certainty ranking and Clark et al. (2015) have shown that a subduction earthquake was the most likely cause of subsidence at Mataora-Wairau Lagoon. There is a very narrow age gap of 10 years between the age range of Corr_Eq1 (520–470 years BP) and Eq1 at Ahuriri Lagoon (460–185 years BP). At the full 100% age uncertainty range, these three earthquake ages would have a degree of overlap, suggesting that Corr_Eq1 could extend up to the central region of the Hikurangi margin.

At face value the 10 past possible subduction earthquakes identified offer the potential to assess recurrence intervals along the margin. However, we consider the majority of earthquake ages from individual sites are too poorly constrained to produce reliable subduction zone earthquake ages using the along-strike correlations, and furthermore, there is a high degree of variability in record length along the margin so any recurrence interval (RI) calculation would only apply to a point along the margin rather than the whole margin or a segment. The southern Hawke Bay region, central Hikurangi margin, is the only location where a sufficient number of subduction earthquakes have been resolved to produce recurrence statistics. Using earthquake ages from Ahuriri Lagoon, Hayward et al. (2016) calculated a RI of 900 years. At the same location using our moderate certainty subduction earthquake correlations, the RI increases to 1450 years and using moderate plus low certainty correlations reduces the RI to 800 years (uncertainty ranges on the RI are not calculated as we do not have robustly constrained uncertainty ranges on the correlated earthquake ages). For the southern region of the Hikurangi margin, the record of past subduction earthquakes is much shorter and using only the last two moderate-confidence subduction earthquakes yields a RI of ~435 years with an open interval since the last earthquake of 520–470 years (Table 3). The longer, but less well-constrained, record of 5 subduction earthquakes on the southern margin in the past 4000 years yields a RI of ~800 years. Using the midpoint of the correlated earthquake age ranges, the intervals between earthquakes range from 350 years (between Corr_Eq1 and Corr_Eq2) to 1725 years (between Corr_Eq10 and Corr_Eq9) suggesting high variability of intervals between large earthquakes. In general, the intervals between earthquakes increases further back in time, suggesting older events may be missing. For the past 1800 years when most of the margin has a reasonable number of sites recording earthquakes and tsunamis (Fig. 11, plot A/1) the RI of a large earthquake somewhere along the margin is 450 years. The wide variability in RI demonstrates the difficulty in calculating RI based on the current dataset of subduction earthquakes. Determining reliable recurrence statistics for subduction earthquakes and how they vary along the margin will require improving earthquake ages for existing earthquakes and generating longer earthquake records in regions where records are sparse beyond the last 2000 years.

8.1. The effect of variation in marine reservoir correction on paleoearthquake correlations

Poor constraint of the marine reservoir correction along the Hikurangi margin means where paleoearthquake and paleotsunami ages are calculated using shell radiocarbon ages, there is an increased amount of age uncertainty and this can impact age correlations between sites. We have accommodated uncertainty in ΔR by using relatively wide ranges on the ΔR_R values, and for all paleoearthquake and paleotsunami ages we calculate the age if ΔR was uniform along the margin (ΔR_{NV}) rather than regionally variable (ΔR_R, Tables 1, 3). The earthquake correlations discussed above are based on ΔR_R but here we consider if the temporal correlations hold true if ΔR_{NV} is used.

There is no significant change in the degree of overlap between individual paleoearthquake ages for Corr_Eq9, Corr_Eq8, Corr_Eq7, Corr_Eq5 and Corr_Eq4 when ΔR_{NV} is used rather than ΔR_R. This is largely because the paleoearthquake ages are relatively broad so decadal-scale shifts in the upper and lower limits of the 95% ranges alter the degree of temporal overlap very little. The use of ΔR_{NV} for the paleoearthquake ages of Corr_Eq10 means the age of subsidence at Pakuratahi Valley is slightly older, therefore there is temporal overlap between deformation at Pakuratahi Valley, Ahuriri Lagoon and Te Paeroa/Opoho. When using ΔR_{NV} for Corr_Eq6, there is no overlap at the 95% uncertainty range between uplift at Mahia Peninsula and subsidence at Pakuratahi Valley, therefore this earthquake correlation becomes less certain. For Corr_Eq3 the use of ΔR_{NV} increases the amount of overlap between uplift at Flat Point and the other three paleoearthquake ages, so the temporal correlation is strengthened. The use ΔR_{NV} for Corr_Eq2 does not significantly alter the paleoearthquake correlations but we do note the agreement between the age probability distributions for subsidence at Mataora-Wairau Lagoon and uplift at Honeycomb Rock improves, therefore strengthening the temporal correlation. However, the age range of the Puatai Beach paleotsunami broadens from 260 years to 350 years, weakening the temporal correlation to Corr_Eq2. For Corr_Eq1, agreement between the age probability distribution for coseismic deformation at Mataora-Wairau Lagoon and Honeycomb Rock does not change significantly, but the age range of subsidence at Ahuriri Lagoon has overlap with Corr_Eq1 when ΔR_{NV} is used. In summary, changing the ΔR value in marine radiocarbon age calibrations does not significantly change earthquake ages, but in some cases where age constraints are narrow due to good age control, the change from a locally-appropriate value (ΔR_R) to a regionally-averaged value (ΔR_{NV}) can affect the degree of overlap between earthquake age probability distributions. Until further research is undertaken on marine reservoir corrections along the Hikurangi margin, we maintain the use of ΔR_R is most appropriate.

9. Discussion

9.1. Rupture zones of past subduction earthquakes on the Hikurangi subduction margin

The spatial extent of geologic evidence of past subduction earthquakes can be used to estimate the rupture lengths of past subduction earthquakes (e.g. Cascadia, Nelson et al., 2006; Priest et al., 2017; Nankai-Suruga Trough, Garrett et al., 2016; south central Chile, Moernaut et al., 2014). Rupture lengths are commonly used as a proxy for earthquake magnitude and can be used to characterise the earthquake behaviour and hazard of subduction zones, such as whether "supercycles" or earthquake clustering occurs (Moernaut et al., 2018; Philibosian et al., 2017; Goldfinger et al., 2013). In cases where well-

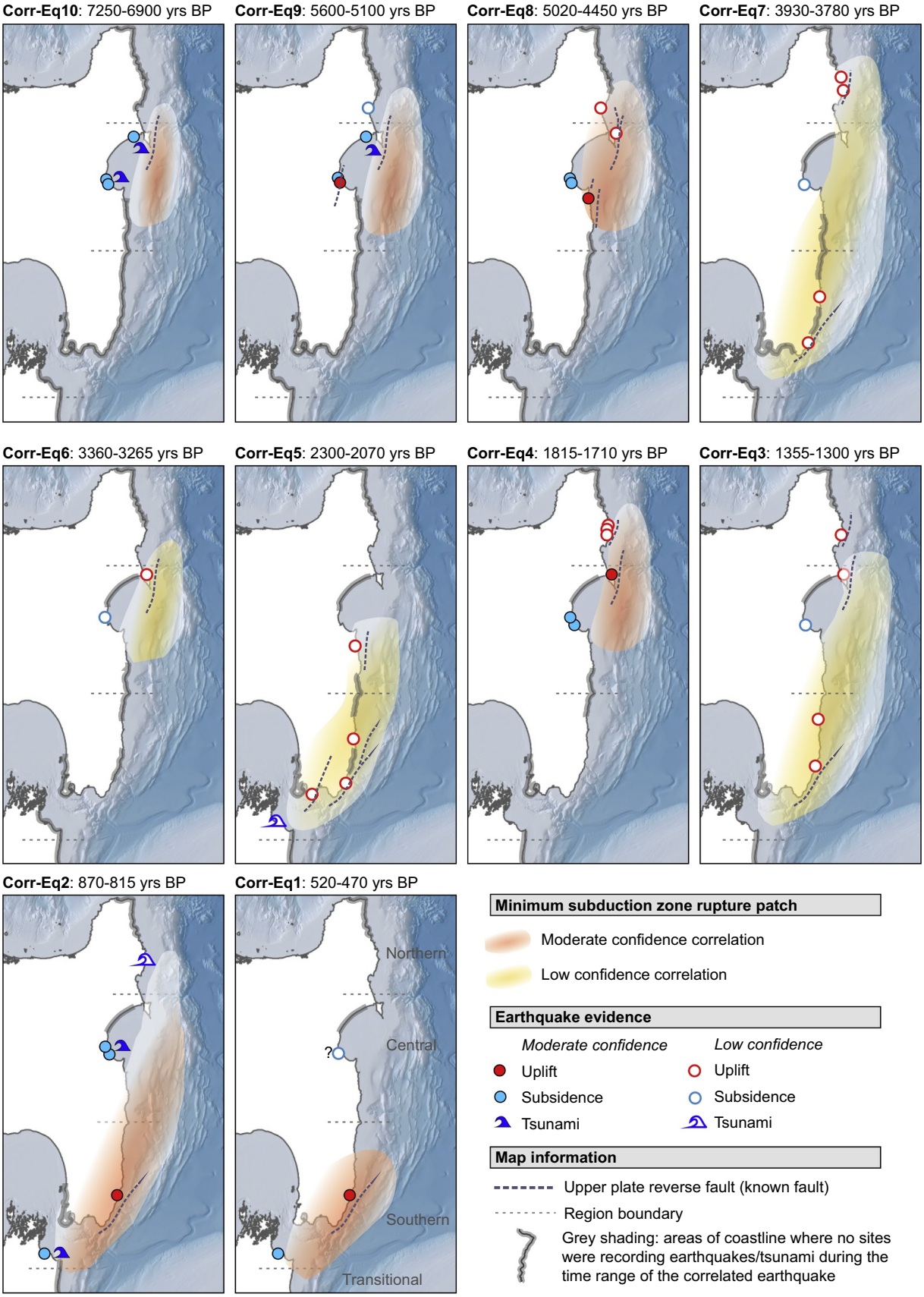

(caption on next page)

Fig. 12. Indicative subduction interface rupture patches for earthquakes Corr_Eq1-Eq10. Where upper plate reverse faults have been mapped offshore of locations with coseismic coastal deformation we have shown these faults in a dark blue dashed line. The rupture patches are highly speculative and assume: (i) all deformation occurred synchronously; (ii) the earthquake was on the subduction interface; (iii) the updip limit of rupture is near the trench; (iv) the downdip limit of rupture was inboard of locations of coseismic uplift and outboard of locations that underwent coseismic subsidence. The ends of each rupture patch are poorly constrained due to data limitations in space and time. Grey-shaded parts of the coastline indicate areas where no sites were recording coastal deformation or paleotsunami records during the time period of the correlated earthquake. The correlated earthquake in question may have extended to the regions of grey shading but the evidence has not been documented due to lack of preservation *or* lack of study/dating. In general, further back in time, there are fewer sites with earthquake or paleotsunami records.

distributed measurements of vertical deformation are available, the dimensions of the rupture patch (i.e. the length plus the up/downdip extent of slip) may be estimated, usually in tandem with forward elastic dislocation modelling (e.g. Cisternas et al., 2017; Shennan et al., 2016; Philibosian et al., 2017).

A compilation of the location of earthquake evidence for Corr_Eq10 (oldest) to Corr_Eq1 (youngest) and estimated minimum subduction interface rupture patches is shown in Fig. 12. The estimated rupture patches are contingent on two assumptions: (1) evidence that correlates within a certain time period relates to the same earthquake; and (2) that vertical deformation is due to rupture of the subduction interface (i.e. no upper plate fault rupture). Previous sections have covered issues involved with the temporal correlation of paleoseismic evidence and in this section we proceed on the assumption that all deformation associated with a correlated earthquake occurred synchronously. Assumptions on fault source are explored in greater detail in Section 9.2, where we also consider the possibility of synchronous interface and upper plate fault ruptures (Fig. 6). Data coverage is not dense enough to estimate the updip and downdip limits of rupture with any certainty so these are indicative only. In Fig. 12, we place the updip limit of rupture near the trench. The downdip rupture extent is placed downdip of uplift sites and updip of subsidence sites. We obtain only minimum estimates of rupture length due to spatial and temporal data limitations, and the likely lack of preservation of small vertical deformation (i.e. tens of centimetres) at the edges of rupture zones. The primary observations that come from the compilation of rupture lengths in Fig. 12 are that: (i) there are no characteristic rupture patches, suggesting segmentation of the margin is not strong, and (ii) whole margin ruptures may have occurred in the past, but are the exception rather than the norm.

Possible rupture segment boundaries are a sought after parameter for seismic hazard assessment of subduction zones due to the proportional relationship between earthquake magnitude and area of fault slip. Our review of subduction earthquake evidence shows no persistent rupture boundaries, with most past subduction ruptures having variable along-margin extents (Figs. 11, 11). The appearance of a persistent rupture patch on the central Hikurangi margin is given in Fig. 12 because Corr_Eq4, 6 and 8–10 rupture a similar extent of the margin but this is an artefact of limited of data coverage. Records of coastal deformation > 2000 years BP become notably sparser on the southern and northern regions of the margin so it appears only the central margin ruptures. Globally, rupture segments are proposed to be controlled by a variety of factors, such as upper plate structure (Song and Simons, 2003; Collot et al., 2004; Melnick et al., 2009), bathymetric anomalies on the subducting plate (Taylor et al., 1987; Chlieh et al., 2008) and megathrust fluids and sediment thickness (reviewed in Bilek and Lay, 2018). On the Hikurangi margin, many physical properties of the margin vary along strike (Barker et al., 2009; Wallace et al., 2009) but no significant structural boundaries have been identified and rupture segments have only tentatively been identified based on interseismic coupling, paleoseismology and geophysical properties of the subducting plate (Stirling et al., 2012). For the purposes of seismic hazard assessment, Stirling et al. (2012) divided the margin into southern, central and northern segments, and single segment ruptures were expected to be M_w 8.1–8.3, while whole margin ruptures could be M_w 9.0 (Stirling et al., 2012).

Our review finds there is no persistent rupture boundary between the southern and central regions of the margin, with Corr_Eq2, 3, 5, and 7 rupturing across both regions (Fig. 12). Corr_Eq1 is the only subduction earthquake that appears to be confined to the southern margin, so further work on refining the age of the last coseismic subsidence of Ahuriri Lagoon is critical for assessing whether the southern region ruptures independently of the central region. The presence or absence of a rupture boundary between the central and northern regions is difficult to evaluate due to sparse high-certainty evidence of past earthquakes on the northern region coastline. Five past subduction earthquakes could have ruptured both segments suggesting there is not a segment boundary between the two regions. However, almost all coseismic coastal deformation recorded on the northern margin is likely to have been caused by upper plate faults (Fig. 11b).

A critical question for the Hikurangi margin is whether the whole margin can rupture in a single great (> M9.0) earthquake and evidence from our review suggests this is possible, but probably infrequent. The strongest evidence for a whole margin rupture is Corr_Eq2 (870–815 years BP), in which the southern and central regions underwent vertical coastal deformation and the northern region has evidence of tsunami runup of up to 9.3 ± 0.5 m. Corr_Eq7 at 3930–3780 years BP and Corr_Eq3 (1355–1300 years BP) may have ruptured the whole margin but both correlated earthquakes have considerably less strength of evidence than Corr_Eq2 (Fig. 11C).

9.2. The role of upper plate faults in subduction earthquakes

On the Hikurangi margin, numerous upper plate faults are located near the coastline, and historic examples of coastal deformation related to upper plate fault earthquakes, mean that upper plate fault ruptures are a realistic proposition for causing coastal deformation and tsunamis (Figs. 1, 2, 6). At other subduction margins such as Cascadia, Chile and Sumatra, there are fewer known upper plate faults close to the coastline that are capable of causing widespread vertical deformation and tsunami. Thus, upper plate faults are rarely considered in compilations of subduction margin paleoseismicity. An exception to this is on the eastern part of the Aleutian subduction margin, where an upper plate reverse fault is considered within the context of uplifted marsh records of subduction earthquakes (Shennan et al., 2014). The presence of many upper plate faults at the Hikurangi margin make resolution of a subduction earthquake paleoseismic record more challenging.

Evaluation of possible upper plate fault involvement in correlated earthquakes Corr_Eq1–10 shows that if deformation were synchronous at each site, then the subduction interface is the most likely source for causing the deformation (and tsunami, if recorded), as opposed to single or multi-fault rupture of upper plate faults. On Fig. 12, we have shown the locations of upper plate faults adjacent to sites where earthquake evidence is most likely related to an upper plate fault. For all correlated earthquakes, except Corr_Eq5, upper plate faults could have been responsible for deformation at some sites but the larger fault source of the underlying subduction interface is required to explain deformation at all sites, if the evidence all relates to a single earthquake. Only Corr_Eq5, comprised of correlated evidence of terrace uplift and tsunami deposition from 5 locations, may be entirely explained by upper plate faults, without requiring subduction interface rupture. Corr_Eq5 could be driven by coastal uplift adjacent to the Wairarapa fault (and offshore fault extensions), the Palliser-Kaiwhata

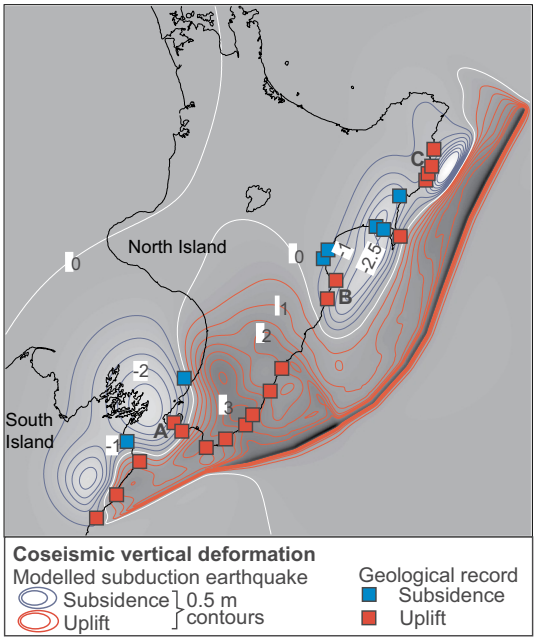

Fig. 13. Comparison between modelled coseismic vertical deformation in a great subduction earthquake and the geological record of coastal coseismic vertical deformation. The modelled deformation, adapted from Wallace et al. (2014) is the predicted vertical deformation for a hypothetical rupture of the entire Hikurangi margin including the interseismically coupled area and offshore slow slip event source areas in the northern and central margin. The slip amounts used in the interseismically coupled area assume reversal of 800 years of accumulated slip deficit (using interseismic slip deficit rates from Wallace et al., 2012b), while the slip amounts within the slow slip event source areas of the central margin are tuned to produce vertical deformation consistent with that observed in Hawkes Bay paleoseismic studies. The use of 800 years of slip deficit does not imply an 800-year recurrence for such events, the spatial pattern of vertical deformation, rather than the values of vertical deformation, are used for comparison with the geological record. Letters A–C represent areas of notable mismatch between the model and the geological data discussed in the text. A: south Wellington coast, B: outboard Hawke Bay, C: north of Gisborne.

fault, and the Kidnappers/Kairakau faults (Figs. 7 and 8). It is unlikely this sequence of 3 non-contiguous faults ruptured in a single multi-fault earthquake, but individual fault ruptures within a ~300 year time period is feasible. Subduction interface rupture for Corr_Eq5 cannot however, be ruled out. Corr_Eq3 and Corr_Eq7 are similar to Corr_Eq5 in lacking strong evidence of a subduction interface source. Deformation could alternatively be explained by a sequence of upper plate fault ruptures or a sequence of smaller subduction earthquakes, analogous to seismic "supercycles" observed on the Mentawai segment of the Sunda margin where periods of strain accumulation culminate in a series of ruptures rather than a single end-to-end rupture (Philibosian et al., 2017). Most offshore upper plate faults along the Hikurangi margin do not have paleoseismic records, the exception are some faults in Cook Strait (Pondard and Barnes, 2010). Paleoseismic records of offshore upper plate faults, independent of coastal deformation records, may help to resolve some uncertainties about upper plate fault involvement in correlated earthquakes but such records will be challenging to obtain.

While the compilation of interface rupture patches with the locations of upper plates results in non-unique solutions for the earthquake source, we suggest this highlights a realistic scenario for the Hikurangi margin in which large to great subduction earthquakes trigger synchronous upper plate ruptures (e.g. scenario 3, Fig. 6). Examples of upper plate fault ruptures with the subduction interface have been seen in several historic subduction earthquakes. For example, rupture of a splay fault during the 2010 M_W 8.8 Maule earthquake uplifted Isla Santa Maria, Chile, by 1.6–2.2 m (Melnick et al., 2012) and rupture of the Patton Bay splay fault uplifted Montague Island by > 6 m during the 1964 M_W 9.2 Alaska earthquake (Plafker, 1967). Splay fault ruptures have been inferred in other subduction earthquakes (Park et al., 2002; Collot et al., 2008) and finite element models also suggest splay faults can rupture with the subduction interface, with the splay faults receiving particular attention due to their role in enhanced tsunami generation (Li et al., 2014; Wendt et al., 2009). Large historic earthquakes in the Hikurangi margin have all been on upper plate faults, but these events may have also involved some degree of slip on the subduction interface. For example, the 1855 Wairarapa (Beavan and Darby, 2005) and 2016 Kaikōura earthquakes (Wallace et al., 2018) demonstrate the close physical connections between major upper plate faults and the interface.

9.3. Comparison between contemporary geodetic coupling and past subduction earthquakes

In several recent large subduction earthquakes, the slip distributions have a close correspondence to plate coupling prior to the earthquake (e.g., Miura et al., 2004; Chlieh et al., 2008; Moreno et al., 2010; Loveless and Meade, 2011; Protti et al., 2013). If such a relationship were consistently true, then future rupture scenarios for the Hikurangi margin could be guided by the contemporary plate coupling pattern. However, it is unknown if seismic rupture zones always correspond with pre-earthquake coupling zones, and furthermore, it is unknown whether coupling distributions vary throughout the interseismic period. To definitively answer these questions, geodetic measurements over multiple earthquake cycles would be needed (Wallace et al., 2014). An alternative approach, though less rigorous, is to compare the contemporary coupling distributions with paleoearthquake records to see if the short- and long-term deformation datasets have a relationship, and therefore if the contemporary interseismically coupled areas of the interface may foreshadow future rupture patches.

A comparison between geodetic plate coupling and geological evidence for past earthquakes in the Hikurangi margin was last undertaken by Wallace et al. (2014) and here we revisit that comparison based on our revisions of past subduction earthquake rupture patches developed in Fig. 12. Wallace et al. (2014) produced a model of vertical deformation produced by a hypothetical rupture of the whole Hikurangi margin with the area of rupture covering the currently interseismically coupled area and the areas of slow slip events offshore of Gisborne and Hawke Bay (Fig. 13). We base our comparison on this model as the subsequent years of geodetic measurements have not altered the spatial distribution of interseismic coupling. The model presented in Fig. 13 assumes slip equivalent to 800 years of accumulated plate motion, but the amount of deformation is scalable to any lesser or larger amount, therefore we do not focus on the magnitude of the modelled earthquake.

In the southern Hikurangi margin there is general consistency between areas of past coseismic subsidence and uplift, and vertical deformation predicted in the model (Fig. 13). Some mismatch occurs where the model predicts subsidence of the Wellington region (area A), where past coseismic uplift is recorded. The mismatch around Wellington is most likely because subduction earthquake deformation is overprinted by uplift on upper plate faults, but the details of vertical deformation around Wellington in a subduction earthquake are highly dependent on where the downdip limit of seismic rupture lies.

In the central Hikurangi margin, there is a good match between geologic records of subsidence (Ahuriri Lagoon, Pakuratahi Valley and northern Hawke Bay), and modelled vertical deformation in a subduction earthquake (Fig. 13). Of note in this area is that fitting coseismic subsidence in inner Hawke Bay (see Fig. 13 caption) requires seismic rupture of the area of slow slip events on the interface beneath Hawke Bay, suggesting different modes of plate interface slip behaviour occur on the central Hikurangi margin on seismic cycle timescales

(Wallace et al., 2014). Areas of coastal uplift in the outboard regions of Hawke Bay (Waimarama - Cape Kidnappers in the south, area B, and Mahia Peninsula in the north) are not matched by the vertical deformation model, suggesting that seismic rupture extends deeper beneath Hawke Bay than suggested by contemporary interseismic coupling, or that nearshore upper plate faults play a role in the coseismic coastal uplift.

In the northern Hikurangi margin geodetic-based modelling predicts subsidence along the coastline where almost all Holocene coseismic deformation is uplift (area C, Fig. 13). This mismatch is likely due to upper plate faults driving coastal uplift, rather than earthquakes on the subduction interface. Only one occurrence of subsidence at 6115–5125 years BP in Poverty Bay on the northern coastline suggests some similarity between the geodetic models and coastal deformation records. The strongest evidence for subduction earthquakes on the northern Hikurangi margin is derived from the submarine turbidite record which suggests ten $M_w > 7.2$ subduction interface earthquakes over the last ~7.5 ka (Pouderoux et al., 2014), but assumptions in deriving the earthquake record mean it is not conclusive that subduction earthquakes are the cause of synchronous turbidites (Section 7.4.1).

Ultimately, evidence for subduction earthquakes in the northern region remains weak, and the misfit between the coastal deformation records, turbidite paleoseismology and geodetic models of plate coupling could indicate complete overprinting of subsidence due to uplift by upper plate faults or an absence of large subduction earthquakes rupturing west of the coastline in the mid-late Holocene. Perhaps the interface typically ruptures in smaller patches, similar to the 1947 tsunami earthquakes, with no detectable coastal deformation but anomalously high tsunamis. The subduction interface at the northern region is generally characterised by weak interseismic coupling and aseismic creep, although the degree of coupling is not well-constrained by land-based geodetic data. Stick-slip behaviour can occur at shallow depths around small asperties created by subducted seamounts (Bell et al., 2010, 2014), thus, it has been suggested that the northern Hikurangi region may be less prone to deeply rupturing subduction earthquakes compared to the southern margin (Wallace et al., 2009, 2014). Evidence such as the paleotsunami at 1065–805 years BP recorded at Puatai Beach that correlates to Corr_Eq2, but not to local marine terrace uplift, could be critical to understanding the potential of the northern subduction interface to rupture with the central and southern Hikurangi margin.

10. Future research directions for Hikurangi subduction margin paleoseismology

Although significant progress has been made toward understanding the seismic and tsunami potential of the Hikurangi subduction margin, many knowledge gaps still remain. Future research directions on the Hikurangi margin fall into three broad categories of: (1) refining and densifying the coastal deformation and tsunami records; (2) integration of multiproxy ground shaking records; and (3) improving underpinning tectonic, sea-level change and chronological datasets.

10.1. Refining and densifying coastal deformation and tsunami records

The coastal deformation record of the Hikurangi margin is the primary dataset that sheds light on the location and timing of past subduction earthquakes along the Hikurangi margin but there are significant spatial and temporal gaps in the record (Figs. 10A, 11). Particular spatial gaps in coastal deformation exist in the transitional region in the south, from Kaikōura up to Kāpara-te-hau (Lake Grassmere), around the Cape Turnagain area (southern-central boundary), and north of Tokomaru Bay up to East Cape (northern area). Illumination of a seismogenic plate interface underlying the transitional region raises the question of whether the region can host large to great subduction earthquakes (Wallace et al., 2018). A detailed study of marine terrace uplift (timing and extent) and paleotsunami is one of the few ways in which we can better understand the seismic potential of the southern Hikurangi margin and constrain how far south into the transitional region large subduction ruptures reach. A further prominent spatial gap is around the Cape Turnagain, this area is of particular relevance to margin segmentation questions as it spans the sharp change in interseismic coupling. The final large spatial gap is at the northern end of the Hikurangi margin. The northern region is undergoing uplift but whether it is aseismic or coseismic uplift remains unclear at many sites; furthermore, if uplift is coseismic, the earthquake source is unresolved. Advances in high-resolution topography and paleoenvironmental studies, along with marine terrace trenching have the potential to reveal more about the uplift mechanisms of the East Cape to Hicks Bay coastline. The northern region should be revisited to advance understanding of the northward extent of plate interface rupture and possible continuation to the Kermadec subduction zone.

Within the existing spatial array of coastal deformation records are prominent temporal gaps in the records, that if filled could greatly increase knowledge of along-margin earthquake correlations. One of the most critical temporal gaps is the < 5000 year record of subsidence and tsunamis in northern Hawke Bay (Te Paeroa/Opoho, Fig. 11). The southern Hawke Bay (Ahuriri) record has seven earthquakes < 5000 years BP and searching for correlative earthquakes and/or tsunamis in northern Hawke Bay would help resolve if the younger earthquakes in southern Hawke Bay were subduction earthquakes, or localised earthquakes. Other temporal gaps in the coastal deformation record relate to the length of record, with both the southern and northern region having no moderate or high certainty earthquakes > 2000 years BP (Fig. 11c). At some locations, the absence of record is due to non-preservation but at others (e.g. the Wairarapa coast) older marine terraces are known to exist but have not been dated due to the difficulty in obtaining reliable radiocarbon dates. Alternative dating techniques, particularly cosmogenic nuclides and luminescence should be investigated for marine terraces where radiocarbon material has degraded. Several particular events within the current record of coastal deformation and tsunamis would benefit from targeted study in order to reduce the uncertainties on along-margin earthquake correlations. For example, in relation to Corr_Eq1, obtaining higher certainty age constraints on the timing of subsidence at Ahuriri Lagoon is a high priority. Better age constraints would allow us to understand whether the last subduction earthquake on the southern Hikurangi margin also ruptured the central Hikurangi margin. This has implications for time-dependent hazard of the central margin and for understanding whether interface ruptures consistently span the locked to unlocked transition zone.

A wholesale improvement of the paleotsunami record of the Hikurangi margin would assist greatly with understanding the seismic and tsunami history of the subduction zone. Paleotsunami datasets from other subduction margins demonstrate the importance of paleotsunami records in understanding subduction zone earthquake behaviour (e.g. Kelsey et al., 2005; Nelson et al., 2015; Rubin et al., 2017). In our review we have noted poorly-constrained evidence of paleotsunami in all regions of the margin, with the primary issues related to: (1) certainty of tsunami evidence; and (2) poorly constrained ages. Much of the reason for the poor paleotsunami record is the lack of targeted paleotsunami research along the margin. Frequently, paleotsunami evidence has been obtained incidentally in the course of paleoseismic studies (e.g. Berryman et al., 2011; Litchfield et al., 2016), therefore the radiocarbon dating tended to prioritise dating paleoearthquakes rather than the inferred tsunami deposits and sites were not optimally sited for preserving tsunamis. In cases where targeted paleotsunami studies have been undertaken the certainty of the tsunami deposits is improved, however, the age constraints remain poor (e.g. Goff et al., 1998, 2004; Goff and Chagué-Goff, 2015). Although tsunamis can be generated by upper plate faults and far-field sources (e.g. the subduction margin of Peru and Chile) as well as subduction earthquakes, the integration of tsunami modelling, upper plate fault paleoseismic chronologies and

coastal deformation can greatly help refine likely tsunami sources (e.g. Clark et al., 2015). Therefore, the abundance of offshore upper plate faults on the Hikurangi margin need not hinder the development of a robust subduction zone paleoseismic record.

10.2. Integrated multiproxy ground shaking records

Beyond coastal deformation and tsunami deposits, other proxy records of ground shaking may provide primary or supporting evidence of past large subduction earthquakes. A particular advantage that proxy ground shaking records have is in most cases there is potential to calibrate the "paleoseismometer" with modern earthquakes, therefore some control can be placed on ground shaking thresholds required to trigger a record. A relatively commonly used proxy for subduction earthquakes is the submarine turbidite records (e.g. Patton et al., 2015; Goldfinger et al., 2012), and research using this technique has been undertaken on the northern Hikurangi margin (Pouderoux et al., 2014) and is currently in progress along the central and southern margin. Turbidite triggering by the 2016 Kaikōura earthquake has revealed a lot about the mobilization and travel distances of turbidites (Mountjoy et al., 2018), and there is potential that earthquakes such as the 1855 Wairarapa and 1931 Hawke's Bay earthquakes may also be found in the turbidite records, allowing refinement of triggering mechanisms of submarine turbidites along the Hikurangi margin.

Lacustrine turbidites have been successfully used as a recorder of great subduction earthquakes along the south-central Chile margin (Moernaut et al., 2014, 2018; Van Daele et al., 2019) and preliminary research shows potential for the technique on the Cascadia and Alaska margins (Morey et al., 2013; Praet et al., 2017). In New Zealand, earthquakes on the Alpine fault have been dated to high precision using lacustrine turbidites (Howarth et al., 2012, 2014, 2016) but similar research is under-explored along the Hikurangi margin. Aside from Lake Tutira (Gomez et al., 2015), no lakes along the Hikurangi margin have been studied for a turbidite record of ground shaking. Alpine fault studies show that the narrowest age constraints, and therefore most reliable along-margin correlations, may come from lacustrine turbidites. As with the Lake Tutira example, all lakes along the Hikurangi margin are likely to record ground shaking from local and regional upper plate fault earthquakes, so a large dataset of lake records and knowledge of triggering thresholds is needed in the search for subduction earthquake signals. Aside from turbidites, other ground shaking proxies include the formation of landslide-dammed lakes and speleothem damage. Cochran et al. (2006) identified a correlation between coseismic subsidence in northern Hawke Bay and large landslide dam lake formation at c. 7100 years BP but beyond that, these proxies have not been explored along the Hikurangi margin.

10.3. Improving underpinning tectonic, sea-level change and chronological datasets

In the Hikurangi margin, as with any other subduction margin globally, the analysis of paleoearthquakes and paleotsunamis is not undertaken in isolation, but relies upon several underpinning datasets that provide context for the identification of extreme and anomalous events. Future research on Hikurangi margin paleoseismology needs to go hand-in-hand with the development and improvement of underpinning datasets. We highlight improving the marine reservoir correction database for the Hikurangi margin as the highest priority step at this point in time, followed by increasing the resolution of the non-tectonic Holocene RSL curve for the Hikurangi margin and further development of knowledge of upper plate fault characteristics.

In Section 6 we have discussed the previous lack of ΔR values from the Hikurangi margin and our contribution of 10 new ΔR values from Wairarapa and Hawke Bay makes only a small advance in our understanding of marine reservoir effects along the margin. Future research should involve: (1) densifying the ΔR database for the Hikurangi margin, with the northern Hikurangi margin as a high priority at this point; (2) understanding how shell habitat (estuarine vs open coast) affects ^{14}C concentrations to help identify the most appropriate species for dating; and (3) constraining the variability of ΔR through the mid-late Holocene because changing climatic conditions impact ocean circulation and precipitation which in turn can alter ΔR (e.g. Hinojosa et al., 2015). As we see from Section 8.1, small changes in ΔR do not usually significantly alter a paleoearthquake age or event correlations. However, as the precision of radiocarbon dating has improved in recent years (currently $\leq \pm 20$ years), the ability to use very small fractions of organic material increases, and statistical event-age modelling techniques improve, we are able to obtain tighter age ranges for past earthquake and tsunamis. This means that the relative importance of the ΔR uncertainty increases. Future research along the Hikurangi margin will increasingly need higher levels of certainty on the marine reservoir values to keep pace with the resolution of our event dating.

The second underpinning dataset that should be improved along the Hikurangi margin is the record of non-tectonic Holocene RSL change because it is useful for (i) evaluating the completeness of the coastal deformation record, (ii) constraining the amount of coastal deformation that occurred in past earthquakes, and (iii) understanding whether any periods of rapid SL change could be misidentified as coseismic deformation. Advances in understanding non-tectonic RSL change will likely come from the development of RSL curves for other, less tectonically active, parts of New Zealand (e.g. Clement et al., 2016) and modelling to extrapolate RSL change to the Hikurangi margin. In particular, better constraint on the elevations and timing of the mid-Holocene highstand, and the rate of RSL change at the end of the highstand would be informative for calculating uplift-per-event from marine terraces.

The third dataset that needs development along with the subduction earthquake record of the Hikurangi margin is our understanding of upper plate fault characteristics, including fault location, geometry, slip rate and paleoseismology. An example of the importance of upper plate paleoearthquake chronologies is at Mataora/Wairau Lagoon, where subsidence at c. 500 years BP could only be assigned to a subduction earthquake because the timing did not match any paleoearthquakes on local and regional upper plate faults (Clark et al., 2015). In the future, when we endeavour to integrate onshore coastal deformation and submarine turbidite records, understanding the location and rates of activity of offshore upper plate faults will be critical to filtering out upper plate fault earthquakes so that large subduction earthquake signatures can be identified. In short, we cannot neglect the study of upper plate faults due to prioritizing subduction earthquake records, as the two are connected. Furthermore, temporal relationships between large upper plate fault earthquakes and subduction earthquakes may reveal insights into the kinematic processes of how plate boundary motion is accommodated at partitioned oblique subduction zones.

11. Conclusions

The Hikurangi subduction margin has a rich geological history of coseismic coastal deformation and tsunamis, but the isolation of evidence specifically relating to past subduction earthquakes remains challenging. We have reviewed evidence of coseismic coastal deformation and tsunamis from 22 locations along the margin and have produced revised age models of 56 paleoearthquakes. Along-margin temporal correlation of subsidence, uplift and tsunamis provides insights into possible past subduction earthquakes and their spatial extent. We find evidence for 10 past subduction earthquakes on the Hikurangi margin in the past 7000 years. The last subduction earthquake (Corr_Eq1) occurred at 520–470 years BP on the southern Hikurangi margin, it possibly also ruptured the central Hikurangi margin. There is strong evidence for a great subduction earthquake at 870–815 years BP (Corr_Eq2) that ruptured the southern, central and possibly northern Hikurangi margin with a minimum rupture length of

350 km. Of significance, Corr_Eq2 shows full margin rupture of the Hikurangi subduction interface is a possibility. Several of the past possible subduction earthquakes, such as Corr_Eq3, 5 and 7, have weak evidence of subduction interface involvement and they could be explicable by a sequence of upper plate fault earthquakes or failure of the interface in a series of smaller earthquakes. Our compilation of past rupture zones shows no characteristic rupture patches, suggesting segmentation of the margin is not strong, although having few long records in the southern and northern margin makes this assessment difficult beyond 2000 years BP. In the southern region of the margin, long term geological deformation matches that expected for ruptures of the interseismically locked portion of the subduction interface. Subsidence on the central region can only be matched if the region of the interface that currently hosts slow slip events also ruptures, demonstrating different modes of slip behaviour occur on the central Hikurangi margin. Understanding subduction earthquake behaviour on the northern Hikurangi margin remains somewhat elusive, as strong deformation signals from upper plate faults dominate the geological record.

Challenges to the identification of past subduction earthquakes mainly relate to wide age uncertainties on many paleoearthquakes, relatively short records at most locations along the margin, ambiguous and sparse paleotsunami evidence, and the involvement of upper plate faults in producing coastal deformation alike subduction earthquakes. Future Hikurangi margin research will be directed toward obtaining recurrence intervals for large subduction earthquakes at multiple locations along the margin. The current record is too sparse to enable robust calculation of recurrence intervals, and while we see no evidence of earthquake clustering, we cannot yet evaluate the occurrence of earthquake supercycle or quasi-periodic earthquake behaviour as is seen on many other plate boundaries with long earthquake records. In the short-term, improving the paleotsunami record, integration of submarine turbidite records and better constraints on the local marine reservoir correction are areas where significant advances may be made. Longer term improvements on the subduction earthquake record will come from refining and densifying the coastal deformation record, integrating multiple ground shaking proxy records and by obtaining a greater understanding of the kinematic relationship between upper plate faults and the subduction interface.

Supplementary data to this article can be found online at https://doi.org/10.1016/j.margeo.2019.03.004.

Acknowledgements

We would like to acknowledge the significant amount of research undertaken along the Hikurangi margin by our colleagues Yoko Ota and Bruce Hayward, and the many valuable discussions and field trips we have shared with them. We appreciate assistance from Bruce Marshall (Te Papa Tongarewa Museum of New Zealand) for facilitating access to the National Collection for obtaining shells for radiocarbon dating, and Regine Morgenstern (GNS Science) provided GIS assistance. This review has been undertaken with support of the MBIE Strategic Science Investment Fund projects: Tectonics and Structure of Zealandia, and Understanding Earthquakes and Tsunamis, and the MBIE Endeavour Fund project “Hikurangi Subduction Earthquakes and Slip Behaviour, C05X1605”. Support from the Earthquake Commission, Natural Hazards Research Platform and the It's Our Fault programme substantially contributed to many of the studies reviewed in this manuscript. Laura Wallace is thanked for many useful discussions about the Hikurangi margin and review comments. This manuscript was improved thanks to the reviews of Jasper Moernaut, Joao Duarte and 2 anonymous reviewers.

References

Atwater, B.F., 1987. Evidence for great Holocene earthquakes along the outer coast of Washington State. Science 236, 942–944.

Bai, Y., Lay, T., Cheung, K.F., Ye, L., 2017. Two regions of seafloor deformation generated the tsunami for the 13 November 2016, Kaikoura, New Zealand earthquake. Geophys. Res. Lett. https://doi.org/10.1002/2017GL073717.

Barrell, D.J.A., 2015. General distribution and characteristics of active faults and folds in the Kaikoura District, North Canterbury GNS Science Consultancy Report 2014/210. In: Environment Canterbury Report No. R15/23, 59 p.

Barker, D.H.N., Sutherland, R., Henrys, S., Bannister, S., 2009. Geometry of the Hikurangi subduction thrust and upper plate, North Island, New Zealand. Geochem. Geophys. Geosyst. 10, Q02007. https://doi.org/10.1029/2008GC002153.

Barnes, P.M., Audru, J.-C., 1999. Quaternary faulting in the offshore Flaxbourne and Wairarapa Basins, southern Cook Strait, New Zealand. N. Z. J. Geol. Geophys. 42, 349–367.

Barnes, P.M., Mercier de Lepinay, B., 1997. Rates and mechanics of rapid frontal accretion along the very obliquely convergent southern Hikurangi margin, New Zealand. J. Geophys. Res. 102, 24931–24952.

Barnes, P.M., Mercier de Lepinay, B., Collot, J.-Y., Delteil, J., Audru, J.-C., 1998. Strain partitioning in the transition area between oblique subduction and continental collision, Hikurangi margin, New Zealand. Tectonics 17, 534–557.

Barnes, P.M., Nicol, A., Harrison, T., 2002. Late Cenozoic evolution and earthquake potential of an active listric thrust complex above the Hikurangi subduction zone, New Zealand. Geol. Soc. Am. Bull. 114, 1379–1405.

Barnes, P., Lamarche, G., Bialas, J., Henrys, S., Pecher, I., Netzeband, G.L., Greinert, J., Mountjoy, J., Pedley, K., Crutchley, G., 2010. Tectonic and geological framework for gas hydrates and cold seeps on the Hikurangi subduction margin, New Zealand. Mar. Geol. 272, 26–48.

Bartlow, N.M., Wallace, L.M., Beavan, R.J., Bannister, S., Segall, P., 2014. Time-dependent modeling of slow slip events and associated seismicity and tremor at the Hikurangi subduction zone, New Zealand. J. Geophys. Res. Solid Earth 119, 734–753. https://doi.org/10.1002/2013JB010609.

Bassett, D., Sutherland, R., Henrys, S., Stern, T., Scherwath, M., Benson, A., Toulmin, S., Henderson, M., 2010. Three-dimensional velocity structure of the northern Hikurangi margin, Raukumara, New Zealand: implications for the growth of continental crust by subduction erosion and tectonic underplating. Geochem. Geophys. Geosyst. 11, Q10013. https://doi.org/10.1029/2010GC003137.

Beanland, S., 1995. The North Island Dextral Fault Belt, Hikurangi Subduction Margin, New Zealand. School of Earth Sciences. Victoria University of Wellington, New Zealand.

Beanland, S., Haines, J., 1998. The kinematics of active deformation in the North Island, New Zealand, determined from geologic strain rates. N. Z. J. Geol. Geophys. 41, 311–323.

Beavan, J., Darby, D., 2005. Fault slip in the 1855 Wairarapa earthquake based on new and reassessed vertical motion observations: did slip occur on the subduction interface? In: Townend, J., Langridge, R., Jones, A. (Eds.), The 1855 Wairarapa Earthquake Symposium. Greater Wellington Regional Council, Wellington, pp. 31–41.

Begg, J., McSaveney, M., 2005. Wairarapa Fault rupture — vertical deformation in 1855 and a history of similar events from Turakirae Head. In: Townend, J., Langridge, R., Jones, A. (Eds.), The 1855 Wairarapa Earthquake Symposium. Greater Wellington Regional Council, Wellington, pp. 21–31.

Bell, R.E., Sutherland, R., Barker, D.H.N., Henrys, S., Bannister, S., Wallace, L., Beavan, R.J., 2010. Seismic reflection character of the Hikurangi subduction interface, New Zealand, in the region of repeated Gisborne slow slip events. Geophys. J. Int. 180, 34–48. https://doi.org/10.1111/j.1365-1246X.2009.04401.x.

Bell, R., Holden, C., Power, W., Wang, X., Downes, G., 2014. Hikurangi margin tsunami earthquake generated by slow seismic rupture over a subducted seamount. Earth Planet. Sci. Lett. 397, 1–9. https://doi.org/10.1016/j.epsl.2014.04.005.

Berryman, K.R., 1993a. Age, height, and deformation of Holocene terraces at Mahia Peninsula, Hikurangi subduction margin, New Zealand. Tectonics 12, 1347–1364.

Berryman, K.R., 1993b. Distribution, age, and deformation of Late Pleistocene marine terraces at Mahia peninsula, Hikurangi subduction margin, New Zealand. Tectonics 12, 1365–1379.

Berryman, K.R., Ota, Y., Hull, A.G., 1992. Holocene coastal evolution under the influence of episodoc tectonic uplift: examples from New Zealand and Japan. Quat. Int. 15 (16), 31–45.

Berryman, K., Marden, M., Eden, D., Mazengarb, C., Ota, Y., Moriya, I., 2000. Tectonic and paleoclimatic significance of Quaternary river terraces of the Waipaoa river, east coast, North Island, New Zealand. N. Z. J. Geol. Geophys. 43, 229–245. https://doi.org/10.1080/00288306.2000.9514883.

Berryman, K., Ota, Y., Miyauchi, T., Hull, A., Clark, K., Ishibashi, K., Iso, N., Litchfield, N., 2011. Holocene paleoseismic history of upper-plate faults in the Southern Hikurangi subduction margin, New Zealand, deduced from marine terrace records. Bull. Seismol. Soc. Am. 101, 2064–2087. https://doi.org/10.1785/0120100282.

Berryman, K., Clark, K., Cochran, U., Beu, A., Irwin, S., 2018. A geomorphic and tectonic model for the formation of the flight of Holocene marine terraces at Mahia Peninsula, New Zealand. Geomorphology 307, 77–92. https://doi.org/10.1016/j.geomorph.2017.10.014.

Bilek, S.L., Lay, T., 2018. Subduction zone megathrust earthquakes. Geosphere 14, 1468–1500. https://doi.org/10.1130/GES01608.1.

Böttner, C., Gross, F., Geersen, J., Crutchley, G.J., Mountjoy, J.J., Krastel, S., 2018. Marine forearc extension in the Hikurangi margin: new insights from high-resolution 3-D seismic data. Tectonics 37, 1472–1491. https://doi.org/10.1029/2017TC004906.

Briggs, R.W., Sieh, K., Meltzner, A., Natawidjaja, D., Galetzka, J., Suwargadi, B., Hsu, Y., Simons, M., Hananto, N., Suprihanto, I., Prayudi, D., Avouac, J.-P., Prawirodirdjo, L., Bock, Y., 2006. Deformation and slip along the Sunda Megathrust in the great 2005 Nias-Simeulue earthquake. Science 311, 1897.

Briggs, R.W., Engelhart, S.E., Nelson, A.R., Dura, T., Kemp, A.C., Haeussler, P.J., Corbett, D.R., Angster, S.J., Bradley, L.-A., 2014. Uplift and subsidence reveal a nonpersistent megathrust rupture boundary (Sitkinak Island, Alaska). Geophys. Res. Lett. 41, 2289–2296. https://doi.org/10.1002/2014GL059380.
Bronk Ramsey, C., 2008. Deposition models for chronological records. Quat. Sci. Rev. 27, 42–60.
Bronk Ramsey, C., 2009. Bayesian analysis of radiocarbon dates. Radiocarbon 51, 337–360.
Bronk Ramsey, C., Lee, S., 2013. Recent and planned developments of the program OxCal. Radiocarbon 55, 720–730.
Brown, L.J., 1995. Holocene shoreline processes at Poverty Bay, a tectonically active area, northeastern North Island, New Zealand. Quat. Int. 26, 21–33.
Cashman, S.M., Kelsey, H.M., Erdman, C.F., Cutten, H.N.C., Berryman, K.R., 1992. Strain partitioning between structural domains in the forearc of the Hikurangi subduction zone, New Zealand. Tectonics 11, 242–257.
Chagué-Goff, C., Dawson, S., Goff, J.R., Zachariasen, J., Berryman, K.R., Garnett, D.L., Waldron, H.M., Mildenhall, D.C., 2002. A tsunami (ca. 6300 years BP) and other Holocene environmental changes, northern Hawke's Bay, New Zealand. Sediment. Geol. 150, 89–102. https://doi.org/10.1016/S0037-0738(01)00269-X.
Chiswell, S.M., Bostock, H.C., Sutton, P.J.H., Williams, M.J.M., 2015. Physical oceanography of the deep seas around New Zealand: a review. N. Z. J. Mar. Freshw. Res. 49, 286–317. https://doi.org/10.1080/00288330.2014.992918.
Chlieh, M., Avouac, J.P., Sieh, K., Natawidjaja, D.H., Galetzka, J., 2008. Heterogeneous coupling of the Sumatran megathrust constrained by geodetic and paleogeodetic measurements. J. Geophys. Res. Solid Earth 113. https://doi.org/10.1029/2007JB004981.
Cisternas, M., Atwater, B., Torrejon, F., Sawai, Y., Machuca, G., Lagos, M., Eipert, A., Toulton, C., Saldago, I., Kamataki, T., Shishikura, M., Rajendran, C.P., Malik, J., Rizal, Y., Husni, M., 2005. Predecessors of the giant 1960 Chile earthquake. Nature 437, 404–407. https://doi.org/10.1038/nature03943.
Cisternas, M., Carvajal, M., Wesson, R., Ely, L.L., Gorigoitia, N., 2017. Exploring the historical earthquakes preceding the Giant 1960 Chile Earthquake in a time-dependent seismogenic zone. Bull. Seismol. Soc. Am. 107, 2664–2675. https://doi.org/10.1785/0120170103.
Clark, K., Berryman, K., Litchfield, N., Cochran, U., Little, T., 2010. Evaluating the coastal deformation mechanisms of the Raukumara Peninsula, northern Hikurangi subduction margin, New Zealand and insights into forearc uplift processes. N. Z. J. Geol. Geophys. 53, 341–358.
Clark, K., Hayward, B., Cochran, U., Grenfell, H.R., Hemphill-Haley, E., Mildenhall, D., Hemphill-Haley, M., Wallace, L., 2011. Investigating subduction earthquake geology along the southern Hikurangi margin using paleoenvironmental histories of intertidal inlets. N. Z. J. Geol. Geophys. 54, 255–271.
Clark, K.J., Hayward, B.W., Cochran, U.A., Wallace, L.M., Power, W.L., Sabaa, A.T., 2015. Evidence for past subduction earthquakes at a plate boundary with widespread upper plate faulting: Southern Hikurangi Margin, New Zealand. Bull. Seismol. Soc. Am. 105, 1661–1690. https://doi.org/10.1785/0120140291.
Clark, K.J., Nissen, E.K., Howarth, J.D., Hamling, I.J., Mountjoy, J.J., Ries, W.F., Jones, K., Goldstien, S., Cochran, U.A., Villamor, P., Hreinsdóttir, S., Litchfield, N.J., Mueller, C., Berryman, K.R., Strong, D.T., 2017. Highly variable coastal deformation in the 2016 MW7.8 Kaikōura earthquake reflects rupture complexity along a transpressional plate boundary. Earth Planet. Sci. Lett. 474, 334–344. https://doi.org/10.1016/j.epsl.2017.06.048.
Clement, A.J.H., Whitehouse, P.L., Sloss, C.R., 2016. An examination of spatial variability in the timing and magnitude of Holocene relative sea-level changes in the New Zealand archipelago. Quat. Sci. Rev. 131, 73–101. https://doi.org/10.1016/j.quascirev.2015.09.025.
Cochran, U., Berryman, K., Mildenhall, D., Hayward, B., Southall, K., Hollis, C., Barker, P., Wallace, L., Alloway, B., Wilson, K., 2006. Paleoecological insights into subduction zone earthquake occurrence, eastern North Island, New Zealand. Geol. Soc. Am. Bull. 118, 1051–1074.
Cochran, U.A., Hannah, M., Harper, M.A., Van Dissen, R., Berryman, K., Begg, J., 2007. Detection of large, Holocene earthquakes using diatom analysis of coastal sedimentary sequences, Wellington, New Zealand. Quat. Sci. Rev. 26, 1129–1147.
Cochran, U.A., Litchfield, N.J., Clark, K.J., Ries, W.F., Villamor, P., Howarth, J.D., Watson, C., Strong, D.T., 2015. Improved Age Control for a Fourteenth Century Earthquake and Tsunami From Okupe Lagoon, Kapiti Island, GNS Science Report 2015/28. GNS Science, Lower Hutt (p. 37 p. + 34 appendices).
Collot, J.-Y., Marcaillou, B., Sage, F., Michaud, F., Agudelo, W., Charvis, P., Graindorge, D., Gutscher, M.-A., Spence, G., 2004. Are rupture zone limits of great subduction earthquakes controlled by upper plate structures? Evidence from multichannel seismic reflection data acquired across the northern Ecuador–southwest Colombia margin. J. Geophys. Res. Solid Earth 109. https://doi.org/10.1029/2004JB003060.
Collot, J.-Y., Agudelo, W., Ribodetti, A., Marcaillou, B., 2008. Origin of a crustal splay fault and its relation to the seismogenic zone and underplating at the erosional north Ecuador–south Colombia oceanic margin. J. Geophys. Res. Solid Earth 113. https://doi.org/10.1029/2008JB005691.
Coulthard, R.D., Furze, M.F.A., Pieńkowski, A.J., Chantel Nixon, F., England, J.H., 2010. New marine ΔR values for Arctic Canada. Quat. Geochronol. 5, 419–434. https://doi.org/10.1016/j.quageo.2010.03.002.
Cousins, W.J., Zhao, J.X., Perrin, N.D., 1999. A model for the attenuation of peak ground acceleration in New Zealand earthquakes based on seismograph and accelerograph data. Bull. N. Z. Soc. Earthq. Eng. 32, 193–217.
Darby, D., Beanland, S., 1992. Possible source models for the 1855 Wairarapa earthquake, New Zealand. J. Geophys. Res. 97, 12375–12389.
Davy, B., Wood, R., 1994. Gravity and megnetic modelling of the Hikurangu Plateau. Mar. Geol. 118, 139–151.
Doser, D.I., Webb, T.H., 2003. Source parameters of large historical (1917–1961) earthquakes, North Island, New Zealand. Geophys. J. Int. 152, 795–832.
Dowling, L.H., Clark, K.J., Howarth, J., Litchfield, N., Cochran, U., 2018. The Hikurangi Margin Coastal Radiocarbon Age Database, GNS Science Report. GNS Science, Lower Hutt (p. 14.10.21420/G2Q35J).
Downes, G., 2006. The 1904 MS6.8 Mw 7.0–7.2 Cape Turnagain, New Zealand, earthquake. Bull. N. Z. Natl. Soc. Earthquake Eng. 39, 182–207.
Downes, G., Barberopoulou, A., Cochran, U., Clark, K., Scheele, F., 2017. The New Zealand Tsunami Database: historical and modern records. Seismol. Res. Lett. 88 (2), 342–353.
Duckmanton, N.M., 1974. The Shore Platforms of the Kaikoura Peninsula. University of Canterbury, pp. 136.
Dura, T., Cisternas, M., Horton, B.P., Ely, L.L., Nelson, A.R., Wesson, R.L., Pilarczyk, J.E., 2015. Coastal evidence for Holocene subduction-zone earthquakes and tsunamis in central Chile. Quat. Sci. Rev. 113, 93–111. https://doi.org/10.1016/j.quascirev.2014.10.015.
Dura, T., Engelhart, S.E., Vacchi, M., Horton, B.P., Kopp, R.E., Peltier, W.R., Bradley, S., 2016a. The role of Holocene relative sea-level change in preserving records of subduction zone earthquakes. Curr. Clim. Chang. Rep. 2, 86–100. https://doi.org/10.1007/s40641-016-0041-y.
Dura, T., Hemphill-Haley, E., Sawai, Y., Horton, B.P., 2016b. The application of diatoms to reconstruct the history of subduction zone earthquakes and tsunamis. Earth Sci. Rev. 152, 181–197. https://doi.org/10.1016/j.earscirev.2015.11.017.
Ely, L.L., Cisternas, M., Wesson, R.L., Dura, T., 2014. Five centuries of tsunamis and land-level changes in the overlapping rupture area of the 1960 and 2010 Chilean earthquakes. Geology. https://doi.org/10.1130/g35830.1.
Fraser, S., Power, W., Wang, X., Wallace, L., Mueller, C., Johnston, D., 2013. Tsunami inundation in Napier, New Zealand, due to local earthquake sources. Nat. Hazards 1–31. https://doi.org/10.1007/s11069-013-0820-x.
Fujiwara, O., Fujino, S., Komatsubara, J., Morita, Y., Namegaya, Y., 2016. Paleoecological evidence for coastal subsidence during five great earthquakes in the past 1500 years along the northern onshore continuation of the Nankai subduction zone. Quat. Int. 397, 523–540. https://doi.org/10.1016/j.quaint.2015.11.014.
Garrett, E., Shennan, I., Woodroffe, S.A., Cisternas, M., Hocking, E.P., Gulliver, P., 2015. Reconstructing paleoseismic deformation, 2: 1000 years of great earthquakes at Chucalén, south central Chile. Quat. Sci. Rev. 113, 112–122. https://doi.org/10.1016/j.quascirev.2014.10.010.
Garrett, E., Fujiwara, O., Garrett, P., Heyvaert, V.M.A., Shishikura, M., Yokoyama, Y., Hubert-Ferrari, A., Brückner, H., Nakamura, A., De Batist, M., 2016. A systematic review of geological evidence for Holocene earthquakes and tsunamis along the Nankai-Suruga Trough, Japan. Earth Sci. Rev. 159, 337–357.
Gehrels, R., Hayward, B., Newnham, R., Southall, K., 2008. A 20th century acceleration of sea-level rise in New Zealand. Geophys. Res. Lett. 35, LO2717 (doi:2710.1029/2007GL032632).
Goff, J., 2008. Tsunami Hazard Assessment for Hawke's Bay Region, NIWA Report. pp. 30.
Goff, J., Chagué-Goff, C., 2015. Three large tsunamis on the non-subduction, western side of New Zealand over the past 700 years. Mar. Geol. 363, 243–260. https://doi.org/10.1016/j.margeo.2015.03.002.
Goff, J., Crozier, M., Sutherland, V., Cochran, U., Shane, P., 1998. Possible tsunami deposits from the 1855 earthquake, North Island, New Zealand. In: Stewart, I., Vita-Finzi, C. (Eds.), Coastal Tectonics. Geological Society, London, pp. 353–374.
Goff, J.R., Rouse, H.L., Jones, S.L., Hayward, B.W., Cochran, U., McLea, W., Dickinson, W.W., Morley, M.S., 2000. Evidence for an earthquake and tsunami about 3100-3400 yr ago, and other catastrophic saltwater inundations in a coastal lagoon, New Zealand. Mar. Geol. 170, 231–249.
Goff, J.R., McFadgen, B.G., Chague-Goff, C., 2004. Sedimentary differences between the 2002 Easter Storm and the 15th-century Okoropunga tsunami, southeastern North Island, New Zealand. Mar. Geol. 204, 235–250.
Goff, J., Chagué-Goff, C., Nichol, S., Jaffe, B., Dominey-Howes, D., 2012. Progress in palaeotsunami research. Sediment. Geol. 243–244, 70–88. https://doi.org/10.1016/j.sedgeo.2011.11.002.
Goldfinger, C., Nelson, C.H., Morey, A., Johnson, J.E., Gutierrez-Pastor, J., Eriksson, A.T., Karabanov, E., Patton, J., Gracia, E., Enkin, R., Dallimore, A., Dunhill, G., Vallier, T., 2012. Turbidite Event History: Methods and Implications for Holocene Paleoseismicity of the Cascadia Subduction Zone. U.S. Geological Survey Professional Paper 1661-F (170 pp.).
Goldfinger, C., Ikeda, Y., Yeats, R., Ren, J., 2013. Superquakes and supercycles. Seismol. Res. Lett. 84, 24–32. https://doi.org/10.1785/0220110135.
Goldfinger, C., Galer, S., Beeson, J., Hamilton, T., Black, B., Romsos, C., Patton, J., Nelson, C.H., Hausmann, R., Morey, A., 2017. The importance of site selection, sediment supply, and hydrodynamics: A case study of submarine paleoseismology on the northern Cascadia margin, Washington USA. Mar. Geol. 384, 4–46. https://doi.org/10.1016/j.margeo.2016.06.008.
Gomez, B., Corral, Á., Orpin, A.R., Page, M.J., Pouderoux, H., Upton, P., 2015. Lake Tutira paleoseismic record confirms random, moderate to major and/or great Hawke's Bay (New Zealand) earthquakes. Geology 43, 103–106. https://doi.org/10.1130/G36006.1.
González, F.I., Geist, E.L., Jaffe, B., Kânoğlu, U., Mofjeld, H., Synolakis, C.E., Titov, V.V., Arcas, D., Bellomo, D., Carlton, D., Horning, T., Johnson, J., Newman, J., Parsons, T., Peters, R., Peterson, C., Priest, G., Venturato, A., Weber, J., Wong, F., Yalciner, A., 2009. Probabilistic tsunami hazard assessment at Seaside, Oregon, for near- and far-field seismic sources. J. Geophys. Res. Oceans 114. https://doi.org/10.1029/2008JC005132.
Gràcia, E., Vizcaino, A., Escutia, C., Asioli, A., Rodés, Á., Pallàs, R., Garcia-Orellana, J., Lebreiro, S., Goldfinger, C., 2010. Holocene earthquake record offshore Portugal (SW Iberia): testing turbidite paleoseismology in a slow-convergence margin. Quat. Sci.

Rev. 29, 1156–1172. https://doi.org/10.1016/j.quascirev.2010.01.010.
Grapes, R., Downes, G., 1997. The 1855 Wairarapa, New Zealand, Earthquake - analysis of historical data. Bull. N. Z. Natl. Soc. Earthquake Eng. 30, 271–368.
Gutiérrez-Pastor, J., Nelson, C.H., Goldfinger, C., Escutia, C., 2013. Sedimentology of seismo-turbidites off the Cascadia and northern California active tectonic continental margins, northwest Pacific Ocean. Mar. Geol. 336, 99–119. https://doi.org/10.1016/j.margeo.2012.11.010.
Hamling, I.J., Hreinsdóttir, S., Clark, K., Elliott, J., Liang, C., Fielding, E., Litchfield, N., Villamor, P., Wallace, L., Wright, T.J., D'Anastasio, E., Bannister, S., Burbidge, D., Denys, P., Gentle, P., Howarth, J., Mueller, C., Palmer, N., Pearson, C., Power, W., Barnes, P., Barrell, D.J.A., Van Dissen, R., Langridge, R., Little, T., Nicol, A., Pettinga, J., Rowland, J., Stirling, M., 2017. Complex multifault rupture during the 2016 Mw 7.8 Kaikōura earthquake, New Zealand. Science 356. https://doi.org/10.1126/science.aam7194.
Hayward, B.W., Grenfell, H.R., Sabaa, A., Carter, R., Cochran, U., Lipps, J.H., Shane, P., Morley, M.S., 2006. Micropaleontological evidence of large earthquakes in the past 7200 years in southern Hawke's Bay, New Zealand. Quat. Sci. Rev. 25, 1186–1207.
Hayward, B., Grenfell, H.R., Sabaa, A., Kay, J., Daymond-King, R., Cochran, U., 2010a. Holocene subsidence at the transition between strike-slip and subduction on the Pacific-Australian plate boundary, Marlborough Sounds, New Zealand. Quat. Sci. Rev. 29, 648–661 (doi:610.1016/j.quascirev.2009.1011.1021).
Hayward, B., Wilson, K.J., Morley, M., Cochran, U., Grenfell, H.R., Sabaa, A., Daymond-King, R., 2010b. Microfossil record of the Holocene evolution of coastal wetlands in a tectonically active region of New Zealand. The Holocene 30, 405–421.
Hayward, B.W., Grenfell, H.R., Sabaa, A.T., 2012a. Marine submersion of an archaic moa-hunter occupational site, Shag River estuary, North Otago. N. Z. J. Geol. Geophys. 55, 127–136. https://doi.org/10.1080/00288306.2012.671181.
Hayward, B.W., Grenfell, H.R., Sabaa, A.T., Clark, K., 2012b. Foraminiferal evidence for Holocene synclinal folding at Porangahau, southern Hawkes Bay, New Zealand. N. Z. J. Geol. Geophys. 55, 21–35. https://doi.org/10.1080/00288306.2011.615845.
Hayward, B.W., Grenfell, H.R., Sabaa, A.T., Clark, K.J., Cochran, U.A., Palmer, A.S., 2015a. Subsidence-driven environmental change in three Holocene embayments of Ahuriri Inlet, Hikurangi Subduction Margin, New Zealand. N. Z. J. Geol. Geophys. 58, 344–363. https://doi.org/10.1080/00288306.2015.1077872.
Hayward, B.W., Sabaa, A.T., Grenfell, H.R., Cochran, U.A., Clark, K.J., Litchfield, N.J., Wallace, L., Marden, M., Palmer, A.S., 2015b. Foraminiferal record of Holocene paleo-earthquakes on the subsiding south-western Poverty Bay coastline, New Zealand. N. Z. J. Geol. Geophys. 58, 104–122. https://doi.org/10.1080/00288306.2014.992354.
Hayward, B.W., Grenfell, H.R., Sabaa, A.T., Cochran, U.A., Clark, K.J., Wallace, L., Palmer, A.S., 2016. Salt-marsh foraminiferal record of 10 large Holocene (last 7500 yr) earthquakes on a subducting plate margin, Hawkes Bay, New Zealand. Geol. Soc. Am. Bull. 128, 896–915. https://doi.org/10.1130/b31295.1.
Heise, W., Caldwell, T.G., Bannister, S., Bertrand, E.A., Ogawa, Y., Bennie, S.L., Ichihara, H., 2017. Mapping subduction interface coupling using magnetotellurics: Hikurangi margin, New Zealand. Geophys. Res. Lett. 44, 9261–9266. https://doi.org/10.1002/2017GL074641.
Higham, T.F.G., Hogg, A.G., 1995. Radiocarbon dating of prehistoric shell from New Zealand and calculation of the ΔR value using fish otoliths. Radiocarbon 37, 409–416.
Hinojosa, J.L., Moy, C.M., Prior, C.A., Eglinton, T.I., McIntyre, C.P., Stirling, C.H., Wilson, G.S., 2015. Investigating the influence of regional climate and oceanography on marine radiocarbon reservoir ages in southwest New Zealand. Estuar. Coast. Shelf Sci. 167 (Part B), 526–539. https://doi.org/10.1016/j.ecss.2015.11.003.
Hogg, A.G., Hua, Q., Blackwell, P.G., Niu, M., Buck, C.E., Guilderson, T.P., Heaton, T.J., Palmer, J.G., Reimer, P.J., Reimer, R.W., Turney, C.S.M., Zimmerman, S.R.H., 2013. SHCal13 Southern Hemisphere calibration, 0–50,000 years cal BP. Radiocarbon 55. https://doi.org/10.2458/azu_js_rc.55.16783.
Howarth, J.D., Fitzsimons, S.J., Norris, R.J., Jacobsen, G.E., 2012. Lake sediments record cycles of sediment flux driven by large earthquakes on the Alpine fault, New Zealand. Geology 40, 1091–1094. https://doi.org/10.1130/g33486.1.
Howarth, J.D., Fitzsimons, S.J., Norris, R.J., Jacobsen, G.E., 2014. Lake sediments record high intensity shaking that provides insight into the location and rupture length of large earthquakes on the Alpine Fault, New Zealand. Earth Planet. Sci. Lett. 403, 340–351. https://doi.org/10.1016/j.epsl.2014.07.008.
Howarth, J., Fitzsimons, S.J., Norris, R., Langridge, R., Vandergoes, M., 2016. A 2000 year rupture history for the Alpine Fault derived from Lake Ellery, South Island, New Zealand. Geol. Soc. Am. Bull. 128, 627–643.
Hull, A., 1986. Pre-A.D. 1931 tectonic subsidence of Ahuriri Lagoon, Napier, Hawkes Bay, New Zealand. N. Z. J. Geol. Geophys. 29, 75–82.
Hull, A.G., 1987. A late Holocene marine terrace on the Kidnappers Coast, North Island, New Zealand: some implications for shore platform development processes and uplift mechanisms. Quat. Res. 28, 183–195.
Hull, A.G., 1990. Tectonics of the 1931 Hawke's Bay earthquake. N. Z. J. Geol. Geophys. 33, 309–320.
Jara-Muñoz, J., Melnick, D., Brill, D., Strecker, M.R., 2015. Segmentation of the 2010 Maule Chile earthquake rupture from a joint analysis of uplifted marine terraces and seismic-cycle deformation patterns. Quat. Sci. Rev. 113, 171–192. https://doi.org/10.1016/j.quascirev.2015.01.005.
Kanamori, H., 1972. Mechanism of tsunami earthquakes. Phys. Earth Planet. Inter. 6, 346–359. https://doi.org/10.1016/0031-9201(72)90058-1.
Kelsey, H.M., Nelson, A.R., Hemphill-Haley, E., Witter, R.C., 2005. Tsunami history of an Oregon coastal lake reveals a 4600 yr record of great earthquakes on the cascadia subduction zone. Geol. Soc. Am. Bull. 117, 1009–1032.
Kelsey, H.M., Engelhart, S.E., Pilarczyk, J.E., Horton, B.P., Rubin, C.M., Daryono, M.R., Ismail, N., Hawkes, A.D., Bernhardt, C.E., Cahill, N., 2015a. Accommodation space, relative sea level, and the archiving of paleo-earthquakes along subduction zones. Geology 43, 675–678. https://doi.org/10.1130/g36706.1.
Kelsey, H.M., Witter, R.C., Engelhart, S.E., Briggs, R., Nelson, A., Haeussler, P., Corbett, D.R., 2015b. Beach ridges as paleoseismic indicators of abrupt coastal subsidence during subduction zone earthquakes, and implications for Alaska-Aleutian subduction zone paleoseismology, southeast coast of the Kenai Peninsula, Alaska. Quat. Sci. Rev. 113, 147–158. https://doi.org/10.1016/j.quascirev.2015.01.006.
Kempf, P., Moernaut, J., Van Daele, M., Vandoorne, W., Pino, M., Urrutia, R., De Batist, M., 2017. Coastal lake sediments reveal 5500 years of tsunami history in south central Chile. Quat. Sci. Rev. 161, 99–116. https://doi.org/10.1016/j.quascirev.2017.02.018.
King, D.N., Goff, J.R., Chagué-Goff, C., McFadgen, B., Jacobsen, G.E., Gadd, P., Horrocks, M., 2017. Reciting the layers: Evidence for past tsunamis at Mataora-Wairau Lagoon, Aotearoa-New Zealand. Mar. Geol. 389, 1–16. https://doi.org/10.1016/j.margeo.2017.05.001.
King, D.N., Shaw, W.S., Meihana, P.N., Goff, J.R., 2018. Māori oral histories and the impact of tsunamis in Aotearoa-New Zealand. Nat. Hazards Earth Syst. Sci. 18, 907–919. https://doi.org/10.5194/nhess-18-907-2018.
Langridge, R.M., Ries, W.F., Litchfield, N.J., Villamor, P., Van Dissen, R.J., Barrell, D.J.A., Rattenbury, M.S., Heron, D.W., Haubrock, S., Townsend, D.B., Lee, J.M., Berryman, K.R., Nicol, A., Cox, S.C., Stirling, M.W., 2016. The New Zealand Active Faults Database. N. Z. J. Geol. Geophys. 59, 86–96. https://doi.org/10.1080/00288306.2015.1112818.
Lay, T., 2015. The surge of great earthquakes from 2004 to 2014. Earth Planet. Sci. Lett. 409, 133–146. https://doi.org/10.1016/j.epsl.2014.10.047.
Li, S., Moreno, M., Rosenau, M., Melnick, D., Oncken, O., 2014. Splay fault triggering by great subduction earthquakes inferred from finite element models. Geophys. Res. Lett. 41, 385–391. https://doi.org/10.1002/2013GL058598.
Litchfield, N.J., Clark, K.J., 2015. Fluvial terrace formation in the lower Awhea and Pahaoa River valleys, New Zealand: implications for tectonic and sea-level controls. Geomorphology 231, 212–228. https://doi.org/10.1016/j.geomorph.2014.12.009.
Litchfield, N.J., Ellis, S., Berryman, K., Nicol, A., 2007. Insights into subduction-related uplift along the Hikurangi Margin, New Zealand, using numerical modeling. J. Geophys. Res. Earth Surf. 112, F02021 (doi:02010.01029/02006JF000535).
Litchfield, N., Wilson, K., Berryman, K., Wallace, L., 2010. Coastal uplift mechanisms at Pakarae River mouth: constraints from a combined Holocene fluvial and marine terrace dataset. Mar. Geol. 270, 72–83.
Litchfield, N.J., Cochran, U.A., Berryman, K.R., Ansell, B., Clark, K., 2013. Timing and amount of uplift of the youngest Holocene marine terrace along the Honeycomb Rock – Riversdale Beach coast, eastern Wairarapa. In: GNS Science Report 2013/54, (44 pp. http://www.gns.cri.nz/static/pubs/2013/SR%202013-202054.pdf).
Litchfield, N.J., Van Dissen, R., Sutherland, R., Barnes, P.M., Cox, S.C., Norris, R., Beavan, R.J., Langridge, R., Villamor, P., Berryman, K., Stirling, M., Nicol, A., Nodder, S., Lamarche, G., Barrell, D.J.A., Pettinga, J.R., Little, T., Pondard, N., Mountjoy, J.J., Clark, K., 2014. A model of active faulting in New Zealand. N. Z. J. Geol. Geophys. 57, 32–56. https://doi.org/10.1080/00288306.2013.854256.
Litchfield, N., Cochran, U., Berryman, K., Clark, K., McFadgen, B., Steele, R., 2016. Gisborne Seismic and Tsunami Hazard: Constraints From Marine Terraces at Puatai Beach, 2016/21. 99 pp., GNS Science Report. Institute of Geological and Nuclear Sciences, Lower Hutt, pp. 99.
Litchfield, N., Clark, K.J., Miyauchi, T., Berryman, K., Barrell, D., Brown, L., Ota, Y., Fujimori, T., 2017. Holocene marine terraces record long-term uplift along the Kaikōura coastline. In: Clark, K.J., Upton, P., Langridge, R., Kelly, K., Hammond, K. (Eds.), Proceedings of the 8th International INQUA Meeting on Paleoseismology, Active Tectonics and Archeoseismology. Handbook and Programme, 13–16 November 2017. GNS Science, Blenheim, pp. 244–247. https://doi.org/10.21420/G2H061.
Litchfield, N.J., Villamor, P., Dissen, R.J.V., Nicol, A., Barnes, P.M., A. Barrell, D.J., Pettinga, J.R., Langridge, R.M., Little, T.A., Mountjoy, J.J., Ries, W.F., Rowland, J., Fenton, C., Stirling, M.W., Kearse, J., Berryman, K.R., Cochran, U.A., Clark, K.J., Hemphill-Haley, M., Khajavi, N., Jones, K.E., Archibald, G., Upton, P., Asher, C., Benson, A., Cox, S.C., Gasston, C., Hale, D., Hall, B., Hatem, A.E., Heron, D.W., Howarth, J., Kane, T.J., Lamarche, G., Lawson, S., Lukovic, B., McColl, S.T., Madugo, C., Manousakis, J., Noble, D., Pedley, K., Sauer, K., Stahl, T., Strong, D.T., Townsend, D.B., Toy, V., Williams, J., Woelz, S., Zinke, R., 2018a. Surface rupture of multiple crustal faults in the 2016 Mw 7.8 Kaikōura, New Zealand, Earthquake. Bull. Seismol. Soc. Am. 108, 1496–1520. https://doi.org/10.1785/0120170300.
Litchfield, N.J., Clark, K., Cochran, U., Palmer, A., Mountjoy, J., Mueller, C., Morgenstern, R., Berryman, K., McFadgen, B., Steele, R., Reitman, N., Howarth, J., Villamor, P., 2018b. Marine terrace paleoseismology reveals complex nearshore upper plate faulting in the northern Hikurangi Margin, New Zealand. Mar. Geol (November; submitted).
Little, T.A., Van Dissen, R., Schermer, E., Carne, R., 2009. Late Holocene surface ruptures on the southern Wairarapa fault, New Zealand: link between earthquakes and the uplifting of beach ridges on a rocky coast. Lithosphere 1, 4–28.
Little, T.A., Van Dissen, R., Kearse, J., Norton, K., Benson, A., Wang, N., 2018. Kekerengu Fault, New Zealand: timing and size of late Holocene surface ruptures. Bull. Seismol. Soc. Am. 108, 1556–1572. https://doi.org/10.1785/0120170152.
Loveless, J.P., Meade, B.J., 2011. Spatial correlation of interseismic coupling and co-seismic rupture extent of the 2011 MW = 9.0 Tohoku-oki earthquake. Geophys. Res. Lett. 38, L17306.
Lowe, D.J., Shane, P.A.R., Alloway, B.V., Newnham, R.M., 2008. Fingerprints and age models for widespread New Zealand tephra marker beds erupted since 30,000 years ago: a framework for NZ-INTIMATE. Quat. Sci. Rev. 27, 95–126. https://doi.org/10.1016/j.quascirev.2007.01.013.
Lowe, D.J., Blaauw, M., Hogg, A.G., Newnham, R.M., 2013. Ages of 24 widespread

tephras erupted since 30,000 years ago in New Zealand, with re-evaluation of the timing and palaeoclimatic implications of the Lateglacial cool episode recorded at Kaipo bog. Quat. Sci. Rev. 74, 170–194. https://doi.org/10.1016/j.quascirev.2012.11.022.
Marshall, J.S., Anderson, R.S., 1995. Quaternary uplift and seismic cycle deformation, Peninsula de Nicoya, Costa Rica. Geol. Soc. Am. Bull. 107, 463–473.
McFadgen, B., 1980. Maori Plaggen Soils in New Zealand: their origin and properties. J. R. Soc. N. Z. 10, 3–18.
McFadgen, B.G., 1987. Beach ridges, breakers and bones: late Holocene geology and archaeology of the Fyffe site, S49/46, Kaikoura Peninsula, New Zealand. J. R. Soc. N. Z. 17, 381–394.
McFadgen, B., Manning, M., 1990. Calibrating New Zealand radiocarbon dates of marine shells. Radiocarbon 32, 229–232. https://doi.org/10.1017/S0033822200040194.
McGinty, P., Darby, D., Haines, J., 2001. Earthquake triggering in the Hawke's Bay, New Zealand, region from 1931 to 1934 as inferred from elastic dislocation and static stress modeling. J. Geophys. Res. Solid Earth 106, 26593–26604. https://doi.org/10.1029/2000JB000031.
McSaveney, M., Graham, I., Begg, J., Beu, A., Hull, A., Kim, K., Zondervan, A., 2006. Late Holocene uplift of beach ridges at Turakirae Head, south Wellington coast, New Zealand. N. Z. J. Geol. Geophys. 49, 337–358.
Melnick, D., Bookhagen, B., Strecker, M.R., Echtler, H.P., 2009. Segmentation of megathrust rupture zones from fore-arc deformation patterns over hundreds to millions of years, Arauco peninsula, Chile. J. Geophys. Res. Solid Earth 114. https://doi.org/10.1029/2008JB005788.
Melnick, D., Moreno, M., Motagh, M., Cisternas, M., Wesson, R.L., 2012. Splay fault slip during the Mw 8.8 2010 Maule Chile earthquake. Geology 40, 251–254. https://doi.org/10.1130/g32712.1.
Merritts, D.J., 1996. The Mendecino triple junction: active faults, episodic coastal emergence, and rapid uplift. J. Geophys. Res. 101, 6051–6070.
Meyers, R.A., Smith, D.G., Jol, H.M., Peterson, C.D., 1996. Evidence for eight great earthquake-subsidence events detected with ground-penetrating radar, Willapa barrier, Washington. Geology 24, 99–102. https://doi.org/10.1130/0091-7613(1996)024<0099:EFEGES>2.3.CO;2.
Miura, S., Suwa, Y., Hasegawa, A., Nishimura, T., 2004. The 2003 M8.0 Tokachi-Oki earthquake – how much has the great event paid back slip debts? Geophys. Res. Lett. 31. https://doi.org/10.1029/2003GL019021.
Miyauchi, T., Ota, Y., Hull, A.G., 1989. Holocene marine terraces and tectonic uplift in the Waimarama coastal plain, eastern North Island, New Zealand. N. Z. J. Geol. Geophys. 32, 437–442.
Moernaut, J., Daele, M.V., Heirman, K., Fontijn, K., Strasser, M., Pino, M., Urrutia, R., De Batist, M., 2014. Lacustrine turbidites as a tool for quantitative earthquake reconstruction: New evidence for a variable rupture mode in south central Chile. J. Geophys. Res. Solid Earth 119, 1607–1633. https://doi.org/10.1002/2013JB010738.
Moernaut, J., Van Daele, M., Fontijn, K., Heirman, K., Kempf, P., Pino, M., Valdebenito, G., Urrutia, R., Strasser, M., De Batist, M., 2018. Larger earthquakes recur more periodically: New insights in the megathrust earthquake cycle from lacustrine turbidite records in south-central Chile. Earth Planet. Sci. Lett. 481, 9–19. https://doi.org/10.1016/j.epsl.2017.10.016.
Moreno, M., Rosenau, M., Oncken, O., 2010. 2010 Maule earthquake slip correlates with pre-seismic locking of Andean subduction zone. Nature 467, 198–202. https://doi.org/10.1038/nature09349.
Morey, A.E., Goldfinger, C., Briles, C.E., Gavin, D.G., Colombaroli, D., Kusler, J.E., 2013. Are great Cascadia earthquakes recorded in the sedimentary records from small forearc lakes? Nat. Hazards Earth Syst. Sci. 13, 1–23.
Mountjoy, J.J., Barnes, P.M., 2011. Active upper plate thrust faulting in regions of low plate interface coupling, repeated slow slip events, and coastal uplift: Example from the Hikurangi Margin, New Zealand. Geochem. Geophys. Geosyst. 12, Q01005. https://doi.org/10.1029/2010gc003326.
Mountjoy, J.J., Barnes, P.M., Pettinga, J.R., 2009. Morphostructure and evolution of submarine canyons across an active margin: Cook Strait sector of the Hikurangi Margin, New Zealand. Mar. Geol. 260, 45–68. https://doi.org/10.1016/j.margeo.2009.01.006.
Mountjoy, J.J., Howarth, J.D., Orpin, A.R., Barnes, P.M., Bowden, D.A., Rowden, A.A., Schimel, A.C.G., Holden, C., Horgan, H.J., Nodder, S.D., Patton, J.R., Lamarche, G., Gerstenberger, M., Micallef, A., Pallentin, A., Kane, T., 2018. Earthquakes drive large-scale submarine canyon development and sediment supply to deep-ocean basins. Sci. Adv. 4. https://doi.org/10.1126/sciadv.aar3748.
Mueller, C.S., Briggs, R.W., Wesson, R.L., Petersen, M.D., 2015. Updating the USGS seismic hazard maps for Alaska. Quat. Sci. Rev. 113, 39–47. https://doi.org/10.1016/j.quascirev.2014.10.006.
Nelson, A.R., Shennan, I., Long, A.J., 1996. Identifying coseismic subsidence in tidal-wetland stratigraphic sequences at the Cascadia subduction zone of western North America. J. Geophys. Res. 101, 6115–6135.
Nelson, A.R., Kelsey, H.M., Witter, R.C., 2006. Great earthquakes of variable magnitude at the Cascadia subduction zone. Quat. Res. 65, 354–365 (wall10.1016/j.yqres.2006.02.009).
Nelson, A.R., Kashima, K., Bradley, L., 2009. Fragmentary evidence of great-earthquake subsidence during Holocene emergence, Valdivia Estuary, south central Chile. Bull. Seismol. Soc. Am. 99, 71–86.
Nelson, A.R., Briggs, R., Dura, T., Engelhart, S.E., Gelfenbaum, G., Bradley, L.-A., Forman, S.L., Vane, C.H., Kelley, K.A., 2015. Tsunami recurrence in the eastern Alaska-Aleutian arc: a Holocene stratigraphic record from Chirikof Island, Alaska. Geosphere 11 (4), 1174–1203.
Nicol, A., Beavan, J., 2003. Shortening of an overriding plate and its implications for slip on a subduction thrust, central Hikurangi margin, New Zealand. Tectonics 22, 1070 (doi:1010.1029/2003TC001521).
Ninis, D., 2018. Upper Plate Deformation and Its Relationship to the Underlying Hikurangi Subduction Interface, Southern North Island, New Zealand. Victoria University of Wellington.
Nodder, S.D., Lamarche, G., Proust, J.-N., Stirling, M., 2007. Characterizing earthquake recurrence parameters for offshore faults in the low-strain, compressional Kapiti-Manawatu Fault System, New Zealand. J. Geophys. Res. 112, B12102. https://doi.org/10.1029/2007jb005019.
NZPD, 2018. New Zealand Paleotsunami Database. https://ptdb.niwa.co.nz.
Orpin, A.R., Carter, L., Page, M.J., Cochran, U.A., Trustrum, N.A., Gomez, B., Palmer, A.S., Mildenhall, D.C., Rogers, K.M., Brackley, H.L., Northcote, L., 2010. Holocene sedimentary record from Lake Tutira: A template for upland watershed erosion proximal to the Waipaoa Sedimentary System, northeastern New Zealand. Mar. Geol. 270, 11–29. https://doi.org/10.1016/j.margeo.2009.10.022.
Ota, Y., Williams, D., Berryman, K., 1981. Late Quaternary Tectonic Map of New Zealand, Parts Sheets Q27, R27 & R28, Wellington, Late Quaternary Tectonic Map of New Zealand 1:50,000. Department of Scientific and Industrial Research, Wellington (p. 1 map + 1 booklet).
Ota, Y., Berryman, K.R., Hull, A.G., Miyauchi, T., Iso, N., 1988. Age and height distribution of Holocene transgressive deposits in eastern North Island, New Zealand. Palaeogeogr. Palaeoclimatol. Palaeoecol. 68, 135–151.
Ota, Y., Berryman, K.R., Brown, L.J., Kashima, K., 1989. Holocene sediments and vertical tectonic downwarping near Wairoa, Northern Hawkes Bay, New Zealand. N. Z. J. Geol. Geophys. 32, 333–341.
Ota, Y., Berryman, K., Fellows, D., Hull, A., Ishibashi, K., Iso, N., Miyauchi, T., Miyoshi, M., Yamasina, K., 1990a. Sections and profiles for the study of Holocene coastal tectonics, Gisborne - Cape Palliser, North Island, New Zealand. New Zealand Geologocal Survey Record. 42 DSIR Geology and Geophysics, Lower Hutt, New Zealand.
Ota, Y., Miyauchi, T., Hull, A.G., 1990b. Holocene marine terraces at Aramoana and Pourerere. N. Z. J. Geol. Geophys. 33, 541–546.
Ota, Y., Hull, A.G., Berryman, K.R., 1991. Coseismic uplift of Holocene marine terraces in the Pakarae River area, eastern North Island. New Zealand. Quaternary Research 35, 331–346.
Ota, Y., Hull, A.G., Iso, N., Ikeda, Y., Moriya, I., Yoshikawa, T., 1992. Holocene marine terraces on the northeast coast of North Island, New Zealand, and their tectonic significance. N. Z. J. Geol. Geophys. 35, 273–288.
Ota, Y., Brown, L.J., Berryman, K.R., Fujimori, T., Miyauchi, T., Beu, A.G., Kashima, K., Taguchi, K., 1995. Vertical tectonic movement in northeastern Marlborough: stratigraphic, radiocarbon, and paleoecological data from Holocene estuaries. N. Z. J. Geol. Geophys. 38, 269–282.
Ota, Y., Pillans, B., Berryman, K., Beu, A., Fujimori, T., Miyauchi, T., Berger, G., Beu, A., Climo, F., 1996. Pleistocene coastal terraces of Kaikoura Peninsula and the Marlborough Coast, South Island, New Zealand. N. Z. J. Geol. Geophys. 39, 51–73.
Paquet, F., Proust, J.-N., Barnes, P., Pettinga, J., 2009. Inner-forearc sequence architecture in response to climatic and tectonic forcing since 150 ka: Hawke's Bay, New Zealand. J. Sediment. Res. 79, 97–124. https://doi.org/10.2110/jsr.2009.019.
Park, J.-O., Tsuru, T., Kodaira, S., Cummins, P.R., Kaneda, Y., 2002. Splay fault branching along the Nankai subduction zone. Science 297, 1157–1160.
Patton, J.R., Goldfinger, C., Morey, A.E., Ikehara, K., Romsos, C., Stoner, J., Djadjadihardja, Y., Udrekh, Ardhyastuti, S., Gaffar, E.Z., Vizcaino, A., 2015. A 6600 year earthquake history in the region of the 2004 Sumatra-Andaman subduction zone earthquake. Geosphere 11, 2067–2129. https://doi.org/10.1130/GES01066.1.
Philibosian, B., Sieh, K., Avouac, J.P., Natawidjaja, D.H., Chiang, H.W., Wu, C.C., Shen, C.C., Daryono, M.R., Perfettini, H., Suwargadi, B.W., Lu, Y., Wang, X., 2017. Earthquake supercycles on the Mentawai segment of the Sunda megathrust in the seventeenth century and earlier. J. Geophys. Res. Solid Earth 122, 642–676. https://doi.org/10.1002/2016JB013560.
Pilarczyk, J.E., Dura, T., Horton, B.P., Engelhart, S.E., Kemp, A.C., Sawai, Y., 2014. Microfossils from coastal environments as indicators of paleo-earthquakes, tsunamis and storms. Palaeogeogr. Palaeoclimatol. Palaeoecol. 413, 144–157. https://doi.org/10.1016/j.palaeo.2014.06.033.
Pillans, B., Huber, P., 1995. Interpreting coseismic deformation using Holocene coastal deposits, Wellington, New Zealand. Quat. Int. 26, 87–95.
Plafker, G., 1967. Surface Faults on Montague Island Associated With the 1964 Alaska Earthquake. U.S. Geological Survey Professional Paper 543-G (42 pp.).
Pondard, N., Barnes, P.M., 2010. Structure and paleoearthquake records of active submarine faults, Cook Strait, New Zealand: Implications for fault interactions, stress loading, and seismic hazard. J. Geophys. Res. 115, B12320. https://doi.org/10.1029/2010jb007781.
Pouderoux, H., Proust, J.-N., Lamarche, G., Orpin, A., Neil, H., 2012a. Postglacial (after 18 ka) deep-sea sedimentation along the Hikurangi subduction margin (New Zealand): characterisation, timing and origin of turbidites. Mar. Geol. 295–298, 51–76. https://doi.org/10.1016/j.margeo.2011.11.002.
Pouderoux, H., Lamarche, G., Proust, J.-N., 2012b. Building an 18,000-year-long paleoearthquake record from detailed deep-sea turbidite characterisation in Poverty Bay, New Zealand. Nat. Hazards Earth Syst. Sci. 12, 2077–2101. https://doi.org/10.5194/nhess-12-2077-2012.
Pouderoux, H., Proust, J.-N., Lamarche, G., 2014. Submarine paleoseismology of the northern Hikurangi subduction margin of New Zealand as deduced from Turbidite record since 16 ka. Quat. Sci. Rev. 84, 116–131. https://doi.org/10.1016/j.quascirev.2013.11.015.
Power, W., Clark, K., King, D.N., Borrero, J., Howarth, J., Lane, E.M., Goring, D., Goff, J., Chagué-Goff, C., Williams, J., Reid, C., Whittaker, C., Mueller, C., Williams, S., Hughes, M.W., Hoyle, J., Bind, J., Strong, D., Litchfield, N., Benson, A., 2017. Tsunami runup and tide-gauge observations from the 14 November 2016 M7.8 Kaikōura earthquake, New Zealand. Pure Appl. Geophys. 174, 2457–2473. https://

doi.org/10.1007/s00024-017-1566-2.
Praet, N., Moernaut, J., Van Daele, M., Boes, E., Haeussler, P.J., Strupler, M., Schmidt, S., Loso, M.G., De Batist, M., 2017. Paleoseismic potential of sublacustrine landslide records in a high-seismicity setting (south-central Alaska). Mar. Geol. 384, 103–119. https://doi.org/10.1016/j.margeo.2016.05.004.
Priest, G.R., Witter, R.C., Zhang, Y.J., Goldfinger, C., Wang, K., Allan, J.C., 2017. New constraints on coseismic slip during southern Cascadia subduction zone earthquakes over the past 4600 years implied by tsunami deposits and marine turbidites. Nat. Hazards 88, 285–313. https://doi.org/10.1007/s11069-017-2864-9.
Protti, M., González, V., Newman, A.V., Dixon, T.H., Schwartz, S.Y., Marshall, J.S., Feng, L., Walter, J.I., Malservisi, R., Owen, S.E., 2013. Nicoya earthquake rupture anticipated by geodetic measurement of the locked plate interface. Nat. Geosci. 7, 117–121.
Ramírez-Herrera, M.T., Kostoglodov, V., Urrutia-Fucugauchi, J., 2011. Overview of recent coastal tectonic deformation in the Mexican subduction zone. Pure Appl. Geophys. 168, 1415–1433. https://doi.org/10.1007/s00024-010-0205-y.
Reimer, P.J., Reimer, R.W., 2001. A marine reservoir correction database and on-line interface. Radiocarbon 43, 461–463. https://doi.org/10.1017/S0033822200038339.
Reimer, P.J., Bard, E., Bayliss, A., Beck, J.W., Blackwell, P.G., Bronk Ramsey, C., Grootes, P.M., Guilderson, T.P., Haflidason, H., Hajdas, I., Hatt, C., Heaton, T.J., Hoffmann, D.L., Hogg, A.G., Hughen, K.A., Kaiser, K.F., Kromer, B., Manning, S.W., Niu, M., Reimer, R.W., Richards, D.A., Scott, E.M., Southon, J.R., Staff, R.A., Turney, C.S.M., van der Plicht, J., 2013. IntCal13 and Marine13 radiocarbon age calibration curves 0–50,000 years cal BP. Radiocarbon 55, 1869–1887.
Rodgers, D., Little, T., 2006. World's largest coseismic strike-slip offset: the 1855 rupture of the Wairarapa Fault, New Zealand, and implications for displacement/length scaling of continental earthquakes. J. Geophys. Res. 111. https://doi.org/10.1029/2005JB004065.
Rubin, C.M., Horton, B.P., Sieh, K., Pilarczyk, J.E., Daly, P., Ismail, N., Parnell, A.C., 2017. Highly variable recurrence of tsunamis in the 7400 years before the 2004 Indian Ocean tsunami. Nat. Commun. 8, 16019. https://doi.org/10.1038/ncomms16019.
Sato, Y., Fujiwara, O., 2017. Microfossil evidence for recurrent coseismic subsidence around Lake Hamana, near the Nankai-Suruga trough, central Japan. Quat. Int. 456, 39–52. https://doi.org/10.1016/j.quaint.2017.08.040.
Sawai, Y., Namegaya, Y., Okamura, Y., Satake, K., Shishikura, M., 2012. Challenges of anticipating the 2011 Tohoku earthquake and tsunami using coastal geology. Geophys. Res. Lett. 39https://doi.org/10.1029/2012GL053692. n/a-n/a.
Shanmugam, G., 2012. Process-sedimentological challenges in distinguishing paleo-tsunami deposits. Nat. Hazards 63, 5–30. https://doi.org/10.1007/s11069-011-9766-z.
Shennan, I., Hamilton, S., 2006. Coseismic and pre-seismic subsidence associated with great earthquakes in Alaska. Quat. Sci. Rev. 25, 1–8.
Shennan, I., Bruhn, R., Barlow, N., Good, K., Hocking, E., 2014. Late Holocene great earthquakes in the eastern part of the Aleutian megathrust. Quat. Sci. Rev. 84, 86–97. https://doi.org/10.1016/j.quascirev.2013.11.010.
Shennan, I., Garrett, E., Barlow, N., 2016. Detection limits of tidal-wetland sequences to identify variable rupture modes of megathrust earthquakes. Quat. Sci. Rev. 150, 1–30. https://doi.org/10.1016/j.quascirev.2016.08.003.
Sieh, K., Natawidjaja, D.H., Meltzner, A.J., Shen, C.-C., Cheng, H., Li, K.-S., Suwargadi, B.W., Galetzka, J., Philibosian, B., Edwards, L., 2008. Earthquake supercycles inferred from sea-level changes recorded in the corals of West Sumatra. Science 322, 1674–1678.
Sikes, E.L., Guilderson, T.P., 2016. Southwest Pacific Ocean surface reservoir ages since the last glaciation: Circulation insights from multiple-core studies. Paleoceanography 31 (2), 298–310. https://doi.org/10.1002/2015PA002855.
Sikes, E.L., Samso, C.R., Guilderson, T.P., Howard, W.R., 2000. Old radiocarbon ages in the southwest Pacific Ocean during the last glacial period and deglaciation. Nature 405, 555–559.
Singh, L., 1971. Uplift and tilting of the Oterei Coast, Wairarapa, New Zealand, during the last ten thousand years. In: Recent Crustal Movements. 9. Royal Society of New Zealand Bulletin, pp. 217–219.
Song, T.-R.A., Simons, M., 2003. Large trench-parallel gravity variations predict seismogenic behavior in subduction zones. Science 301, 630–633. https://doi.org/10.1126/science.1085557.
Stirling, M., McVerry, G., Gerstenberger, M., Litchfield, N., Van Dissen, R., Berryman, K., Barnes, P., Wallace, L., Bradley, B., Villamor, P., Langridge, R., Lamarche, G., Nodder, S., Reyners, M., Rhoades, D.A., Smith, W., Nicol, A., Pettinga, J.R., Clark, K., Jacobs, K., 2012. National seismic hazard model for New Zealand: 2010 update. Bull. Seismol. Soc. Am. 102, 1514–1542 (doi:1510.1785/0120110170).
Taylor, F.W., Frohlich, C., Lecolle, J., Strecker, M., 1987. Analysis of partially emerged corals and reef terraces in the central Vanuatu Arc: comparison of contemporary coseismic and nonseismic with quaternary vertical movements. J. Geophys. Res. Solid Earth 92, 4905–4933. https://doi.org/10.1029/JB092iB06p04905.
Van Daele, M., Araya-Cornejo, C., Pille, T., Vanneste, K., Moernaut, J., Schmidt, S., Kempf, P., Meyer, I., Cisternas, M., 2019. Distinguishing intraplate from megathrust earthquakes using lacustrine turbidites. Geology 47, 127–130. https://doi.org/10.1130/G45662.1.
Wallace, L.M., Beavan, J., 2010. Diverse slow slip behavior at the Hikurangi subduction margin, New Zealand. J. Geophys. Res. 115, B12402. https://doi.org/10.1029/2010jb007717.
Wallace, L.M., Beavan, J., McCaffrey, R., Darby, D., 2004. Subduction zone coupling and tectonic block rotations in the North Island, New Zealand. J. Geophys. Res. 109. https://doi.org/10.1029/2004JB003241.
Wallace, L., Reyners, M., Cochran, U., Bannister, S., Barnes, P., Berryman, K., Downes, G., Eberhart-Philips, D., Fagereng, A., Ellis, S., Nicol, A., McCaffrey, R., Beavan, J., Henrys, S., Sutherland, R., Barker, D., Power, W., Litchfield, N., Townend, J., Robinson, R., Bell, R.E., Wilson, K., Power, W.L., 2009. Characterizing the seismogenic zone of a major plate boundary subduction thrust: the Hikurangi Margin. Geochem. Geophys. Geosyst. 10. https://doi.org/10.1029/2009GC002610.
Wallace, L.M., Barnes, P., Beavan, J., Van Dissen, R., Litchfield, N., Mountjoy, J., Langridge, R., Lamarche, G., Pondard, N., 2012a. The kinematics of a transition from subduction to strike-slip: an example from the central New Zealand plate boundary. J. Geophys. Res. 117, B02405. https://doi.org/10.1029/2011jb008640.
Wallace, L.M., Beavan, J., Bannister, S., Williams, C., 2012b. Simultaneous long-term and short-term slow slip events at the Hikurangi subduction margin, New Zealand: implications for processes that control slow slip event occurrence, duration, and migration. J. Geophys. Res. Solid Earth 117. https://doi.org/10.1029/2012JB009489.
Wallace, L.M., Cochran, U.A., Power, W.P., Clark, K.J., 2014. Earthquake and tsunami potential of the Hikurangi subduction thrust, New Zealand: insights from paleoseismology, GPS, and tsunami modeling. Oceanography 27, 104–117.
Wallace, L.M., Kaneko, Y., Hreinsdóttir, S., Hamling, I., Peng, Z., Bartlow, N., D'Anastasio, E., Fry, B., 2017. Large-scale dynamic triggering of shallow slow slip enhanced by overlying sedimentary wedge. Nat. Geosci. 10, 765. https://doi.org/10.1038/ngeo3021. https://www.nature.com/articles/ngeo3021#supplementary-information.
Wallace, L.M., Hreinsdóttir, S., Ellis, S., Hamling, I., D'Anastasio, E., Denys, P., 2018. Triggered slow slip and afterslip on the southern Hikurangi subduction zone following the Kaikōura earthquake. Geophys. Res. Lett. 45, 4710–4718. https://doi.org/10.1002/2018GL077385.
Wang, T., Wei, S., Shi, X., Qiu, Q., Li, L., Peng, D., Weldon, R.J., Barbot, S., 2018. The 2016 Kaikōura earthquake: simultaneous rupture of the subduction interface and overlying faults. Earth Planet. Sci. Lett. 482, 44–51. https://doi.org/10.1016/j.epsl.2017.10.056.
Wellman, H.W., 1971a. Holocene tilting and uplift on the White Rocks Coast, Wairarapa, New Zealand. In: Recent Crustal Movements. 9. Royal Society of New Zealand Bulletin, pp. 211–215.
Wellman, H.W., 1971b. Holocene tilting and uplift on the Glenburn Coast, Wairarapa, New Zealand. In: Recent Crustal Movements. 9. Royal Society of New Zealand Bulletin, pp. 221–223.
Wendt, J., Oglesby, D.D., Geist, E.L., 2009. Tsunamis and splay fault dynamics. Geophys. Res. Lett. 36. https://doi.org/10.1029/2009GL038295.
Williams, C.A., Eberhart-Phillips, D., Bannister, S., Barker, D.H.N., Henrys, S., Reyners, M., Sutherland, R., 2013. Revised interface geometry for the Hikurangi subduction zone, New Zealand. Seismol. Res. Lett. 84, 1066–1073. https://doi.org/10.1785/0220130035.
Wilson, K.J., Berryman, K.R., Litchfield, N.J., Little, T.A., 2006. A revision of Mid to Late Holocene marine terrace distribution and chronology at New Zealand's most tectonically active coastal location, Pakarae River, North Island, New Zealand. N. Z. J. Geol. Geophys. 49, 477–489.
Wilson, K., Berryman, K., Cochran, U., Little, T., 2007a. Holocene coastal evolution and uplift mechanisms of the northeastern Raukumara Peninsula, North Island, New Zealand. Quat. Sci. Rev. 26, 1106–1128.
Wilson, K.J., Litchfield, N., Berryman, K.R., Little, T.A., 2007b. Distribution, age and uplift patterns of Pleistocene marine terraces of the northwestern Raukumara Peninsula, North Island, New Zealand. N. Z. J. Geol. Geophys. 50, 181–191.
Witter, R.C., Kelsey, H.M., Hemphill-Haley, E., 2003. Great Cascadia earthquakes and tsunamis of the past 6700 years, Coquille River estuary, southern coastal Oregon. Geol. Soc. Am. Bull. 115, 1289–1306. https://doi.org/10.1130/b25189.1.
Witter, R.C., Zhang, Y., Wang, K., Goldfinger, C., Priest, G., Allan, J.C., 2012. Coseismic slip on the southern Cascadia megathrust implied by tsunami deposits in an Oregon lake and earthquake-triggered marine turbidites. J. Geophys. Res. 117. https://doi.org/10.1029/2012JB009404.
Witter, R.C., Zhang, Y.J., Wang, K., Priest, G.R., Goldfinger, C., Stimely, L., English, J.T., Ferro, P.A., 2013. Simulated tsunami inundation for a range of Cascadia megathrust earthquake scenarios at Bandon, Oregon, USA. Geosphere 9, 1783–1803. https://doi.org/10.1130/GES00899.1.
Witter, R., Nelson, A., Briggs, R., Engelhart, S.E., Gelfenbaum, G., La Selle, S., Koehler, R.D., Corbett, R., Wallace, K., 2018. Evidence for Frequent, Large Tsunamis Spanning Locked and Creeping Parts of the Aleutian Megathrust. https://doi.org/10.1130/b32031.1.
Wolinsky, M.A., Swenson, J.B., Litchfield, N., McNinch, J.E., 2010. Coastal progradation and sediment partitioning in the Holocene Waipaoa Sedimentary System, New Zealand. Mar. Geol. 270, 94–107. https://doi.org/10.1016/j.margeo.2009.10.021.